

**People's Democratic Republic of Algeria
Ministry of Higher Education and Scientific Research
Mhamed Bouguera University of Boumerdes
Faculty of Engineering
Industrial Maintenance Department**



**IN PARTIAL FULLFILLMENT
OF THE REQUIREMENTS FOR
THE DEGREE MASTER IN
MECHANICS AND SYSTEMS
ENGINEERING**



TOPIC

**Study of honeycomb panels under tensile
stresses and bending**

Realized by:

Amira DJELLAB

Nabil HAMZAoui

Supervised by:

Dr. Ahmed Tidjani SETTET

:

في إطار هذه المذكرة، نهدف إلى دراسة الإجهادات المطبقة على ألواح الشطائر ذوي النواة السداسية المستوحاة من خلية النحل. ومن أجل تحقيق ذلك، قمنا بإعداد ثلاث عينات من الألواح بنفس النواة و بأوجه من مواد وهي نسيج ألياف الكربون و نسيج ألياف الزجاج، ثم طبقنا عليها نوعين من الإجهادات وهي جهد الجذب و الانثناء. أما النوع الثالث وهو الجهد القاطع فقد قمنا بمحاكاته باستعمال برنامج جاهز ANSYS. وفي الأخير قمنا بجمع البيانات وتحليلها من أجل معرفة الاختلاف في مقاومة الألواح لمختلف الإجهادات انفة الذكر، ومعرفة اللوح الأكثر مقاومة بينها.

Abstract:

In this paper, we study the stresses applied to honeycomb sandwich panels. To do this we have prepared three samples of panels with the same core and faces of different materials and these are carbon fiber fabrics and glass fibers and then applied two types of stresses: tensile and flexural. The third type, shear stress, was illustrated using ANSYS software. The results obtained allowed us to distinguish the critical zones from the stress concentrations on the sandwich panel.

Résumé:

Dans ce document, nous cherchons à étudier les contraintes appliquées aux panneaux sandwich en nid d'abeille. Pour ce faire, nous avons préparé trois échantillons de panneaux avec le même noyau et des faces de différents matériaux et ce sont des tissus de fibre de carbone et des fibres de verre, où on a appliqué deux types de contraintes : traction et flexion. Le troisième type, l'effort de cisaillement, a été illustré à l'aide d'un logiciel ANSYS. Les résultats obtenu nous ont permis de distingué les zones critique des concentrations des contraintes sur le panneau sandwich.

كلمات مفتاحية: ألواح الشطائر ذوي النواة السداسية، جهد الجذب، جهد الانثناء، الجهد القاطع.

Keywords: honeycomb sandwich panels, traction, bending, cut-off effort.

Mots-clés: Panneaux sandwich en nid d'abeille, traction, flexion, effort de coupure.

ACKNOWLEDGMENTS

In the Name of Allah, the Most Merciful, the Most Compassionate all praise is to Allah, the Lord of the worlds; and prayers and peace be upon Mohamed His servant and messenger.

First and foremost, we must acknowledge our limitless thanks to Allah, the Ever-Magnificent, the Ever-Thankful, for His help and bless. We are totally aware that this work would have never seen the light without Him saying so.

We owe a deep debt of gratitude to our university for giving us an opportunity to complete this work. We are grateful to some people, who worked hard with us from the beginning till the completion of the present research particularly our supervisor **Dr. Ahmed Tidjani Settet**, who has been always generous during all phases of this work, and we highly appreciate the help offered to us by **Dr. S. Aghib, Dr. H. Mechakra**, from laboratory of dynamics and vibro-acoustics. And to **Dr. M. Faghi** from USTHB. We recognize also, the precious help from engineers at composite materials workshop at repairs base of Algerian airlines **Mr. Gherbi Amar, Mr. M. N. Tolba, and Mr. K. malik, and Mr. M. Makhdoumi.**

We are grateful for all teachers of laboratory of dynamics and vibroacoustics under the leading ship of **Pr. A. K. Noor**, starting with **Mr. T. Djeddid, Dr. S. Lecheb, and Dr. F. Brahimi**, we want to say thank you it was a good experience being your students, and it makes us sad that it comes to its end, but, life goes on, and with Allah help we'll make you proud of us.

We would like to take this opportunity to say warm thanks to our friends, who supported us and comrades who are now most like family, beside our differences, we want to say to each one apart that we are lucky to meet someone like you on this journey it is always better sooner than later. We also would like to express our wholehearted thanks to our parents and families for their generous support they provided us throughout our entire life and particularly through the process of pursuing the master degree. Because of their unconditional love and prayers, we have the chance to complete this thesis.

In the end, we just want to express our deepest thanks to all people who took part in making this thesis real.

Dedication

Every challenging work needs self-efforts as well as support from the closest persons to our hearts. My humble effort I dedicate to the most precious persons in my life, my parents

Hamzaoui Omar and Hamaz Nora

And for her hard work and her patience and discipline, to my dear friend and partner

Djellab Amira

And to save the best for last, this work is highly dedicated for you, our supervisor

Dr. Settet Ahmed Tidjani

Your passion to learn and teach, and work ethics are truly inspiring and motivating to always keep going forward and further

Without forgetting in the end my brothers and sisters, my friends, my colleagues, and everyone who believed in me and gave me the strength.

Dedication

I dedicate this thesis to my beloved mother

Belhachemi Fatma Zohra

Who has worked for my success, thanks to her love, her support,

All the sacrifices she has made and her precious advice

You have successfully made me the person I am becoming

And to my beloved father

Djellab El-yazid

A special feeling of gratitude to a special person to my great friend and partner

Nabil Hamzaoui.

*I dedicate this work and give special thanks to my professor for the many hours of
proofreading*

Dr. Settet Ahmed Tidjani

Who must see in this work the pride of a knowledge well acquired.

*I also dedicate this dissertation to my many friends and comrades who have
supported me throughout the process, and to my fiancé, who always brings me out
the best in me*

And to all those whom I do not name, but who will recognize themselves

I will always appreciate all they have

*"I have not failed 700 times. I have not failed once.
I have succeeded in proving that those 700 ways will not work.*

When I have eliminated the ways that will not work, I will find the way that will work."

Thomas Edison

Summary

List of figures

List of tables

Nomenclatures

General introduction1

Chapter I: Composite materials and sandwich structures

1	Introduction	5
2	Composite materials	5
3	Components of a composite material.....	7
3.1	Matrix.....	7
3.1.1	Organic.....	7
3.1.2	Inorganic.....	7
3.2	Reinforcement.....	8
3.2.1	Fiber	8
3.2.2	Other reinforcements.....	8
4	Classification of composite materials.....	9
4.1	According to the form of components	10
4.1.1	Fiber composites.....	10
4.1.2	Particle composites.....	10
4.2	According to the nature of components	11
5	Composite sandwich structures.....	12
6	Constituents of sandwich structure.....	13
6.1	Face sheets.....	13
6.2	Core material	13
6.3	Kinds of cores	14
6.3.1	Honeycomb cores	14
6.3.2	Corrugated cores.....	14
6.3.3	Foam cores.....	15

6.4	Adhesive	15
7	Properties of the sandwich structure	16
7.1	Low density	16
7.2	Bending stiffness	16
7.3	Tensile and compressive strength	16
7.4	Damage tolerance	17
8	Application Areas of Sandwich Structures	17
9	Honeycomb structures	18
10	Definition of the unit cell	19
11	Unit cell configurations	20
12	Conclusion	21

Chapter II: Equilibrium theories and failure criteria

1	Introduction	22
2	Derivation of the governing equations for sandwich plates	22
2.1	Plate equilibrium equations	22
2.2	The bending of composite material sandwich plates (classical theory)	26
2.3	Classical plate theory boundary conditions	29
2.3.1	Simply-supported edge	29
2.3.2	Clamped edge	29
2.3.3	Free edge	29
3	Failure criteria [37]	30
3.1	Hill criterion	30
3.2	Tsai-hill criterion	32
3.3	Hoffman criterion	32
3.4	Tsai-Wu criterion	33
4	Anisotropy- Orthotropy	35
5	Calculation of the elastic constants of orthotropic material	37
5.1	Calculation of E_3	39

5.2	Calculation of E_1 & E_2	42
5.3	Calculation of θ_1 , θ_1 , θ_2	48
5.4	Calculation of G_1 , G_1 , G_2	49
6	Conclusion:	50

Chapter III: study of honeycomb sandwich plate

1	Introduction	51
2	Manufacturing of sandwich plate	51
2.1	Manufacturing process	51
2.2	Tensile and bending tests specimens	53
3	Tensile test	54
3.1	Tensile experiment process.....	55
4	Experimental data	56
4.1	Plate with glass fiber texture faces sheets (GFT)	56
4.2	Plate with glass fiber and carbon fiber textures faces sheets (GFT-CFT) ...	56
4.3	Plate with carbon fiber texture faces sheets (CFT)	57
4.4	Honeycomb core	58
5	Flexural strength.....	59
5.1	Three points bending experiment process	60
6	Experimental data	61
6.1	Plate with glass fiber texture faces sheets (GFT)	61
6.2	Plate with glass fiber and carbon fiber textures faces sheets (GFT-CFT) ...	61
6.3	Plate with carbon fiber texture faces sheets (CFT)	62
7	Results and discussion	62
7.1	Tensile test.....	62
7.2	Three point Bending test.....	64
8	Simulation.....	65
8.1	Tensile test.....	66
8.1.1	GFT (glass fiber texture)	66

8.1.2	GFT-CFT (glass fiber texture – carbon fiber texture)	67
8.1.3	CFT (carbon fiber texture)	68
8.2	Bending test.....	69
8.2.1	GFT (glass fiber texture)	69
8.2.2	GFT-CFT (carbon fiber texture- glass fiber texture)	70
8.2.3	CFT (carbon fiber texture)	71
9	Conclusion	72

Conclusion general	74
--------------------------	----

Bibliography

Annex

General conclusion.....73

References

Annex

List of figures

List of figures

Chapter I

Figure. I. 1 Composite basic structure	6
Figure. I. 2 Composite material [37].....	9
Figure. I. 3 Examples of fibers.....	9
Figure. I. 4 Reinforcements configurations [45].....	11
Figure. I. 5 Different configurations of honeycomb cores [46]	14
Figure. I. 6 Different configurations of corrugated cores [46]	15
Figure.I. 7 Sandwich structure with foam core [45]	15
Figure.I. 8 Composite materials in modern airplane structure [62]	18
Figure. I. 9 Some applications of composites in car structure [63]	18
Figure. I. 10 Unit cell [48]	20
Figure. I. 11 Common honeycomb types [48]	21

Chapter II

Figure. II. 1 Positive directions of sandwich panel [30]	23
Figure. II. 2 Unit cell of honeycomb [60]	39
Figure. II. 3 Regular honeycomb core [60].....	40
Figure. II. 4 Walls of honeycomb [60]	43
Figure. II. 5 Deformation in 2nd directions [60]	43
Figure. II. 6 Idealized unit cell [60]	44
Figure. II. 7 deformation in 1st direction [60]	46

Chapter III

Figure. III. 1 preparation of resin (adhesive)	51
Figure. III. 2 (a), (c), Skins and, (b) core materials	52
Figure. III. 3 Final phase of manufacturing process (a), (b)	52

Figure. III. 4 GFT- CFT	53
Figure. III. 5 (a) GFT	53
Figure. III. 6 CFT	53
Figure. III. 7 Stress-strain curve	54
Figure. III. 8 HOYTOM universal traction machine	55
Figure. III. 9 stress-strain curve for the second experiment of GFT plate.....	56
Figure. III. 10 stress-strain curve for first experiment of GFT plate	56
Figure. III. 11 stress-strain curve for the second experiment of GFT-CFT plate.	56
Figure. III. 12 stress-strain curve for the first experiment of GFT-CFT plate.....	56
Figure. III. 13 Stress-strain curve for the second experiment of CFT Plate.	57
Figure. III. 14 stress-strain curve for the first experiment of CFT plate.....	57
Figure. III. 15 deformation caused by the gripping force of jaws	58
Figure. III. 16 Stress-strain curve for honeycomb core in tensile test	58
Figure. III. 17 Three points bending test machine	60
Figure. III. 18 Stress-strain curve for GFT honeycomb sandwich plate.....	61
Figure. III. 19 Stress-strain curve for GFT-CFT honeycomb sandwich plate	61
Figure. III. 20 stress strain curve for CFT honeycomb sandwich plate	62
Figure. III. 21 (a),(b) stress by strain curve of the first tensile experiment for the test specimens.....	62
Figure. III. 22 (c),(d) stress by strain curve of the second tensile experiment for the test specimens	63
Figure. III. 23 Stress by strain for the bending test of the three specimens	64
Figure. III. 24 Maximum stress by deformation for bending test specimens	64
Figure. III. 25 Shear stress in tensile test for the GFT plate	66
Figure. III. 26 Maximum shear stress in tensile test for the GFT plate	66
Figure. III. 27 Maximum shear deformation in tensile test for the GFT plate	66
Figure. III. 28 shear stress in tensile tests for the GFT-CFT plate.....	67
Figure. III. 29 Maximum shear stress in tensile test for the GFT-CFT plate	67
Figure. III. 30 Maximum shear deformation in tensile test for the GFT-CFT plate.....	67
Figure. III. 31 shear stress in tensile tests for the CFT plate	68
Figure. III. 32 Maximum shear stress in tensile test for the CFT plate	68

Figure. III. 33 Maximum shear deformation in tensile test for the CFT plate.....	68
Figure. III. 34 shear stress in three point bending tests for the GFT plate.....	69
Figure. III. 35 Maximum shear stress in three point bending tests for the GFT plate	69
Figure. III. 36 Maximum shear deformation in three point bending tests for the GFT plate	69
Figure. III. 37 shear stress in three point bending tests for the GFT plate.....	70
Figure. III. 38 Maximum shear stress in three point bending tests for the GFT-CFT plate	70
Figure. III. 39 Maximum shear deformation in three point bending tests for the GFT-CFT plate.....	70
Figure. III. 40 shear stress in three point bending tests for the GFT plate.....	71
Figure. III. 41 Maximum shear stress in three point bending tests for the CFT plate	71
Figure. III. 42 Maximum shear deformation in three point bending tests for the CFT plate	71
Figure. III. 44 shear stress by shear deformation for tensile specimens	72
Figure. III. 43 shear stress by shear deformation for three points bending specimens	72

List of tables

List of tables

Chapter III

Table. III. 1 Dimension of test specimens	53
Table. III. 2 Characteristics obtained from the first tensile experiment	63
Table. III. 3 Characteristics obtained from the second tensile experiment.....	64
Table. III. 4 Flexural characteristics obtained from bending test	65
Table. III. 5 data obtained from software analysis.....	72

Nomenclatur

Nomenclatures

x, y, z : rectangular coordinates.

1, 2, and 3: honeycomb sandwich plate coordinates.

d : honeycomb cell size [mm].

a : honeycomb cell edge [mm].

t_c : fail thickness [mm].

L : length [mm].

W : width [mm].

H_c : hight of cell unit [mm].

t : thickness [mm].

$[C]$: stiffness matrix of the material.

E : Young's modulus (elasticity) [MPa].

b : width of the plate [mm].

M : applied moment [mm. N].

Y : the distance between natural axes.

Y_{max} : farthest distance from natural axes.

M_{max} : maximum moment [mm.N].

σ_{max} : maximum allowable stress [MPa].

F : applied force [N]

C_{ij} : stiffness matrix $i, j=1, \dots, 6$

E_i : young's modulus in i direction [MPa] $i, j=1, 2, 3$.

E_{hc} : young's modulus of the honeycomb core [MPa].

ν_{ij} : Poisson's ratio in $i, j=1, 2, 3$

ν_{hc} : Poisson's ratio for the honeycomb core material .

G_{ij} : shear modulus in i direction $i=1, 2, 3$ [MPa].

G_{hc} : shear modulus for honeycomb core [MPa].

A_{hc} : area of honeycomb in 1-2 planes.

ϵ_{hc} : strain of the honeycomb .

k: plate stiffness [N/mm]

$w_{,\bar{x}}$: partial derivate of w in \bar{x} .

$w_{,\bar{x}\bar{x}}$: 2nd partial derivate.

$w_{,\bar{x}\bar{x}\bar{x}}$: 3rd partial derivate

$w_{,\bar{x}\bar{x}\bar{x}\bar{x}}$: 4th partial derivate

α : angle of cell honeycomb longitudinal [°]

β : transversal angle of honeycomb cell [°]

γ : angle between horizontal and diagonal walls ($\gamma = \pi/4$)

$\bar{\alpha}, \bar{\beta}$: The negative of the first derivative of the lateral displacement equal respectively $-(\partial w / \partial \bar{x})$, $-(\partial w / \partial \bar{y})$.

N: stress resultants

Q: shear resultants

M: stress couples

V_n : the effective “shear resultant “

τ : shear stress

X: is the tensile stress (or compression) in L direction

Y: is the tensile stress (or compression) in T direction

Z: is the tensile stress (or compression) in T' direction

S_{LT} : shear stress in the plane (L, T)

γ : angle between horizontal and diagonal walls of the unit cell

[D]: stiffness matrix.

General Introduction

General introduction

Composites are one of the most advanced and adaptable engineering materials known to men. Progress in the field of materials science and technology have given birth to these fascinating and wonderful materials [1]

Innovative, high performance design of load-bearing component is always sought in high-tech application, such as aircraft, spacecraft, satellites or F1 racing cars. These structures should be as light as possible, while having high stiffness, sufficient strength, and some damage tolerance. This requires structurally efficient construction. Structural efficiency can be maximized by using the most efficient materials and optimizing the structure's geometry. To produce an optimum design, both of these factors need to be considered throughout the design process [2]. Ashby [3] proposed a material selection procedure, using material selection charts. Birmingham et al [4] have introduced an integrated approach to the assessment of alternative materials and structural forms at the stage of structural design based on the above methodology.

Emergence of strong and stiff reinforcement like carbon fiber and glass-fiber along with advances in polymer research to produce high performance resins as a matrix materials have helped meet the challenges posed by the complex design of modern aircraft. The large scale use of advanced composites in current programs of development of military fighter aircraft, small and big civil transport aircraft, helicopters, satellites, launch vehicles and missiles all around the world is perhaps the most glowing examples of the utilization of potential of such composites materials [5].

The use of composites keeps expanding thanks to the multiple physical advantages they offer (light weight, magnetic properties, resistance to corrosion, adaptable material ...etc). The techniques of fabrication are improved and the development of the technique using the couple polyester resin and glass-fiber helped to build up a starting point to use composites in the naval industry, more civil than military field (J.Odorico et al.1988) [6]

The choice of composites was motivated by its resistance to corrosion, which results in a reduction in the maintenance costs, also for its magnetic properties. These advantages led a number of state institutions and arms fabricators of different countries to invest in the development researches of new composite materials (M.L Sanmartin, 1988) [7], that's what induced the concept of performance index.

General introduction

The numerical methods construction an important tool of research in the development of new composite materials. The evaluation of the convergence of the results obtained from these methods aroused the use of error estimation, there, we distinguished three important types:

- An estimator using the smoothing of constraints (Zienkiewicz and Zhu 1987 [7])
- An estimator constructed on equilibrium residus (Babushka and Rheinblt , 1978 [8])
- An estimator based on the error in relation with the behavior (Ladeveze and leguillon 1983 [9] , Ladeveze and Oden 1998 [10],Landevez and Pell 2001 [11])

Regardless of the importance of these approaches, there are no guarantees that the model used will represent perfectly the reality of the studied mechanical phenomenon. With the confrontation with an experimental reference, a numerous method was developed for the registration of the stiffness matrix, and damping in dynamic models, from the result of

Try-outs in forced or free vibration (D.Lang, 1988 [12]). Other research like mottershead and friswell (1993) [13] have drawn up a state off the art of the various existing techniques of registration. The most commonly used are the so-called parametric methods for which the correction of the elementary matrix of the finite element model are related to the variation of certain physical parameters of the model (Golinval and collignon 1996 [14], Moine and al 1997 [15], Pascal Gimenez and al 1998 [16]. Humburt and al 1999 [17], Balmes 2000 [18]). In particular, the method developed within the LMT-Cachan and based on the error relation with the behavior, modified (Ladevez 1993 [19], Ladevaz and chouaki 1999 [20]) and recently expanded to the domain of acoustics (Deouvreure and al 2004 [21]) deserve to be mentioned. However, a numerical model could not govern a certain phenomenon correctly. In general there are some error sources:

- On the masses and their side effect, as in a piloting problem in Aerospatiale, for example constituting a crucial point.
- Structural, because a disruption in the characteristics of the used material in the manufacturing of the structure can occur.

Numerous studies have been carried out in recent years to model honeycomb composite structures (Y.Yang, 1986 [22]), (Young W.kwon, 1997 [23]). Without being exhaustive, an overview of the direction of the direction of the research carried out up to the present day can be given, namely (M.GREDLAC in 1993 [24]) (K.RENJI and al. 1996 [25] and flat

sandwiches, which made it possible to offer certain optimum manufacturing solutions and for specific economic objectives. In 1998, W becher [26] studied the stiffness in the plane for a bee midrange, and in particular studied the influence of the variation in the thickness of the material.

Honeycomb sandwich panels were used in the manufacture of spacecraft , due to their strain which can undergo flexural deformations on the one hand and to reduce the masse and optimize the design of the vehicle on the other hand (K.Renji and al 2002 [27]).

A structural sandwich is a special form of a laminated composite comprised of combination of different materials that are bonded to each other so as to utilize the properties of each separate component to the structural advantage of the whole assembly. The sandwich structure is composed of two faces and a core. Usually the faces are identical in material and thickness the variety of types of sandwich constructions basically depends upon the configuration of the core, not to mention the material constituents. The most common types of core are: foam, honeycomb and web core [28]. The faces that must be stiff, strong and thin; are separated and bonded to a light, weaker and thick core. The adhesion of both materials is very important for the load transferring and therefore the functioning of the sandwich as a whole Honeycomb structures are widely used in many areas for their material characteristics such as high strength to weight ratio, stiffness, dynamic, and other properties. Honeycomb structures are constructed from periodically spaced unit cells. The effective stiffness properties of honeycomb are controlled by the local geometry and wall thickness of the unit cells.

Many of the research have dealt with the bending behavior and failure of sandwich structure Foo, Seah and Chai Study the failure response of aluminum sandwich panels subjected to low-velocity impact is discussed. A three-dimensional geometrically correct finite element model of the honeycomb sandwich plate and a rigid impact. [29], V. Crupi, et al investigated the analysis of static and low-velocity impact response of two typologies of aluminum honeycomb sandwich structures with different cell size.[30], H R Ali. B.Manafi.et al investigated the effects of core shape, cell wall height, wall thickness and skin thickness on critical bending load of honeycomb sandwich panels.[31], Sakhi Jan et al. study the flexure behavior of the honeycomb sandwich panels are experimentally and analytically investigated. Aluminum honeycomb core and glass fiber composite face sheets were utilized for the manufacture of the test specimens. [32],Sushrut Vaidya et al study the quasi-static response of corrugated core sandwich beams with various core layer arrangements of uniform and graded thicknesses, and perform parametric study of structural size beams [33],Abadi et al used

General introduction

important experimental fatigue data for honeycomb sandwich panels with artificial defects and without defects. Was compared the fatigue tests on honeycomb sandwich panels from the aluminum alloy skin (the reference case) [34].

Therefore, the present study is focused on studying the honeycomb sandwich panel in plan and in bending, also to learn the difference between the shear stress in both experiments. The focus of this study relies on the change of the mechanical characteristics by modifying the skins materials of the panels.

Chapter I

*Composite materials and sandwich
structures*

1 Introduction

From the earliest days, humans were concerned about developing the life style and comfort in every and each part of living, this necessity to obtain a better, easy, and more developed way to live was the reason to reach many victories in different major domains as health care, scientific research, and transportation. In this chapter we are going to talk about composite materials, one the most advanced kind of materials used in modern industry.

2 Composite materials

A composite material can be identified as a combination of two or more components (matrix and reinforcement), which when combined gives properties superior to the properties of the individual components.

Generally, a composite material consists of two or more discontinuous phases plugged-in a continuous phase. In the case of multiple discontinuous phases with different natures the composite is called hybrid. The discontinuous phase is usually more rigid with superior mechanical characteristics compared to the continuous phase. An important exception to the previous description is the case of modified polymers by elastomeres, for which a rigid polymer matrix is charged with elastomeres particles. For this type of materials the static characteristics of polymer (Young`s modulus, yield stress, ...etc) are not practically modified with the addition of elastomeres particles, however, the characteristics at shock are improved.

The properties of composite materials results of:

- Properties of the components.
- Their geometric distribution.
- Their interaction, etc.

Also, to get access to the description of a composite material, it is important to specify:

- The nature of components.
- The geometry of reinforcement, and its distribution.
- The nature of interface matrix/reinforcement.

The geometry of reinforcement will be characterized by its form, size, concentration, disposition (orientation), etc. The concentration of reinforcement is usually measured by volume fraction or masse fraction. The concentration of matrix is an important parameter to determine the properties of composite material.

For a given concentration, the distribution of reinforcement in the composite is also an important parameter. A distribution that is uniform will ensure the homogeneity of the material, on the other hand, a non-uniform distribution will cause a weak zones in the material in which crack initiates causing in its turn a diminution in the resistance of the material.

In the case of composite material with fiber reinforcement, the orientation of fibers determines the anisotropy of the material. This aspect represents one of the fundamental characteristics of composites, that is the possibility to control the anisotropy of the final product with desired properties.

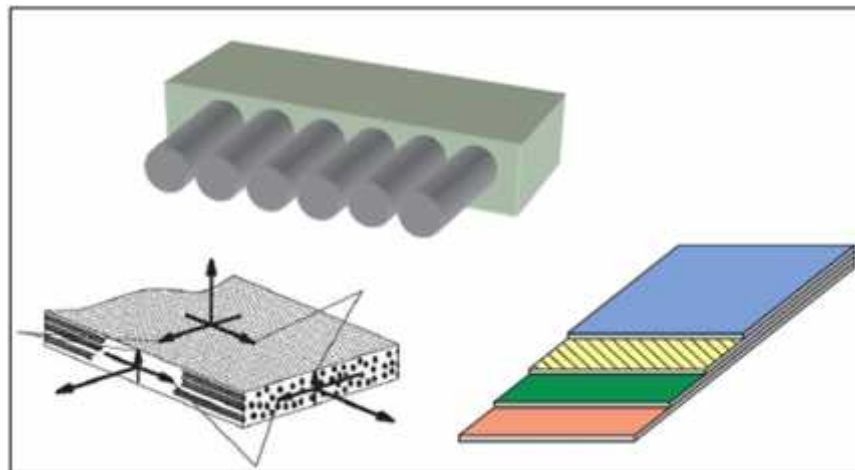


Figure. I. 1 Composite basic structure

3 Components of a composite material

3.1 Matrix

3.1.1 Organic

Polymers are common matrices (especially used for fiber reinforced plastic). Road surfaces are often made from asphalt concrete which uses bitumen as a matrix. Mud (wattle and dumb) has seen extensive use. Typically, most common polymer-based composite materials include at least two parts, the substrate and resin.

Polyester resin tends to have yellowish tint, and it is suitable for most backyard projects. its weakness is that it is UV sensitive and can be tend to degrade over time, and thus generally is also coated to help preserve it. It is often used in the making of surfboards and for marine applications, its hardener is a peroxide often MEKP (methyl, ethyl, ketene, peroxide). When the peroxide is mixed with resin, it decomposes to generate free radicals, which initiate the current reaction. Hardeners in the system are commonly called catalysts, but since they do not re-appear unchanged in the end of the reaction, they do not fit strictest chemical definition of a catalyst.

Vinyl ester resin tends to have a purplish to bluish to greenish tint. This resin has a lower viscosity than polyester resin, and it is more transparent. This resin is often billed as being fuel resistant, but will melt in contact with gasoline. This resin tends to be more resistant over time to degradation than polyester resin, and it is more flexible. It uses the same hardener as polyester resin (at a similar mix ratio) and the cost is approximately the same.

Epoxy resin is almost totally transparent when crude. In aerospace industry, epoxy is used as a structural matrix material or structural glue [36].

3.1.2 Inorganic

Cement (concrete), metals, ceramics, and sometimes glasses are employed. Unusual matrices such as ice are sometimes proposed as in pykecrete [36].

3.2 Reinforcement

3.2.1 Fiber

Reinforcement usually adds rigidity and greatly impedes crack propagation. Thin fibers, can have a very high strength, and provided they are mechanically well attached to the matrix. They can greatly improve the composite's overall properties.

Fiber-reinforced composite materials can be divided into two main categories normally referred to as short fiber-reinforced materials and continuous fiber-reinforced materials. The woven and continuous fiber styles are typically available in a variety of forms, being pre-impregnated with the given matrix (resin), dry, unidirectional tapes of various widths, plain weave, harness satins, braided, and stitched.

The short and long fibers are typically employed in compression molding and sheet molding operations. These come in form of flakes, chips, and random mat (which can also be made from a continuous fiber laid in random fashion until the desired thickness of the ply/laminate is achieved).

Common fiber used for reinforcement includes glass fibers, carbon fibers, cellulose (wood/paper fibers and straw) and high strength polymers for example aramid. Silicon carbide fibers are used for some high temperature applications [36].

3.2.2 Other reinforcements

Concrete uses aggregate, and reinforced concrete additionally uses steel bars (rebar) to tension the concrete. Steel mesh or wires are also used in some glass and plastic products

[36].

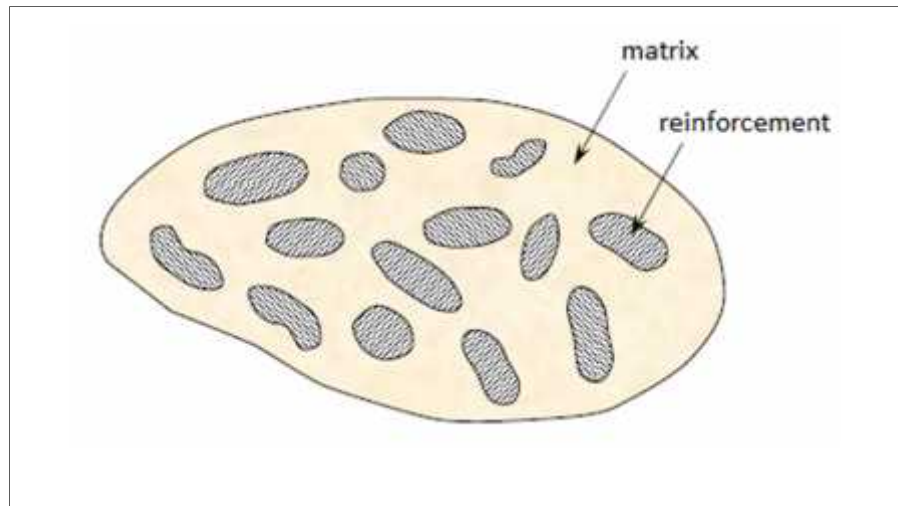


Figure. I. 2 Composite material [37]



Figure. I. 3 Examples of fibers

4 Classification of composite materials

Composites can be classified in more than way, depending on the different parameters that these materials can offer; the classification could change from way to another. Here, we take in consideration the form and the nature of components [37]:

4.1 According to the form of components

4.1.1 Fiber composites

The most common man-made composites are composed of glass or carbon fiber in a plastic resin. Resins can be of the form of thermoset or thermoplastic materials which each have their own unique advantages and disadvantages. The glass or carbon fibers are significantly stronger than the plastic matrix but they also tend to be brittle.

A composite construction, therefore, allows one to take advantage of the excellent stiffness and strength properties of glass or carbon by embedding the fibers in a more compliant matrix.

When a composite structure is manufactured, a “dry” carbon fiber and a “wet” resin is used. The dry carbon fiber will be wetted with the resin and put inside a oven so that the resin can solidify and “block” the carbon fibers creating stiffness [37].

4.1.2 Particle composites

Particulate reinforced composites with concrete being a good example. The aggregate of coarse rock or gravel is embedded in a matrix of cement. The aggregate provides stiffness and strength while the cement acts as the binder to hold the structure together.

There are many different forms of particulate composites. The particulates can be very small particles (< 0.25 microns), chopped fibers (such as glass), platelets, hollow spheres, or new materials such as bucky balls or carbon nano-tubes. In each case, the particulates provide desirable material properties and the matrix acts as binding medium necessary for structural applications.

Particulate composites offer several advantages. They provide reinforcement to the matrix material thereby strengthening the material. The combination of reinforcement and matrix can provide for very specific material properties. For example, the inclusion of conductive reinforcements in a plastic can produce plastics that are somewhat conductive. Particulate composites can often use more traditional manufacturing methods such as injection molding which reduces cost [37].

4.2 According to the nature of components

Composite materials are classed by the nature of matrix to: organic (ceramic) composites, metallic composites, mineral composites. Different reinforcements are associated to these matrices, but, only some of these association couples are used in industry, the rest are subjects of search and development in research laboratories [37].

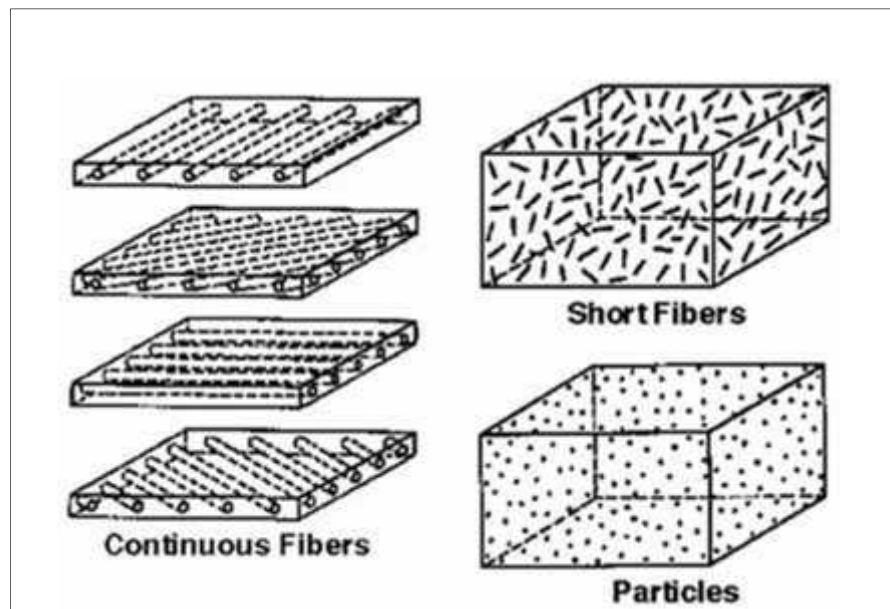


Figure. I. 4 Reinforcements configurations [45]

5 Composite sandwich structures

Sandwich structures can be classed as composite materials in that they consist of two or more individual components of differing properties which when combined result in a high performance material. In contrast to monolithic composites - which consist of an intimate mixture of fibres (glass, kevlar, carbon, metal, etc) supported within a continuous matrix (e.g. thermoplastic or thermoset resin) - sandwich structures have a discrete structure in which a core material is bonded to, and faced with, a skin material.

The skin material usually has a high stiffness, whereas the core typically has high compressive and shear strength. When these are bonded together, this combination gives the sandwich structure a high flexural modulus. The skins are bonded to the core with film, liquid or paste adhesives and normally cured using heat and pressure, although some adhesives can cure at room temperature. It is important to note that the chosen adhesive needs to have the appropriate mechanical and thermal properties to achieve compatibility between the skin and core materials, especially with respect to thermal expansion differences. Sandwich panels are used in preference to conventional composites where the characteristics of low weight and high resistance to bending are required [37].

6 Constituents of sandwich structure

There are various types of face sheet and core materials and every different combination of these components results with sandwich constructions having different mechanical behaviors. It is important to produce a sandwich structure having required properties according to the working environment. In order to employ the proper components the following conditions must be satisfied:

1. Determination of the absolute minimum weight for a given structural geometry, loading and material system.
2. Comparison of one type of sandwich construction with others

3. Comparison of the best sandwich construction with alternative structural configurations (monocoque, rib-reinforced, etc.)
4. Selection of the best face sheet and core materials in order to minimize structural weight.
5. Selection of the best stacking sequence for faces composed of laminated composite materials.
6. Comparison of the optimum construction weight with weights required by some restrictions; i.e., the weight penalty due to restrictions of cost, minimum gage, manufacturing, material availability, etc.

Main components of the composite sandwich structures are investigated separately in a detailed manner [40].

6.1 Face sheets

In a sandwich structure the face sheets can be made of many different materials, it can be isotropic monocoque material, anisotropic monocoque material or a composite material. Aluminum, fiberglass, graphite and aramid are the widely used face sheet materials. However, in order to minimize the weight of the structure generally composite face sheets are preferred [40].

6.2 Core material

The core has several vital functions. It must be stiff enough to resist loads acting in perpendicular direction to the panels, so the distance between the upper and lower face sheets remains fixed. Also, enough in shear to prevent the sliding of the face sheets over each other. If this condition is not fulfilled, the face sheets acts as two independent panels and the sandwich effect is lost. In addition, the core should be stiff enough to stabilize the thin face sheets, otherwise, wrinkling (local buckling) of the face sheets may occur. Further, it increases the moment of inertia of the cross section of the outer faces and enables them to work together as a single beam. Both the critical buckling stress and the ultimate compressive strength of the compressed face are significantly rises by the presence of the core in comparison to similar plates without such support [41].

6.3 Kinds of cores

6.3.1 Honeycomb cores

Honeycomb cores have a unit cell that is either square, triangular, or hexagonal that can be translated and repeated in two or three dimensions. These cores can be manufactured from slotted metal sheets and can be attached to face sheets by a number of joining methods such as adhesive bonding, brazing, diffusion bonding [41][42]. However, and there is no access into the core region unless the webs are deliberately perforated which can significantly degrade their strength.

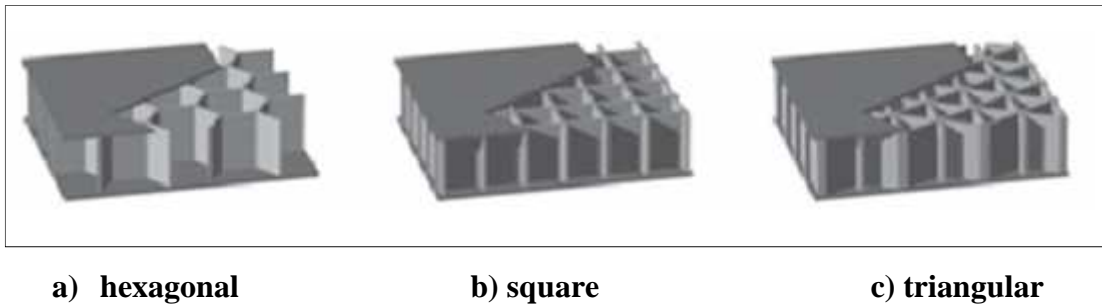
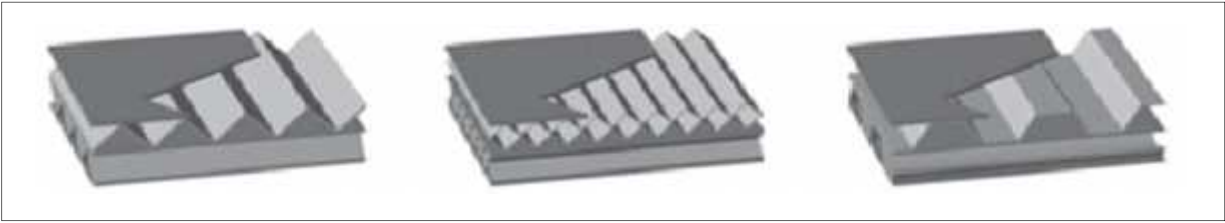


Figure. I. 5 Different configurations of honeycomb cores [46]

6.3.2 Corrugated cores

Corrugated cores have a unit cell that can be triangular, diamond or trapezoidal shaped. These cores can be manufactured by bending metal sheets and sandwich structures are then made by brazing or welding them to face sheets [41]. Unlike honeycomb cores, corrugated cores are an open celled geometry in one direction and do not restrict one directional lateral access into the core region after face sheets bonding. Oftentimes, however, smaller face sheets core nodal joints made corrugated cores more susceptible to face sheets debonding than honeycomb cores [42][43].



d) Triangular

e) diamond

f) trapezoid

Figure. I. 6 Different configurations of corrugated cores [46]

6.3.3 Foam cores

These lightweight materials inexpensive, easily machined and yet they have very low mechanical characteristics. Foam materials, are classed as 3-dimensional cellular materials, as the arrangement of the cells varies throughout the solid.

**Figure.I. 7 Sandwich structure with foam core [45]**

6.4 Adhesive

The adhesive keeps the faces and the core cooperating with each other, the adhesive between the face sheets and core must be able to transfer the shear forces between them. It must also be able to carry shear and tensile stresses. It is hard to specify the demands

on the joints. A simple rule is that the adhesive should be able to take up the same shear stress as the core [45].

7 Properties of the sandwich structure

Main advantage of any type of composite material is the possibility of tailoring their properties according to the application. The same advantage also applies to sandwich structure. Proper choice of core and environmental conditions. Some general characteristics of sandwich structures are described below:

7.1 Low density

Choice of the lightweight core or expanded structures of high-density materials decrease the overall density of the sandwich structure. Volume of the core is considerably higher in the sandwich structure compared to the volume of skins so any decrease in the density of the core material has significant effect on the overall sandwich density [47].

7.2 Bending stiffness

This property comes from the skin part of the sandwich, due to a higher specific stiffness sandwich and higher natural frequencies compared to other structures [47].

7.3 Tensile and compressive strength

The Z-direction properties are controlled by the properties of the core and X and Y directions properties are controlled by properties of the skin [47].

7.4 Damage tolerance

Use of flexible foam as core makes sandwich material highly damage tolerant structure. For this reason foam core or corrugated core sandwich structured material are popular materials in packaging applications [47].

8 Application Areas of Sandwich Structures

The use of composite sandwich structures in aeronautical, automotive, aerospace, marine and civil engineering applications is getting wider as these structures have excellent stiffness to weight ratios that leads to weight reduction and fuel consumption. Various combinations of core and face sheet materials are being studied by researchers worldwide in order to achieve improved crashworthiness (Mamalis, et al. 2005) [35].

In aerospace applications various honeycomb cored sandwich structures were used for space shuttle constructions also they are used for both military and commercial aircrafts. The U.S. Navy and the Royal Swedish Navy has used honeycomb sandwich bulkhead to reduce the weight of the ship and to withstand underwater explosions for more than 20 years. Moreover, locomotives are designed in order to resist the pressure waves occurring during the crossing of two high-speed trains in tunnels. More recently, sandwich constructions are commonly used in civil engineering projects such as bridge decks, wall and roof claddings for buildings because of their low cost and thermal performance. Also, railcars for rapid transit trains, busses, sailboats, racing boats, racing cars, snow skis, water skis and canoes are all employing sandwich constructions (Vinson 1999) [30].

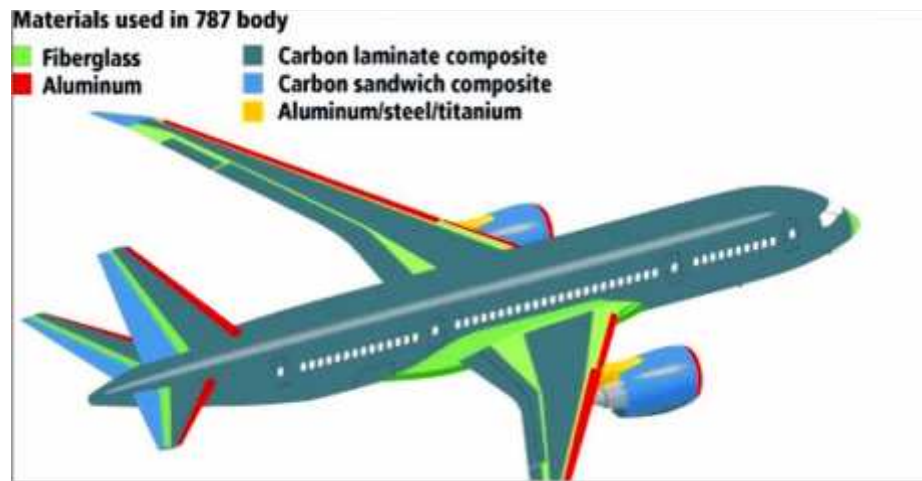


Figure.I. 8 Composite materials in modern airplane structure [62]

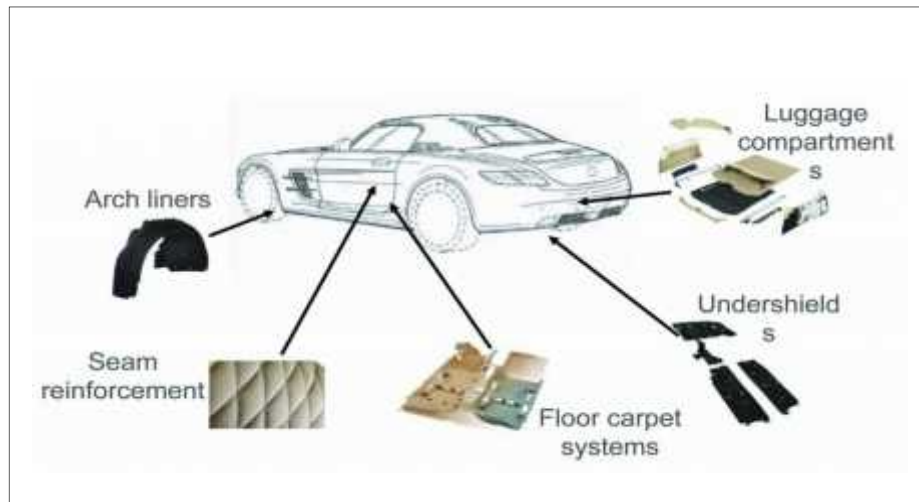


Figure. I. 9 Some applications of composites in car structure [63]

9 Honeycomb structures[47]

Honeycomb structures are natural or man-made structures that have the geometry of a honeycomb to allow the minimization of the amount of used materials to reach a

minimal weight and minimal material cost. The geometry of honeycomb structures can vary widely but the common features of all such structures are an array of hollow cells formed between thin vertical walls. A honeycomb shopped structure provides a material with minimal density and relative high out-of-plane compression and out-of-plane shear properties [46]. Man-made honeycomb structures materials are commonly made by layering a honeycomb material between two thin layers that provide strength in tension. This forms a plat-like assembly.

Honeycomb materials are widely used in aerospace industry for this reason, and honeycomb materials in aluminum, fiberglass and advanced composite materials have been featured in aircraft and rockets since 1950s [46].

Due to the efficient hexagonal configuration of the honeycomb, where the walls support each other, the compression strength of the cores is typically higher than other sandwich core configurations of the same weight. The honeycomb cell structure is typically light in weight and its out-of-plane (x3 direction) effective Young's modulus is considerably greater than the isotropic in-plane (x1–x2) moduli. The proposed metamaterial can be considered as a composite composed of an isotropic membrane and a homogenized, transversely isotropic material. The effective static mass density for the metamaterial composite can be obtained from the following equation:

$$\rho = \frac{\rho_m h_m + \rho_c h_c}{h} \quad (I.1)$$

Where $\rho_c = \frac{2\rho_0 t}{[(1 + \cos \theta)(1 + \sin \theta)]}$ is the effective static mass density of the honeycomb cell structure.

ρ_0 is the mass density of the honeycomb material.

ρ_m is the membrane density.

$$h = h_m + h_c \quad (I.2)$$

10 Definition of the unit cell

The unit cell is a hexagonal cell. In fact with a hexagonal cell, it's possible to describe the entire honeycomb core. The periodicity of the structures is used here. In the second time the unit cell is built up with one quarter of one central wall and one quarter of one inclined wall. This reduction in the size of the cell to be studied is because of the different symmetries [48].

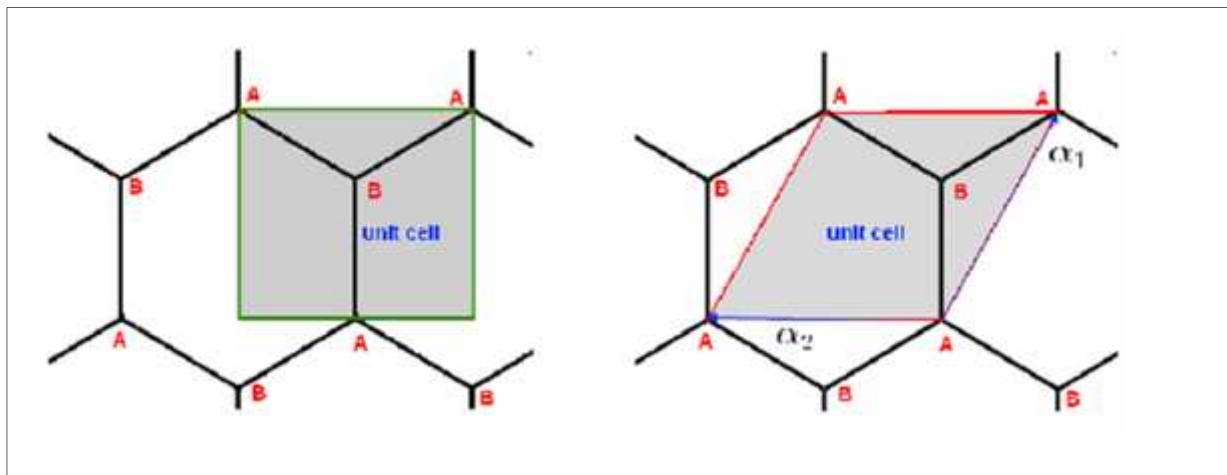


Figure. I. 10 Unit cell [48]

11 Unite cell configurations

Honeycomb can be made and cut to the standard hexagonal style which is and the most common cellular configuration or it can be over-expanded in the W direction to form the corrugated or over-expanded (OX) configuration, where the cells look rectangular. The OX process tends to increase W sheer properties and slightly reduce L shear properties compared to hexagonal honeycomb core [49]. There are also other configurations as showed in the following figure:

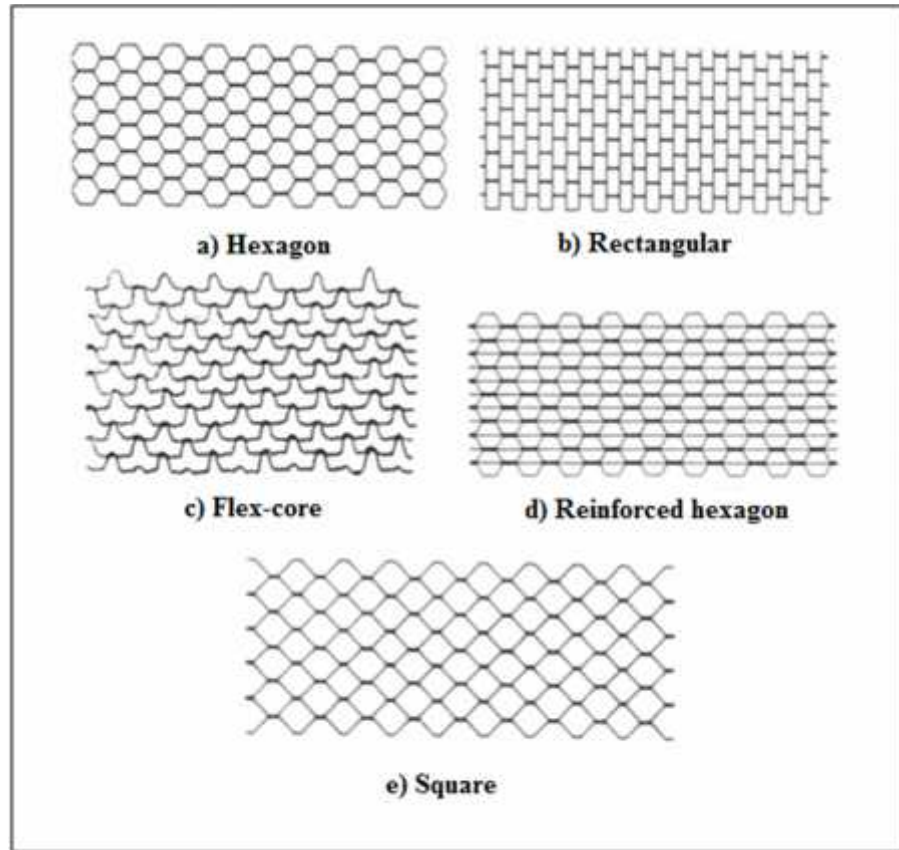


Figure. I. 11 Common honeycomb types [48]

12 Conclusion

In this chapter, we learned about composite materials, sandwich structures, and honeycomb cores. We notice at the end of this chapter the importance of composite materials and their major participation in modern industry.

Chapter II

*Equilibrium theories and failure
criteria*

1 Introduction

The purpose of this chapter is to determine the equations relating to the mechanical behaviour of sandwich structures based of nomex honeycomb core. It is an extremely lightweight, high strength, non-metallic product manufactured with aramid fiber paper impregnated with a heat resistant phenolic resin.

This core material offers unique combination of properties which allows superior electrical insulation. Aramid paper is used in boat hulls, auto racing bodies and military shelters. Furthermore it's very appreciated by the aeronautical, railway and shipyard industry.

2 Derivation of the governing equations for sandwich plates

2.1 Plate equilibrium equations

The integrated stress resultants (N), shear resultants (Q), and stress couples (M), with approximately subscripts, are defined by equation (II.1)

$$\begin{Bmatrix} N_x \\ N_y \\ N_x \\ Q_x \\ Q_y \end{Bmatrix} = \int_{-h/2}^{h/2} \begin{Bmatrix} \sigma_x \\ \sigma_y \\ \sigma_x \\ \sigma_x \\ \sigma_y \end{Bmatrix} d \quad , \quad \begin{Bmatrix} M_x \\ M_y \\ M_x \end{Bmatrix} = \int_{-h/2}^{h/2} \begin{Bmatrix} \sigma_x \\ \sigma_y \\ \sigma_x \end{Bmatrix} Z.d \quad (\text{II.1})$$

For a rectangular plate, defined as a body of length a in the x -direction, width b in the y -direction, and thickness h in the z -direction, where $h \ll b$ and $h \ll a$, a thin plate. It is now necessary to derive the equilibrium relations that exist for this plate structure. Keep in mind that this derivation for a laminated composite plate applies as well to a sandwich plate or panel [30].

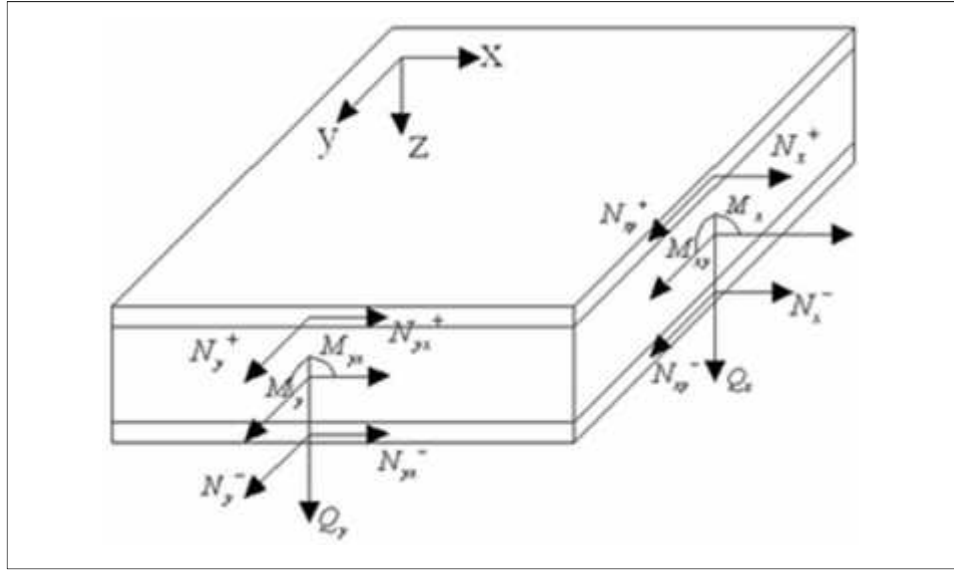


Figure. II. 1 Positive directions of sandwich panel [30]

A force balance can now be made in the x, y and z directions resulting in this equation of equilibrium. For instance, a force balance on the x-direction would yield:

$$\left(\sigma_x + \frac{\partial \sigma_x}{\partial x} dx \right) dy dz + \left(\sigma_y + \frac{\partial \sigma_y}{\partial y} dy \right) dx dz + \left(\sigma_z + \frac{\partial \sigma_z}{\partial z} dz \right) dx dy - \sigma_x dx dy dz - \sigma_y dx dy dz - \sigma_z dx dy dz + F_x dx dy dz = 0$$

Cancelling terms and dividing the remaining terms by the volume v (where v =dx dy dz), the results are the following:

$$\frac{\partial \sigma_x}{\partial x} + \frac{\partial \sigma_y}{\partial y} + \frac{\partial \sigma_z}{\partial z} + F_x = 0 \quad (\text{II.2})$$

Similarly, equilibrium in the y and z directions yields:

$$\frac{\partial \sigma_x}{\partial x} + \frac{\partial \sigma_y}{\partial y} + \frac{\partial \sigma_z}{\partial z} + F_y = 0 \quad (\text{II.3})$$

$$\frac{\partial \sigma_x}{\partial x} + \frac{\partial \sigma_y}{\partial y} + \frac{\partial \sigma_z}{\partial z} + F_z = 0 \quad (\text{II.4})$$

These three equations comprise the equilibrium equation for three-dimensional elasticity. However, for beam, plate, and shell theory, whether involving composite materials or not, one must integrate the stresses across the thickness of the thin-walled structures to obtain solution.

Recalling the definitions in literature [30], the stress resultants and stress couples are:

$$\begin{Bmatrix} N_x \\ N_y \\ N_x \\ Q_x \\ Q_y \end{Bmatrix} = \int_{-h/2}^{h/2} \begin{Bmatrix} \sigma_x \\ \sigma_y \\ \sigma_x \\ \sigma_x \\ \sigma_y \end{Bmatrix} dz = \sum_{k=1}^N \int_{h_{k-1}}^{h_k} \begin{Bmatrix} \sigma_x \\ \sigma_y \\ \sigma_x \\ \sigma_x \\ \sigma_y \end{Bmatrix} dz_k \quad (\text{II.5})$$

$$\begin{Bmatrix} M_x \\ M_y \\ M_x \end{Bmatrix} = \int_{-h/2}^{h/2} \begin{Bmatrix} \sigma_x \\ \sigma_y \\ \sigma_x \end{Bmatrix} z dz = \sum_{k=1}^N \int_{h_{k-1}}^{h_k} \begin{Bmatrix} \sigma_x \\ \sigma_y \\ \sigma_x \end{Bmatrix} z_k dz_k \quad (\text{II.6})$$

The first form of each is applicable to a single-layer plate, while the second form is necessary for a laminated plate due to the stress discontinuities associated with different material and/or differing orientations in the various plies. The second form is, therefore, necessary for a sandwich plate because of the different face and core material properties.

Turning now to equation (II.2), neglecting the body force term, F_x , for simplicity of example, integrating term by term across each ply, and summing across the plate provides:

$$\sum_{k=1}^N \int_{h_{k-1}}^{h_k} \frac{\partial \sigma_{xk}}{\partial z} dz + \sum_{k=1}^N \int_{h_{k-1}}^{h_k} \frac{\partial \sigma_{yk}}{\partial z} dz + \sum_{k=1}^N \int_{h_{k-1}}^{h_k} \frac{\partial \sigma_{zk}}{\partial z} dz = 0 \quad (\text{II.7})$$

In the first two terms integration and differentiation can be interchanged, hence:

$$\frac{\partial}{\partial z} \left[\sum_{k=1}^N \int_{h_{k-1}}^{h_k} \sigma_{xk} dz \right] + \frac{\partial}{\partial z} \left[\sum_{k=1}^N \int_{h_{k-1}}^{h_k} \sigma_{yk} dz \right] + \sum_{k=1}^N \sigma_{zk} \Big|_{h_{k-1}}^{h_k} = 0 \quad (\text{II.8})$$

In the first two terms N_x and N_{yx} appear explicitly as the bracketed quantities. In the third term it is clear that between all plies and between the face and core materials of the sandwich panel, the interlinear shear stresses cancel each other out, and one can define externally applied surface shear stresses on the top ($z = h_N$) and ($z = h_0$) surfaces

$$\partial_z (h_N) = \tau_{1x} \text{ And } \partial_z (h_0) = \tau_{2x} \quad (\text{II.9})$$

Equation (II.8) can therefore be written as:

$$\frac{\partial x}{\partial z} + \frac{\partial x}{\partial z} + \tau_{1x} - \tau_{2x} = 0 \quad (\text{II.10})$$

Similarly, integrating the equilibrium equation in the y-direction provides:

$$\frac{\partial x}{\partial z} + \frac{\partial y}{\partial z} + \tau_{1y} - \tau_{2y} = 0 \quad (\text{II.11})$$

$$\text{Where: } \partial_z (h_N) = \tau_{1y} \text{ and } \partial_z (h_0) = \tau_{2y} \quad (\text{II.12})$$

Likewise equilibrium in the z-direction upon integration and summing provides:

$$\frac{\partial x}{\partial z} + \frac{\partial y}{\partial z} + p_1 - p_2 = 0 \quad (\text{II.13})$$

$$\text{Where: } \partial_z (h_N) = p_1 \text{ and } \partial_z (h_0) = p_2 \quad (\text{II.14})$$

In addition to the integrated force equilibrium equation above, two equations of moment equilibrium are also needed, one for the x-direction and one for the y-direction. Multiplying equation (II.1) through by $z \, dz$, integrating across each ply, and summing across all laminate results the following

$$\sum_{k=1}^N \frac{h_k}{h_{k-1}} \frac{\partial x_k}{\partial z} z \, dz + \sum_{k=1}^N \frac{h_k}{h_{k-1}} \frac{\partial y_k}{\partial z} z \, dz + \sum_{k=1}^N \frac{h_k}{h_{k-1}} \frac{\partial z_k}{\partial z} z \, dz = 0 \quad (\text{II.15})$$

Again, in the first two terms integration and summation can be interchanged with differentiation with the result that the first two terms become $(\frac{\partial x}{\partial z}) + (\frac{\partial x'}{\partial z})$.

However, the third term must be integrated by parts as follows:

$$\sum_{k=1}^N \frac{h_k}{h_{k-1}} \frac{\partial z_k}{\partial z} z \, dz = \sum_{k=1}^N \left\{ z \, z \Big|_{h_{k-1}}^{h_k} - \frac{h_k}{h_{k-1}} \partial_z z \, dz \right\} \quad (\text{II.16})$$

Here the last term is seemed to be Q_x . Again in the first term on the right, clearly the moments of all the interlinear stresses between plies cancel each other out, and the only

none zero terms are the moments of the applied surface shear stresses, hence, that term becomes:

$$h_N \tau_{1x} - h_0 \tau_{2x} = \frac{h}{2} [\tau_{1x} + \tau_{2x}] \quad (\text{II.17})$$

Using the former expression, the equation of equilibrium of moments in the x-direction is:

$$\frac{\partial}{\partial x} + \frac{\partial}{\partial} - Q_x + \frac{h}{2} [\tau_{1x} + \tau_{2x}] = 0 \quad (\text{II.18})$$

Similarly in the y-direction the moment equilibrium equation is:

$$\frac{\partial}{\partial x} + \frac{\partial}{\partial y} - Q_y + \frac{h}{2} [\tau_{1y} + \tau_{2y}] = 0 \quad (\text{II.19})$$

Where all terms are defined above, thus, there are five equilibrium equations for a rectangular plate, regardless of what material or materials are utilized in the plate (II.10),(II.11), (II.13), (II.15), and(II.16).

2.2 The bending of composite material sandwich plates (classical theory)

Consider a plate composed of a sandwich composite material that is mid-plane symmetric, i.e, $B_{ij}=0$, and has no other coupling terms, no surface shear stresses and no hygrothermal effects [30]. The plate equilibrium equations for the bending of the plate subjected to lateral loads given by equations (II.15), (II.16), and (II.13) become:

$$\frac{\partial}{\partial x} + \frac{\partial}{\partial} - Q_x = 0 \quad (\text{II.20})$$

$$\frac{\partial}{\partial x} + \frac{\partial}{\partial y} - Q_y = 0 \quad (\text{II.21})$$

$$\frac{\partial Q_x}{\partial} + \frac{\partial}{\partial y} - p_{(x,y)} = 0 \quad (\text{II.22})$$

Where,

$$p_{(x,y)} = p_{1(x,y)} - p_{2(x,y)} \quad (\text{II.23})$$

These three equations apply also to a sandwich plate. Solving for Q_x and Q_y equations (II.17) and (II.18) can be substituted into equation (II.19) with the result that:

$$\frac{\partial^2 M_x}{\partial y^2} + 2 \frac{\partial^2 M_{xy}}{\partial x \partial y} + \frac{\partial^2 M_y}{\partial x^2} = -P(x,y) \quad (II.24)$$

The above equations are derived from equilibrium consideration alone. For the case of mid-plane symmetry ($B_{ij}=0$) and no coupling terms,

$$M_x = D_1 k_x + D_1 k_y \quad (II.25)$$

$$M_y = D_1 k_x + D_2 k_y \quad (II.26)$$

$$M_{xy} = 2D_6 k_{xy} \quad (II.27)$$

Where:

$$k_x = \frac{\partial \bar{\alpha}}{\partial y}, \quad k_y = \frac{\partial \bar{\beta}}{\partial x}, \quad k_{xy} = \frac{1}{2} \left(\frac{\partial \bar{\alpha}}{\partial x} + \frac{\partial \bar{\beta}}{\partial y} \right) \quad (II.28)$$

It is well known that transverse shear deformation (that is $\epsilon_x = 0, \epsilon_y = 0$) effects are important for plates composed of composite materials and also sandwich plates in determining maximum deflections, vibration natural frequencies, and critical buckling loads. However, it is appropriate to use a simple stress analysis involving classical theory that neglects transverse shear deformation for preliminary design to determine a "first cut" for stresses, the required overall stacking sequence, and required plate thickness.

If, in fact, transverse shear deformation is neglected,

$$\epsilon_x = 0 = \frac{1}{2} \left(\bar{\alpha} + \frac{\partial}{\partial y} \right) a, \quad \epsilon_y = 0 = \frac{1}{2} \left(\bar{\beta} + \frac{\partial}{\partial x} \right) b \quad (II.29)$$

Hence,

$$\bar{\alpha} = -\frac{\partial}{\partial y}, \quad a = \bar{\beta} = -\frac{\partial}{\partial x} \quad (II.30)$$

$$\text{And} \quad k_x = -\frac{\partial^2 w}{\partial y^2}, \quad k_y = -\frac{\partial^2 w}{\partial x^2}, \quad k_{xy} = -\frac{\partial^2 w}{\partial x \partial y} \quad (II.31)$$

So, substituting equation (II.28) into equation (II.25) through equation (II.27), the results are:

$$M_x = -D_1 \frac{\partial^2 w}{\partial x^2} - D_1 \frac{\partial^2 w}{\partial y^2} \quad (\text{II.32})$$

$$M_y = -D_1 \frac{\partial^2 w}{\partial x^2} - D_2 \frac{\partial^2 w}{\partial y^2} \quad (\text{II.33})$$

$$M_x = -2D_6 \frac{\partial^2 w}{\partial x \partial y} \quad (\text{II.34})$$

Substituting these three equations in turn into equation (II.24) results in:

$$D_1 \frac{\partial^4 w}{\partial x^4} + 2(D_1 + 2D_6) \frac{\partial^4 w}{\partial x^2 \partial y^2} + D_2 \frac{\partial^4 w}{\partial y^4} = p(x,y) \quad (\text{II.35})$$

The above coefficients can be simplified to:

$$D_1 = D_1, D_2 = D_2, (D_1 + 2D_6) = D_3 \quad (\text{II.36})$$

With the simplified notation, equation (II.32) becomes:

$$D_1 \frac{\partial^4 w}{\partial x^4} + 2D_3 \frac{\partial^4 w}{\partial x^2 \partial y^2} + D_2 \frac{\partial^4 w}{\partial y^4} = p(x,y) \quad (\text{II.37})$$

This is the governing differential equation for the bending of a plate composed of a composite material, including transverse shear deformation, with no coupling terms, and no hygrothermal terms (that is, $T = m = 0$) subjected to a lateral distributed load $p(x,y)$, it can be shown that if the plate materials are isotropic then, $D_1 = D_2 = D_3 = 0$. As started previously, neglecting transverse shear deformation and

hygrothermal effects can lead to significant errors, as will be shown, but in preliminary design to ``size`` the plate initially.

Solutions of equation (II.36) can be obtained generally in two ways: direct solution of the governing differential equation (II.37), or utilization of an energy principle solution. The latter offers more latitude in finding approximate solutions, often needed.

Direct solutions of the governing differential equation for plate of composite materials fall into three categories: Navier, levy, and perturbation solutions.

Each has its advantages and disadvantages. However, prior to that, boundary conditions need to be discussed [30].

2.3 Classical plate theory boundary conditions

In the ``classical`` plate theory two and only two boundary conditions can be satisfied at each edge of the plate. The boundary conditions for a simply-supported edge and a clamped edge, shown below, are identical to those of classical beam theory, where n is the direction normal to the plate edge and t is the direction parallel or tangent to the edge [30]:

2.3.1 Simply-supported edge

$$w = 0 \quad M_{nt} = 0 \quad (II.38)$$

$M_{nt} = 0$ Implies $\frac{\partial^2 w}{\partial^2} = 0$, because in equations (II.30) and (II.31) there is no curvature (that is $\frac{\partial^2 w}{\partial^2}$) along the edge of the simply-supported plate because $w = 0$ along that edge.

2.3.2 Clamped edge

$$w = 0 \quad \frac{\partial w}{\partial n} = 0 \quad (II.39)$$

2.3.3 Free edge

For a free edge of a plate, that is, on which there are no loads nor any displacement or slope requirement, it is clear that M_n , Q_n , and M_{nt} all should be zero. However, with classical plate theory only two boundary conditions can be satisfied. This was a major problem for the solid mechanists of the early nineteenth century. Then Kirchhoff brilliantly formulated an approximate solution to the problem which is developed in many texts. He reasoned that for the free edge.

$$M_{nt} = 0$$

Where now, because there is curvature along the edge, the full expressions of equations (II.30), (II.31) must be utilized. The approximate expression for the second boundary condition is

$$V_n = Q_n + \frac{\partial n}{\partial \theta} = 0 \quad (\text{II.40})$$

Where V_n is the ``effective`` shear resultant, and Q_n is given by equation (II.20) or (II.21), M_n is given by equation (II.30) or (II.31), and M_{nt} is given by equation (II.32).

3 Failure criteria [37]

3.1 Hill criterion

One of the first interactive criteria of rupture applied to anisotropic materials was introduced by R.Hill .This criterion can be formulated by stating that the limiting state of constraints of anisotropic materials is not reached, the following inequality shall be verified:

$$F(\sigma_T - \sigma_{T'})^2 + G(\sigma_{T'} - \sigma_L)^2 + H(\sigma_L - \sigma_T)^2 + 2L\sigma_T^2 + 2M\sigma_L^2 + 2N\sigma_L^2 < 1 \quad (\text{II.41})$$

The breaking of a material therefore occurs when the equality is verified, namely:

$$F(\sigma_T - \sigma_{T'})^2 + G(\sigma_{T'} - \sigma_L)^2 + H(\sigma_L - \sigma_T)^2 + 2L\sigma_T^2 + 2M\sigma_L^2 + 2N\sigma_L^2 = 1 \quad (\text{II.42})$$

This equality constitutes the criterion of Hill, relative to the main axes (L, T, and T') of the material.

It can also be put in another form as follows:

$$(G + H)\sigma_L^2 + (F + H)\sigma_T^2 + (F + G)\sigma_{T'}^2 - 2H\sigma_L\sigma_T - 2G\sigma_L\sigma_{T'} - 2F\sigma_T\sigma_{T'} + 2L\sigma_{TT'}^2 + 2M\sigma_{LT'}^2 + 2N\sigma_{LL}^2 = 1 \quad (\text{II.43})$$

The parameters F, G, H, L, M and N are characteristic parallels of the material in question, which are connected to the rupture stresses X, Y and S of the material.

In the case of a tensile (or compression) test in the L direction, Hill's criterion is reduced:

$$G + H = \frac{1}{X^2} \quad (\text{II.44})$$

Where X is the tensile stress (or compression) in the L direction. Similarly, we find:

$$F + H = \frac{1}{Y^2} \quad (\text{II.45})$$

$$F + H = \frac{1}{Z^2} \quad (\text{II.46})$$

Where Y and Z are the tensile (or compressive) tensile stresses in the T and T' directions. In the case of a shear test in the plane (L, T), the Hill criterion reduces to

$$2N = \frac{1}{S_{LT}^2} \quad (\text{II.47})$$

where S_{LT} is the shear stress in the plane (L, T).

$$2M = \frac{1}{S_{LT'}^2} \quad (\text{II.48})$$

$$2L = \frac{1}{S_{T'}^2} \quad (\text{II.49})$$

Where $S_{LT'}$, and $S_{T'}$ are the shear failure stresses, respectively in the planes (L, T') and (T, T').

The expressions (II.A) to (II.F) are used to determine the fracture parameters F, G, L, M, and N and write the Hill criterion in the form:

$$\left(\frac{\sigma_L}{X}\right)^2 + \left(\frac{\sigma_T}{Y}\right)^2 + \left(\frac{\sigma_{T'}}{Z}\right)\left(\frac{1}{X^2} + \frac{1}{Y^2} - \frac{1}{Z^2}\right)\sigma_L\sigma_T\left(\frac{1}{X^2} + \frac{1}{Z^2} - \frac{1}{Y^2}\right)\sigma_L\sigma_{T'}\left(\frac{1}{Y^2} + \frac{1}{Z^2} - \frac{1}{X^2}\right)\sigma_T\sigma_{T'} +$$

$$\left(\frac{\sigma_L}{S_L}\right)^2 + \left(\frac{\sigma_{LT'}}{S_{LT'}}\right)^2 + \left(\frac{\sigma_{T'}}{S_{T'}}\right)^2 = 1 \quad (\text{II.50})$$

It should be noted that the criterion of Hill does not take into account the difference in the behavior of the materials in tension and compression:

In the case of a state of plane stresses in the plane (L; T) of the layer:

$$\sigma_{T'} = \sigma_{LT'} = \sigma_{T'} = 0 \quad (\text{II.51})$$

Hill's criterion is simplified as follows:

$$\left(\frac{\sigma_L}{X}\right)^2 + \left(\frac{\sigma_T}{Y}\right)^2 - \left(\frac{1}{X^2} + \frac{1}{Y^2} - \frac{1}{Z^2}\right)\sigma_L\sigma_T + \left(\frac{\sigma_L}{S_L}\right)^2 = 1 \quad (\text{II.52})$$

3.2 Tsai-hill criterion

The prior rupture criterion in plane stresses has been simplified by V.D AZZI and S.W.Tsai [37] in the case of unidirectional composite materials. Indeed,

In this case: $Z = Y$ and the criterion is written:

$$\left(\frac{\sigma_L}{X}\right)^2 + \left(\frac{\sigma_T}{Y}\right)^2 - \frac{\sigma_L\sigma_T}{X^2} + \left(\frac{\sigma_L}{S_L}\right)^2 = 1 \quad (\text{II.53})$$

This criterion is generally known as the Tsai-hill criterion. In the case of traction or compression outside the main axes. The main constraints are given by the expressions. By deferring these expressions in the relations. Criterion of Tsai-hill is written:

$$\frac{\cos^4 \theta}{X^2} + \left(\frac{1}{S_L^2} - \frac{1}{X^2}\right) \sin^2 \theta \cos^2 \theta + \frac{\sin^4 \theta}{Y^2} = \frac{1}{\sigma^2_x} \quad (\text{II. 54})$$

3.3 Hoffman criterion

A generalization of Hill's criterion, taking into account the difference in the behavior of the materials in tension and compression, was formulated by O. Hoffman [37]

The criterion of Hoffman admits that the rupture of the material occurs when the following equality is verified:

$$C_1(\sigma_T - \sigma_{T'})^2 + C_2(\sigma_{T'} - \sigma_L)^2 + C_3(\sigma_L - \sigma_T)^2 + C_4\sigma_L + C_5\sigma_T + C_6\sigma_{T'} + C_7\sigma_{T'}^2 + C_8\sigma_L^2 + C_9\sigma_L^2 = 1 \quad (\text{II.55})$$

The constants $C_1, C_2, C_3, C_4, C_5, C_6, C_7, C_8$, and C_9 are characteristics of the materials and related to the stresses at break of the materials by the relations:

$$C_1 = \frac{1}{2} \left[\frac{1}{Y_T Y_C} + \frac{1}{Z_T Z_C} - \frac{1}{X_T X_C} \right] \quad (\text{II.56})$$

$$C_2 = \frac{1}{2} \left[\frac{1}{Z_t Z_c} + \frac{1}{X_t X_c} - \frac{1}{Y_t Y_c} \right] \quad (\text{II.57})$$

$$C_3 = \frac{1}{2} \left[\frac{1}{X_t X_c} + \frac{1}{Y_t Y_c} - \frac{1}{Z_t Z_c} \right] \quad (\text{II.58})$$

$$C_4 = \frac{1}{X_t} - \frac{1}{X_c}$$

$$C_7 = \frac{1}{S_T^2}$$

$$C_5 = \frac{1}{Y_t} - \frac{1}{Y_c}$$

$$C_8 = \frac{1}{S_L^2}$$

$$C_6 = \frac{1}{Z_t} - \frac{1}{Z_c}$$

$$C_9 = \frac{1}{S_L^2}$$

In the case of a state of plane stresses in the plane (L, T), the Hoffman criterion is reduced to:

$$\frac{\sigma_L^2}{X_t X_c} + \frac{\sigma_T^2}{Y_t Y_c} - \frac{\sigma_L \sigma_T}{X_t X_c} + \frac{X_c - X_t}{X_t X_c} \sigma_L + \frac{Y_c - Y_t}{Y_t Y_c} \sigma_T + \frac{\sigma_L^2}{S_L^2} = 1 \quad (\text{II. 59})$$

3.4 Tsai-Wu criterion

The Von-Misses criterion, introduced in strength-of-materials courses for studying yielding of metals, can be written as:

$$\frac{((\sigma_1 - \sigma_2)^2 + (\sigma_1 - \sigma_3)^2 + (\sigma_2 - \sigma_3)^2)}{2(\sigma_y)^2} = 1 \quad (\text{II.60})$$

According to the Von-Misses criterion if

$$F(\sigma_1, \sigma_2, \sigma_3) < 1$$

Then the material has not yielded. Equation (II.40) represents the well-known Von-Misses ellipsoid and thus a surface in $\sigma_1 - \sigma_2 - \sigma_3$, principal stress space, and equation (II.41) represent the volume inside this surface. Because rolled metals have slightly different properties in the roll direction than in the other two perpendicular directions, hill assumed that the yield criterion for these orthotropic metals was of the form

$$F((\sigma_1 - \sigma_2)^2 + G(\sigma_1 - \sigma_3)^2 + H(\sigma_2 - \sigma_3)^2 + 2L\tau_{12}^2 + 2M\tau_{13}^2 + 2N\tau_{23}^2 = 1 \quad (\text{II.61})$$

The constants F,G,H and so forth, are related to the yield stresses in the different direction, like σ_y in equation (II.38) and either the 1,2 or 3 direction is aligned with the roll direction. This view of a failure criterion can be extended to composite materials, which are, of course, orthotropic in the principal material coordinate system, by assuming an equation of the form,

$$F(\sigma_1, \sigma_2, \sigma_3, \tau_{12}, \tau_{13}, \tau_{23}) = 1 \quad (\text{II.62})$$

Can be used to represent the failure condition of a composite, while the condition of no failure is given by

$$F(\sigma_1, \sigma_2, \sigma_3, \tau_{12}, \tau_{13}, \tau_{23}) < 1 \quad (\text{II.63})$$

For a state of plane stress, if the power of the stress components is maintained at 2, as in equation (II.43) and (II.44), the most general form of F is

$$F(\sigma_1, \sigma_2, \sigma_3) = F_1\sigma_1 + F_2\sigma_2 + F_6\tau_{12} + F_{11}\sigma_1^2 + F_{22}\sigma_2^2 + F_{66}\tau_{12}^2 + 2F_{12}\sigma_1\sigma_2 + 2F_{16}\sigma_1\tau_{12} + 2F_{26}\sigma_2\tau_{12} \quad (\text{II.64})$$

Where in the above $F_1, F_2, F_6, F_{11}, F_{22}, F_{66}, F_{12}, F_{16}$ and F_{26} are constants. With the above consideration, the failure criterion that we are seeking takes the form:

$$F_1\sigma_1 + F_2\sigma_2 + F_6\tau_{12} + F_{11}\sigma_1^2 + F_{22}\sigma_2^2 + F_{66}\tau_{12}^2 + 2F_{12}\sigma_1\sigma_2 + 2F_{16}\sigma_1\tau_{12} + 2F_{26}\sigma_2\tau_{12} = 1 \quad (\text{II.65})$$

And the condition of no failure is given by the inequality

$$F_1\sigma_1 + F_2\sigma_2 + F_6\tau_{12} + F_{11}\sigma_1^2 + F_{22}\sigma_2^2 + F_{66}\tau_{12}^2 + 2F_{12}\sigma_1\sigma_2 + 2F_{16}\sigma_1\tau_{12} + 2F_{26}\sigma_2\tau_{12} < 1 \quad (\text{II.66})$$

Where $F_6=F_{16}=F_{26}=0$

$$F_{12} = -1/2 (F_{11} F_{22})^{1/2} \quad (\text{II.67})$$

Using this relation for composite materials, the Tsai-Wu criterion becomes:

$$F_1 \sigma_1 + F_2 \sigma_2 + F_1 \sigma_1^2 + F_2 \sigma_2^2 + F_6 \tau_1^2 - \sigma_1 \sigma_2 (F_1 F_2)^{1/2} = 1 \quad (\text{II.68})$$

Where

$$F_1 = (1/\sigma_1^T) + (1/\sigma_1^C)$$

$$F_2 = (1/\sigma_2^T) + (1/\sigma_2^C)$$

$$F_{11} = 1/\sigma_1^T \sigma_1^C$$

$$F_{22} = 1/\sigma_2^T \sigma_2^C$$

$$F_{66} = (1/\tau_1^F)^2$$

4 Anisotropic- Orthotropic

In this section, information on anisotropy-orthotropic will be given. Orthotropic is an important concept not only the core material but also the face sheets may shows orthotropic behavior. Honeycomb cores are highly orthotropic materials.

The generalized Hooke's law that relates the stresses to strains can be written as:

$$\sigma_i = C_{ij} \cdot \varepsilon_j \quad i, j=1 \dots 6$$

C_{ij} is the stiffness matrix and it has 36 constants . however, it can be easily shown that less than 36 of the constants are independent for elastic material. In fact, the elastic stiffness matrix is symmetric and it has only 21 independent constant [50]

$$\begin{Bmatrix} \sigma_1 \\ \sigma_2 \\ \sigma_3 \\ \tau_2 \\ \tau_3 \\ \tau_1 \end{Bmatrix} = \begin{bmatrix} C_1 & C_1 & C_1 & C_1 & C_1 & C_1 \\ C_2 & C_2 & C_2 & C_2 & C_2 & C_2 \\ C_3 & C_3 & C_3 & C_3 & C_3 & C_3 \\ C_4 & C_4 & C_4 & C_4 & C_4 & C_4 \\ C_5 & C_5 & C_5 & C_5 & C_5 & C_5 \\ C_6 & C_6 & C_6 & C_6 & C_6 & C_6 \end{bmatrix} \cdot \begin{Bmatrix} \varepsilon_1 \\ \varepsilon_2 \\ \varepsilon_3 \\ \gamma_2 \\ \gamma_3 \\ \gamma_1 \end{Bmatrix} \quad (\text{II.69})$$

Equation (II.69) is the most general expression for linear elasticity. In fact, this equation defines the stresses-strain relationship of anisotropic materials. An anisotropic

material is the one that exhibits material properties that are directionally independent, i.e., a given material property can have different values in different direction [51].

Unlike anisotropic materials, orthotropic materials show symmetric material properties. If there are two orthogonal planes of materials property symmetry for a material, symmetry will exist relative to a third mutually orthogonal plane.

This defines an orthotropic material [52]. The independent elastic coefficient reduces to 9 for an orthotropic material.

The stress-strain relations for an orthotropic material are given by:

$$\begin{Bmatrix} \sigma_1 \\ \sigma_2 \\ \sigma_3 \\ \tau_2 \\ \tau_3 \\ \tau_1 \end{Bmatrix} = \begin{bmatrix} C_1 & C_2 & C_3 & 0 & 0 & 0 \\ C_1 & C_2 & C_2 & 0 & 0 & 0 \\ C_1 & C_2 & C_3 & 0 & 0 & 0 \\ 0 & 0 & 0 & C_4 & 0 & 0 \\ 0 & 0 & 0 & 0 & C_5 & 0 \\ 0 & 0 & 0 & 0 & 0 & C_6 \end{bmatrix} \cdot \begin{Bmatrix} \varepsilon_1 \\ \varepsilon_2 \\ \varepsilon_3 \\ \gamma_2 \\ \gamma_3 \\ \gamma_1 \end{Bmatrix} \quad (\text{II.70})$$

The stiffness coefficients in equation (II.70) C_{ij} for an orthotropic material may be expressed in terms of engineering constants by [51]:

$$C_{11} = \frac{1 - \nu_2 \nu_3}{E_2 E_3} \quad (\text{II.71})$$

$$C_{12} = \frac{\nu_1 + \nu_3 \nu_2}{E_2 E_3} = \frac{\nu_1 + \nu_2 \nu_3}{E_1 E_2} \quad (\text{II.72})$$

$$C_{13} = \frac{\nu_3 + \nu_2 \nu_3}{E_2 E_3} = \frac{\nu_1 + \nu_1 \nu_2}{E_1 E_2} \quad (\text{II.73})$$

$$C_{22} = \frac{1 - \nu_1 \nu_3}{E_1 E_3} \quad (\text{II.74})$$

$$C_{23} = \frac{\nu_3 + \nu_1 \nu_3}{E_1 E_3} = \frac{\nu_2 + \nu_2 \nu_1}{E_1 E_3} \quad (\text{II.75})$$

$$C_{33} = \frac{1 - \nu_1 \nu_2}{E_1 E_2} \quad (\text{II.76})$$

$$C_{44} = G_{23} \quad (\text{II.77})$$

$$C_{55} = G_{13} \quad (\text{II.78})$$

$$C_{66} = G_{12} \quad (\text{II.79})$$

$$\nu = \frac{1 - \nu_1 \nu_2 - \nu_2 \nu_3 - \nu_3 \nu_1 - 2\nu_2 \nu_3 \nu_1}{E_1 E_2 E_3} \quad (\text{II.80})$$

5 Calculation of the elastic constants of orthotropic material

As figured in the previous section, there are 9 constant to be determined in order to construct the stiffness matrix of an orthotropic material. Since the honeycomb core will be modeled as an orthotropic material, the calculation of these constants is very crucial. The coefficient are functions of engineering constants, and they are given in equations (II.71) to (II.79).

Therefore, to determine these coefficients, the following 9 engineering constants are needed:

* E_1, E_2, E_3

* ν_1, ν_{13}, ν_2

* G_{12}, G_{13}, G_{23}

The suffixes of the constants represent the axis system that is given in figure (II.1) [honeycomb axis system] for a honeycomb core.

There have been various studies investigating one or more of these constants, but it is hard to find a study which gives the complete set of nine elastic constants for a honeycomb core material Masters and Ivans [52] developed a theoretical model for predicting E_1, E_2, ν_1, G_1 in 2D. they studied flowing, hinging and stretching mechanisms. They considered both regular honeycomb cells and re-entrant honeycomb cells. After

separately investigating the three mechanisms they combined the results to get a general model that includes the three models.

Qunli Lin [53] gave the calculation for E_3 , G_{13} , and G_{23} . Abd-el-Sayed, Jones, and Burger [54] Concentrated on E_1 , E_2 , ν_1 in 2D. In their work, they also considered the effect of filling the honeycomb cell with a low modulus infill. Prior to that, they solved the mechanical properties of unfilled honeycomb. When F_1 and F_2 (in plan forces) are applied to the cell, the double thickness members (where the two strips are glued) remain straight and parallel to each other whereas the single members deform elastically with points contra flexure at their mid-lengths. Displacements in both directions are calculated and then Poisson's ratio and Young's modulus are calculated.

Grediac [55] and Shi & Tong [56] separately worked on the calculation of G_{13} , G_{23} , they both continued on the studied of Kelsey & Al [57]. Grediac used a quarter portion of a cell and, using the symmetries of the honeycomb, calculated the shear modulus using FEM.

Shi & Tong used the two scale method of homogenization of periodic media and later also performed FEM studies. Becker [58] formed the E_1 , E_2 , ν_1 , ν_3 , G_1 while considering the core thickness effect.

Zhang and Ashby [59] gave the formulas for E_3 , ν_3 , ν_1 , G_1 , G_2 . They analyzed the collapse behavior in the out of plane direction. Buckling, deboning, and fracturing are identified as possible failure mechanisms.

E. Nast [60] performed a study similar to those of abd-El Sayed, Jones, and Burgess. Nast applied different boundary conditions in order to get the constants and finally managed to get a set all 9 elastic constants.

In the following sub-section, sample derivations of the equivalent elastic constants for a honeycomb core will be described to give in sight to the typical procedures used in the literature.

4.1 Calculation of E_3 [60]

Of all the constants E_3 calculation is the most direct one. This is a generally accepted calculation and there is no other approach that conflicts with this one. The calculation of E_3 basically depends on the equivalent area, equal displacement concept. Reconsider the unit honeycomb cell given in figure (II.5), a honeycomb cell is a thin walled structure and therefore its cross section area can be calculated by:

$$A_{hc} = 8 * a * t_c \quad (II.81)$$

In the figure, the basic parameters of a honeycomb are shown, d is the cell size, a is the edge length, t_c is the wall thickness, L is the length and W is the width, and h_c is the height of the unit cell. If the cell forms a regular hexagonal then it is called “regular cell”. It is the most common cell type, although irregular honeycomb can also be found. For a regular honeycomb cell figure (II.6), the following relations hold

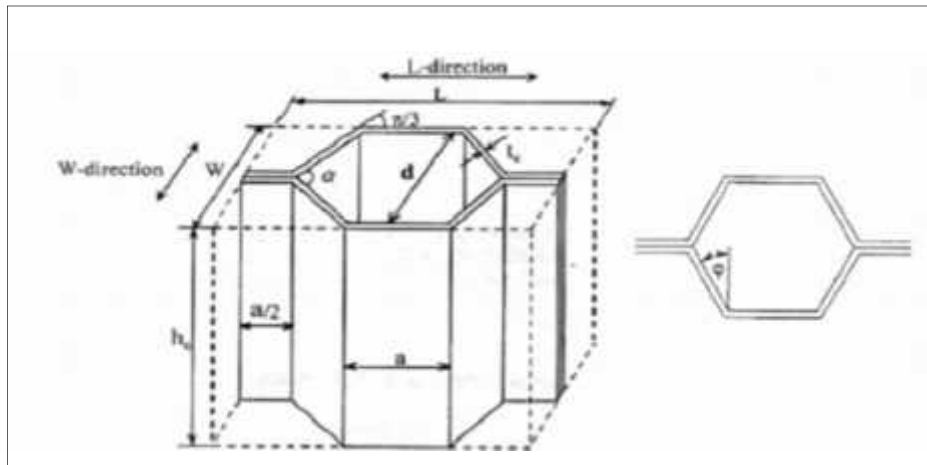


Figure. II. 2 Unit cell of honeycomb [60]

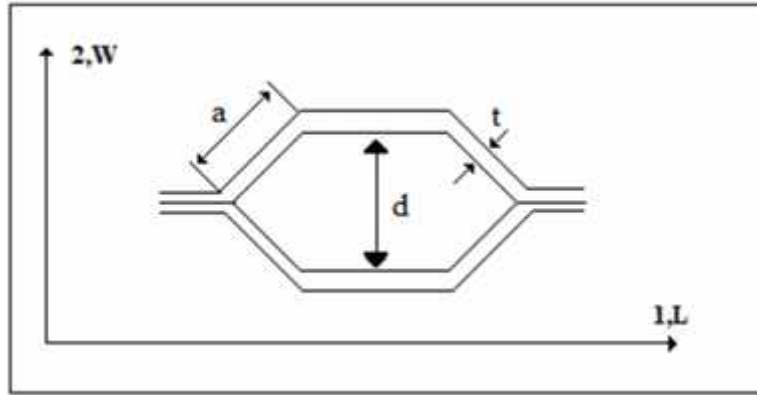


Figure. II. 3 Regular honeycomb core [60]

$$\varphi = \frac{a}{d} = \frac{\pi}{4} \quad (\text{II.82})$$

Where: $a = d \cdot \tan(\varphi)$

$$L = 2 \cdot (a + a \cdot \sin(\varphi)) \quad (\text{II.83})$$

$$w = d + 2 \cdot t_c \quad (\text{II.84})$$

From figure (II.5), the corresponding area for the rectangular prism is

$$A_3 = L \cdot w \quad (\text{II.85})$$

Where:

$$L = 2 \cdot (a + a \cdot \cos \varphi)$$

$$W = 2 \cdot a \cdot \sin \varphi$$

And

$$\varphi = \pi/4$$

$$A_3 = (2d + 2d \cos \varphi) \cdot 2 \cdot d \sin \varphi \quad (\text{II.86})$$

$$A_3 = 4d^2 \cdot \sin \varphi \cdot (1 + \cos \varphi) \quad (\text{II.87})$$

$$\frac{A_{hc}}{A_3} = \frac{2.t_c}{d.(1+c)s} \quad (II.88)$$

Now, we can calculate the equivalent modulus of elasticity. Let's assume that both of the two blocks (unit honeycomb cell and equivalent prism) are loaded by F in transverse direction (3rd direction). For an equivalent model, the deflections, we can get the equivalent E , after the following steps:

$$\varepsilon_{hc} = \frac{\sigma_{hc}}{E_{hc}} = \frac{F}{A_{hc}E_{hc}} \quad (II.89)$$

Similarly:

$$\varepsilon_3 = \frac{\sigma_3}{E_3} = \frac{F}{A_3E_3} \quad (II.90)$$

It is important to note that the height of both is the same, hence, if we want to have equal deflection, we must have equal strains and therefore equation (II.88) must be satisfied in order to have an equivalent modulus.

$$A_{hc} \cdot E_{hc} = A_3 \cdot E_3 \quad (II.91)$$

The equivalent elastic modulus E_3 can be calculated as in equation (II.92)

$$E_3 = \frac{A_{hc}}{A_3} E_{hc} \quad (II.92)$$

If we plug-in the A_{hc}/A_3 ratio from equation (II.91), (II.92), we get

$$E_3 = \left[\frac{2.t_c}{d.(1+c)s} \right] E_{hc} \quad (II.93)$$

Or

$$E_3 = \left[\frac{2.t_c}{d.(1+c)s} \right] \left(\frac{t_c}{d} \right)$$

4.2 Calculation of E_1 & E_2

The calculation of the in-plane equivalent elastic moduli for a honeycomb core will be demonstrated based on the work of Nast [60].

According to Nast, calculation of E_1 and E_2 depend on the fact that in-plane loading, horizontal walls do not deform, whereas diagonal walls deform. (figure.II.4) shows the horizontal and diagonal walls of typical honeycomb cores. Thus, the deformation of the walls can be reduced to the problem of solving a plate equation [60].

$$w_{,x} = 0 \quad (II.94)$$

In the first load case, an external stress σ_2 with respect to the whole projected cross-section is applied in the second direction, and the central point is assumed to be clamped. The other end of the plate is assumed to have a rotation and the external stress is applied as a shear force boundary condition. Thus, the following boundary conditions are applied:

$$w(x = 0) = 0 \quad (II.95)$$

$$w_{,x}(x = 0) = 0 \quad (II.96)$$

$$w_{,x}(x = a) = 0 \quad (II.97)$$

$$w_{,x}(x = a) = -\frac{\sigma_2}{k} a (1 + \sin(\varphi)) \sin(\varphi) \quad (II.98)$$

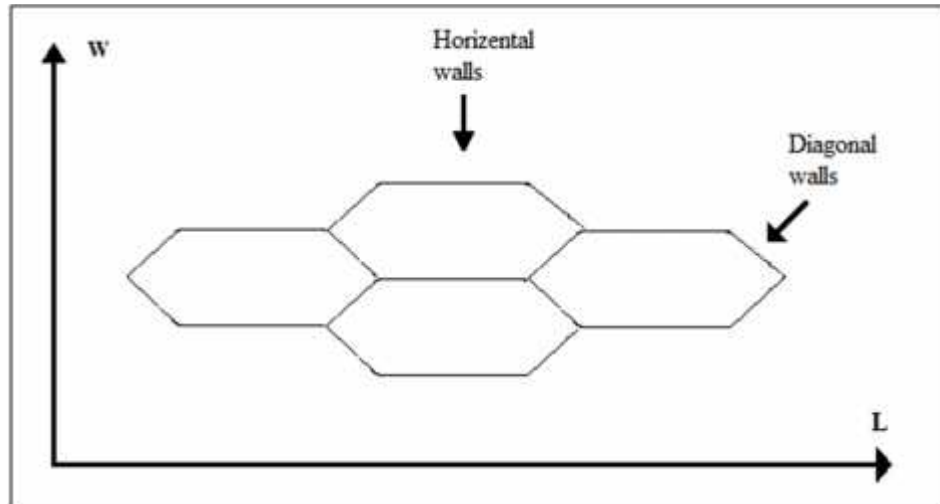


Figure. II. 4 Walls of honeycomb [60]

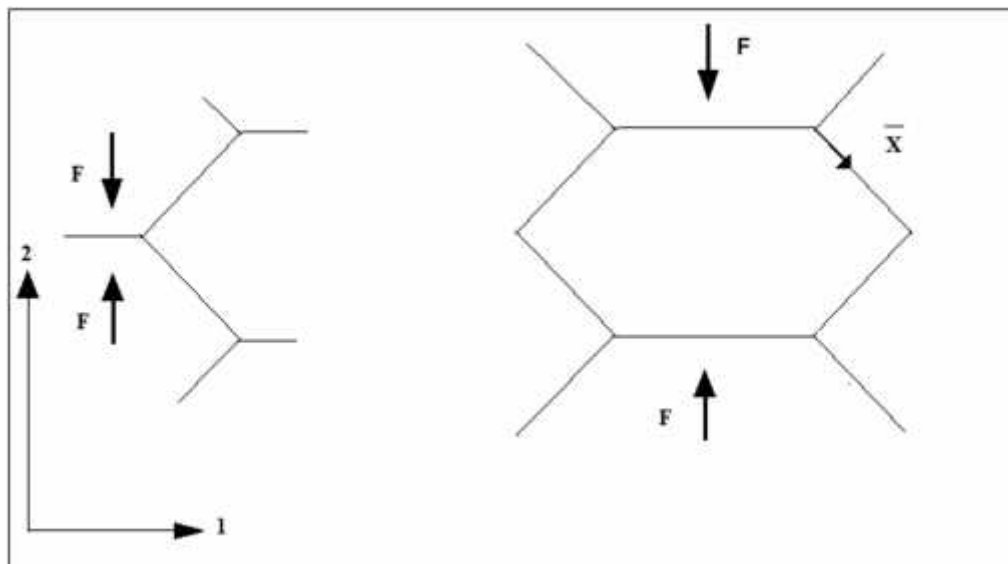


Figure. II. 5 Deformation in 2nd directions [60]

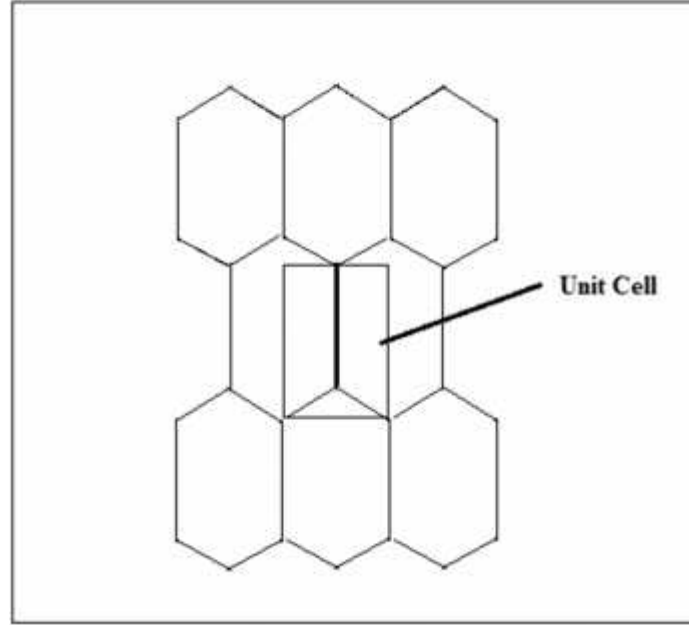


Figure. II. 6 Idealized unit cell [60]

Where k is the plate stiffness and it is equal to:

$$K = \frac{E_{hc} t^3}{12(1-\nu_{hc})} \quad (\text{II.99})$$

(x) is the plate coordinate with its origin at the intersection point of diagonal walls (figure.II.8).

Integrating the plate equation in equation (II.91) four times gives:

$$W(x) = C_1 \frac{x^2}{6} + C_2 \frac{x^2}{2} + C_3 x + C_4 \quad (\text{II.100})$$

From the first boundary condition equation (II.95)

$$W(x=0) = 0 \quad C_4 = 0 \quad (\text{II.101})$$

From the first boundary condition equation (II.93)

$$W'(x=0) = 0 \quad C_3 = 0 \quad (\text{II.102})$$

From the second boundary condition equation (II.97)

$$W(x=0) = 0 \quad w(x=0) = C_1 \cdot a^2/2 + C_1 \cdot a = 0 \quad (\text{II.103})$$

$$C_1 = -2 C_2/a \quad (\text{II.104})$$

From the fourth boundary condition equation (II.104)

$$w_x(x=a) = -\frac{\sigma_2}{K} a(1 + \sin \varphi) \cdot \sin \varphi \quad (\text{II.105})$$

$$C_1 = -\frac{\sigma_2}{K} a(1 + \sin \varphi) \sin \varphi \quad (\text{II.106})$$

From equation (II.104) and (II.105)

$$C_2 = \frac{\sigma_2}{2K} a(1 + \sin \varphi) (\sin \varphi) \quad (\text{II.107})$$

Then equation (II.100) becomes:

$$w_x = -\frac{\sigma_2}{K} a(1 + \sin \varphi) \sin(\varphi) \frac{x^3}{6} + \frac{\sigma_2}{2K} (1 + \sin \varphi) \sin(\varphi) \frac{x^3}{2} \quad (\text{II.108})$$

$$\varepsilon_2 = \frac{D_1}{O} \frac{\text{in the } S_1}{l_0} \frac{d}{h} \quad (2) \quad (\text{II.109})$$

$w(x)$ gives the displacement in x coordinate, therefore we need to find its components in 2 direction. Since we are dealing only with the upper section of the cell, original length is half of the cell size. Hence,

$$\varepsilon_2 = \frac{\sigma_2}{E_2} = \frac{w(x=a) \cdot \sin \varphi}{a \cdot \cos \varphi} \quad (\text{II.110})$$

$$E_2 = \frac{\sigma_2 \cdot a \cdot \cos \varphi}{w(x=a) \cdot \sin \varphi} \quad (\text{II.111})$$

If we replace in equation (II.108) with $(x = a)$ we get:

$$E_2 = \frac{\sigma_2 \cdot a \cdot \cos \varphi}{-\frac{\sigma_2}{K} a(1 + \sin \varphi) \sin \varphi \frac{a^3}{6} + \frac{\sigma_2}{2K} (1 + \sin \varphi) \sin \varphi \frac{a^3}{2} \sin \varphi} \quad (\text{II.112})$$

Using equation (II.108), equation (II.112) becomes:

$$E_2 = \frac{t^3 \cdot \cos^2(\varphi)}{(1 + \sin^2(\varphi)) a^3 \cdot \sin^2(\varphi) \cdot (1 - \cos^2(\varphi))} \cdot E_{hc} \quad (\text{II.113})$$

Thus, equation (II.114) gives the equivalent modulus of the honeycomb core in the 2 direction.

Similar procedure is followed for the calculation of E_1 .

Based on the microscopic view of the deformation of the unit cell and the finite element modeling of the unit cell, Nast [60] proposed the boundary conditions, given by equations (II.108), (II.115) for calculation of E_1 .

In the second load case, an external stress σ_1 with respect to the whole projected cross section is applied in the 1 direction.

$$w(x = 0) = 0 \quad (\text{II.114})$$

$$w_x(x) = 0 \quad (\text{II.115})$$

$$w_x(x = a) = -\frac{\sigma_1}{k} \cdot a \cdot \cos^2(\varphi) \quad (\text{II.116})$$

$$w(x = a) = -\frac{\sigma_1}{k} \cdot a^2 \cdot \frac{\cos^2(\varphi)}{4} \cdot (1 + \cos(\varphi)) \quad (\text{II.117})$$

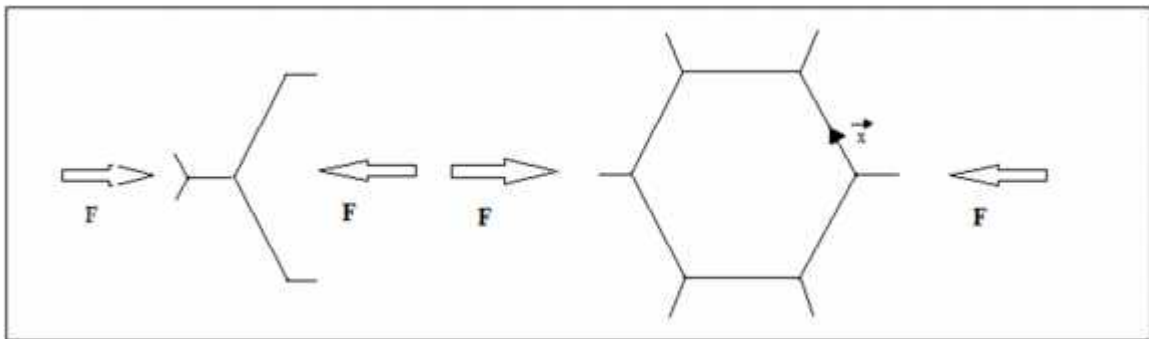


Figure. II. 7 deformation in 1st direction [60]

If we re-call equation (II.107) and apply the first and second boundary conditions equation (II.113) and equation (II.114) we get:

$$C_3 = 0$$

$$C_4 = 0$$

From the third boundary condition equation (II.116)

$$C_1 = -\frac{\sigma_1}{k} \cdot a \cdot \cos^2 \varphi \quad (\text{II.118})$$

From the fourth boundary condition equation (II.118)

$$w_{\bar{x}}(x = a) = C_1 \cdot a + C_2 \quad (\text{II.119})$$

$$C_2 = \frac{\sigma_1}{k} \cdot a^2 \cdot \left(-\frac{\cos^3(\varphi) + 3 \cos^2(\varphi)}{4} \right) \quad (\text{II.120})$$

Hence, equation (II.73) for the second case becomes:

$$w(x) = -\frac{\sigma_1}{k} \cdot a \cdot \cos^2(\varphi) \frac{x^3}{6} + \frac{\sigma_1}{k} \cdot a^2 \cdot \left(\frac{-\cos^3(\varphi) + 3 \cos^2(\varphi)}{4} \right) \frac{x^2}{6} \quad (\text{II.121})$$

$$\varepsilon_1 = \frac{Dl}{a} \frac{dw}{dx} \quad (1) \quad (\text{II.122})$$

Once again, $w(x)$ gives the displacement in the x coordinate, therefore, we need to find its component in 1 direction.

Hence:

$$\varepsilon_1 = \frac{w(x) \cdot \cos(\varphi)}{a \cdot (1 + \sin(\varphi))} = \frac{\sigma_1}{E_1} \quad (\text{II.123})$$

$$E_1 = \frac{\sigma_1 \cdot a \cdot (1 + \sin(\varphi))}{\left[\frac{\sigma_1}{k} \cos^2(\varphi) \frac{a^4}{6} + \frac{\sigma_1}{k} \left(\frac{-\cos^3(\varphi) + 3 \cos^2(\varphi)}{4} \right) \frac{a^4}{2} \right] \cos(\varphi)} \quad (\text{II.124})$$

Rearranging:

$$E_1 = \frac{r^3(1+s(\varphi))}{1 - a^3 \cdot c^2(\varphi) \left(\frac{5c(\varphi)-3}{2} \right)} \cdot \frac{E_{hc}}{(1-\vartheta_{hc}^2)} \quad (\text{II.125})$$

4.3 Calculation of ϑ_1 , ϑ_1 , ϑ_2

Poisson`s ratio is defined as follow:

$$\vartheta_1 = -\varepsilon_2 / \varepsilon_1 \quad (\text{II.126})$$

Then, by using equations (II.115) and (II.123), we can calculate ϑ_1 :

$$\vartheta_1 = \frac{\sigma_2 / E_2}{\sigma_1 / E_1} = \frac{\sigma_2}{\sigma_1} \cdot \frac{E_1}{E_2} \quad (\text{II.127})$$

In order to obtain the Poisson`s ratio ϑ_1 , we need to calculate the σ_2 / σ_1 ratio. The applied force is the same for both cases. Therefore, σ_2 / σ_1 reduced to the ratio of areas that the F force is applied.

call height is the same for both cases, therefore, from figure (II.6) and figure (II.7) the area ratio is obtained as follow:

$$\frac{\sigma_2}{\sigma_1} = \frac{F/A_2}{F/A_1} = \frac{A_1}{A_2} = \frac{c(\varphi)}{(1+s(\varphi))} \quad (\text{II.128})$$

If we re-call equation (II.119) and plug-in equation (II.114) and equation (II.118) and equation (II.120), then we make simplification we obtain:

$$\vartheta_1 = \frac{(1+s(\varphi)) s^2(\varphi)}{1 - c^2(\varphi) \left[\frac{\cos(\varphi)}{3} - \frac{1-c(\varphi)}{8} \right]} \quad (\text{II.129})$$

There is also an upper limit for a positive definite stiffness matrix:

$$\nu_1 = \sqrt{E_1/E_2} \quad (\text{II.130})$$

If the value obtained from equation (II.130) is bigger than the result from equation (II.131), then, the second one should be used.

Zhang & Ashby [59] stated that the Poisson's ratios ν_1 and ν_2 are simply equal to those for the solid core it-self, and we have: $\nu_1 = \nu_2 = \nu_{hc}$.

The Poisson's ratios ν_1 and ν_2 can be found using reciprocal relations:

$$\nu_1 = \frac{E_1}{E_3} \nu_{hc} \quad (\text{II.131})$$

$$\nu_2 = \frac{E_2}{E_3} \nu_{hc} \quad (\text{II.132})$$

Since: $E_3 = E_1$ and $E_3 = E_2$ Ashby concluded that:

$$\nu_1 = \nu_2 = \nu_{hc}$$

Nast [60] calculated the Poisson's ratios using equation (II.115), (II, 123), (II.131), and (II.132) in equation (II.101). In this calculation based on the unite cell definition figure (II.6) defined in equation (II.101):

$$\nu_1 = \frac{t^2(s(\varphi)+1)^2}{2 \cdot a^2 \cdot c(\varphi) \left[\frac{c(\varphi)}{3} - \frac{1-c(\varphi)}{E} \right]} \cdot \frac{\nu_{hc}}{(1-\nu_{hc}^2)} \quad (\text{II.133})$$

$$\nu_2 = \frac{t^2 c^2(\varphi)}{2 \cdot a^2 \cdot s^2(\varphi) (1-\nu_{hc}^2)} \quad (\text{II.134})$$

4.4 Calculation of G_1 , G_1 , G_2

Due to the shear deformation, the calculation of G is quite complicated process; in this calculation the vertical and the diagonal parts of the honeycomb are involved.

The details of this calculation process was introduced by Nast [60], and based on his analysis, the shear moduli of the honeycomb core are well predicted by the following equations:

$$G_1 = \frac{t^3(1+s(\varphi))}{a^3c(\varphi)(6.2-6.5s(\varphi))} \cdot \frac{E_{hc}}{(1-\nu_{hc}^2)} \quad (\text{II.135})$$

$$G_1 = \frac{2t}{a.c(\varphi)(1+s(\varphi))} \cdot G_{hc} \quad (\text{II.136})$$

$$G_2 = \frac{1.t}{9.a.c^3(\varphi)(1+s(\varphi))} \cdot G_{hc} \quad (\text{II.137})$$

5 Conclusion:

In this chapter we demonstrated the equations relating to the mechanical behaviour of sandwich structures, some failure criteria, and anisotropic-orthotropic material are presented. In addition the calculation of the elastic constant of orthotropic material are given

Chapter III

Study of honeycomb sandwich plate

1 Introduction

We learned previously that the importance of composite materials and sandwich structures is in their high performance characteristics, and to determine these characteristics there is some procedures to follow and experiments to perform, in this chapter, we are going to see two of the basic experiments used to characterize a sandwich plate: tensile test, and three point flexural test, and a simulation using ANSYS software.

2 Manufacturing of sandwich plate

2.1 Manufacturing process

The manufactures of the plates were made at the level of plastic and composite workshop at Algerian airlines reparation base. We start with the preparation of place and material needed for this process. First we mixes the resin and the hardener at 15/100 ratio (figure.III.1)



Figure. III. 1 preparation of resin (adhesive)

After that, we cut the tissues of carbon (a) and glass fiber (c) and the honeycomb (b) with the desired measurements (100x200 mm), the tissue is deposited on the impregnation layer and then spread another resin layer on each layer (one layer for the carbon tissue (a) and 3 layers for fiber glass tissue (c)). The honeycomb core (b) is placed directly after the last impregnated ply by a layer of resin. Then we put another layer of the tissue (fiber glass (c) or carbon (a)) then spread another resin layer on this fold



a) Carbon fiber texture

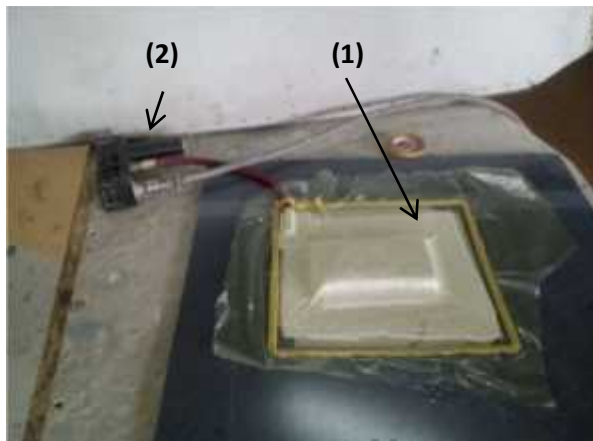
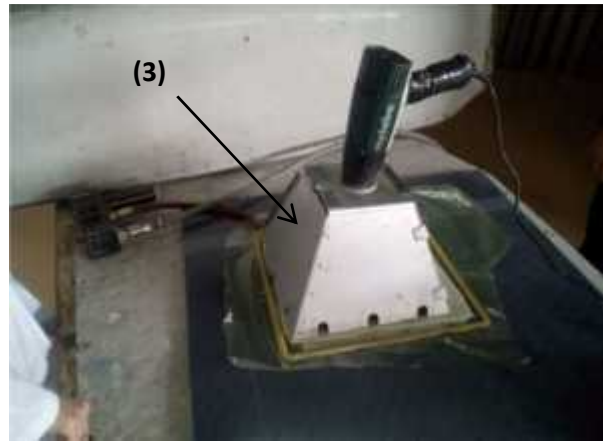
b) Aramide paper (Nomex)
honeycomb core

c) Glass fiber texture

Figure. III. 2 (a), (c), Skins and, (b) core materials

The next step is to cut the tear-off fabric widely enough to cover the sandwich plate and then placed on it and we cut also the absorption fabric in rectangular form which covers the entire previous surface without trespass the sealing tape.

Finally, the vacuum bag system is closed by using the plastic film; the purpose of its use is to seal the system assembly and to achieve the protection of the mold, and to have mostly perfect resin absorption (figure.III.3. (a)), then we put a heat chamber over this system (figure.III.3. (b)).

a) (1) Vacuum bag system
(2) Vacuum pump

b) (3) Heat chamber

Figure. III. 3 Final phase of manufacturing process (a), (b)

2.2 Tensile and bending tests specimens



Figure. III. 5 (a) GFT



Figure. III. 4 GFT- CFT



Figure. III. 6 CFT

- (a) GFT: Glass Fiber Texture faces sheets plate: each face contains 3 layers of GFT.
- (b) GFT-CFT: Glass Fiber Texture and Carbon Fiber Texture faces sheets plate: one face sheet made with 1 layer of CFT, the other one is made with 3 layers of GFT.
- (c) CFT: Carbon Fiber Texture faces sheets plate: each face contains 1 layer of CFT.

Table. III. 1 Dimension of test specimens

Length L (mm)	Width b (mm)	Depth d (mm)
100	30	10

3 Tensile test

Tensile testing is a fundamental material science test in which a sample is subjected to a controlled tension until failure. Properties that are directly measured via a tensile test are ultimate tensile strength, maximum elongation and reduction in area. From these measurements the following properties can also be determined: Young's modulus, Poisson's ratio, yield strength, and strain-hardening characteristics. These characteristics can be determined from stress-strain curve (figure.III.5) obtained from the experimental data.

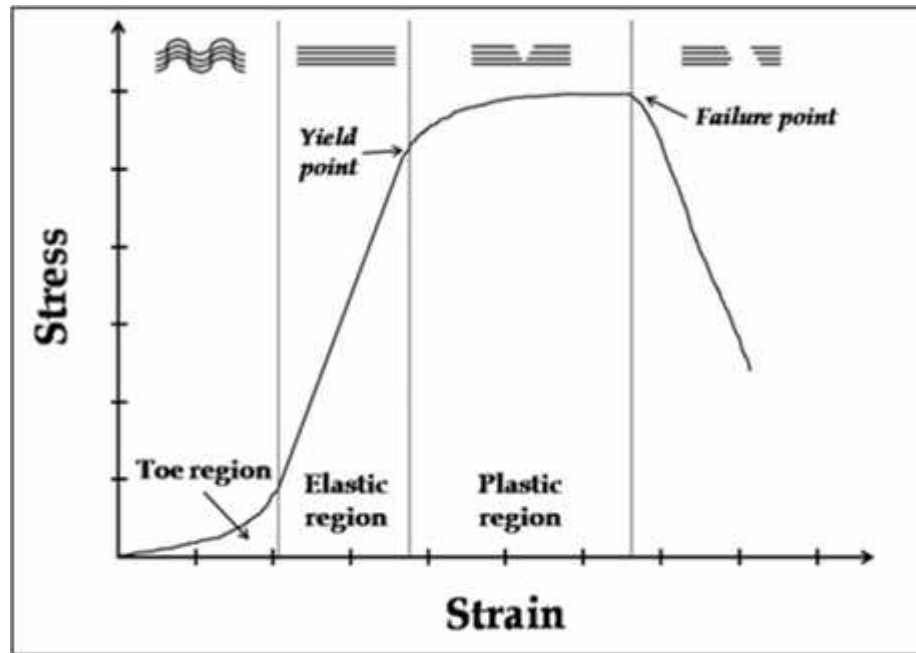


Figure. III. 7 Stress-strain curve

In the following paragraph, we are going to represent three test cases performed in two separate occasions; the first was at the laboratory of mechanics at the higher college of aerial defense of the territory at Reghaia (ESDAT). The second one was at materials science laboratory located at the department of mechanical engineering at HOUARI BOUMEDIENE Sciences and Technology University, but, in this case we putted hills in both ends of the test specimens glued with the adhesive used in patch repairs.

3.1 Tensile experiment process

The tensile test is generally carried out by introducing a test piece into a Universal traction machine (figure.III.6). This machine consists of a flat base and a piston Hydraulic system having a linear motion perpendicular to this same base. Jaws (hydraulic or manual) are located on the piston as well as on the piston based. The latter are installed in such a way that their axes are collinear with that of the piston. Then, once the test piece is inserted into the jaws, the piston is displaced vertically and the axial force required for this displacement is recorded. In addition, strain gauges are glued to the test piece to measure deformations involved in the calculation of the mechanical properties.



Figure. III. 8 HOYTOM universal traction machine

Our work is to recover and process and analyze these Tests using a spreadsheet (Excel) to determine the values of the characteristics Mechanical properties of the 3 test specimens. The maximum force of the test machine is 50 KN, and the test speed is 50 mm/min.

4 Experimental data

4.1 Plate with glass fiber texture faces sheets (GFT)

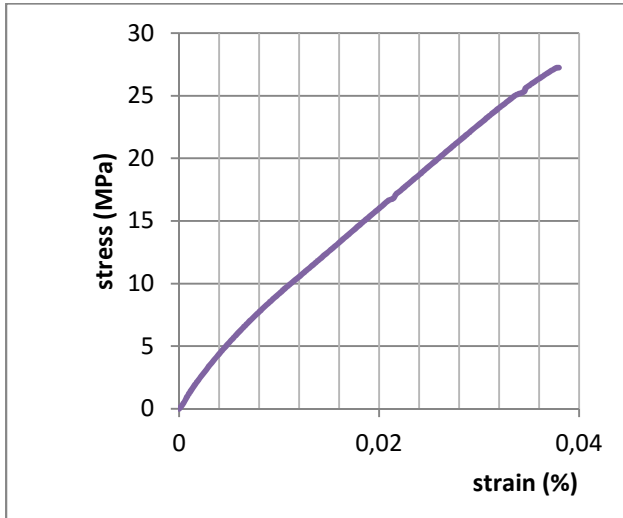


Figure. III. 10 stress-strain curve for first experiment of GFT plate

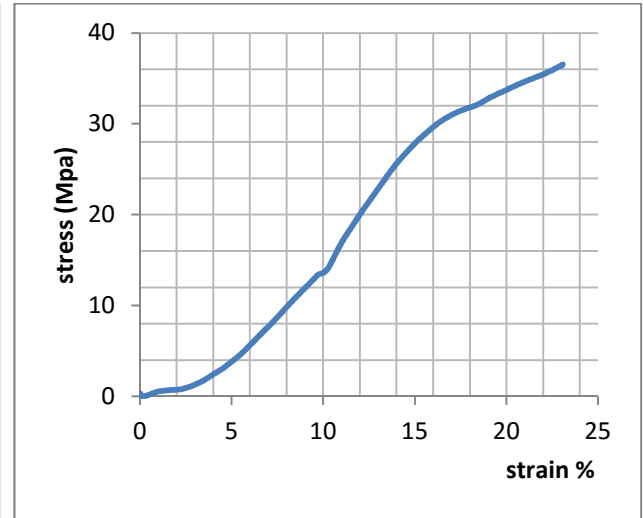


Figure. III. 9 stress-strain curve for the second experiment of GFT plate

From figure III.10 we see that curve is mostly linear, the maximum stress is 27.23 MPa, and the yield stress is 25.2 MPa. The maximum deformation is 3 %. From figure.III.9 we notice that the maximum stress is about 36.54 MPa, and the yield stress 19.42 MPa, and the maximum deformation after the yielding point 23.1%. We also observe a small disturbance at the beginning of the curve; it was due to a small sliding between the grips and the test specimen.

4.2 Plate with glass fiber and carbon fiber textures faces sheets (GFT-CFT)

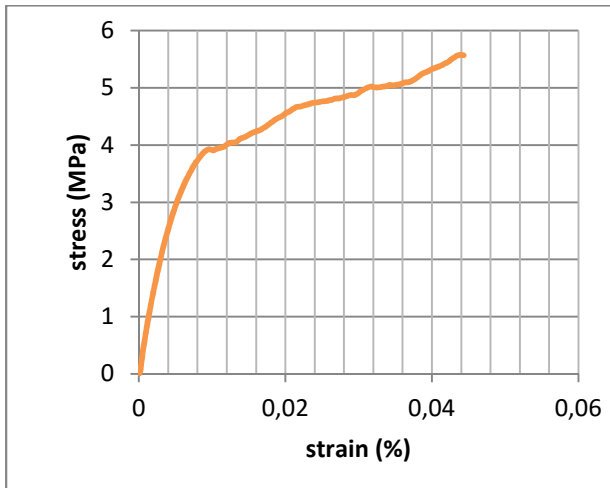


Figure. III. 12 stress-strain curve for the first experiment of GFT-CFT plate

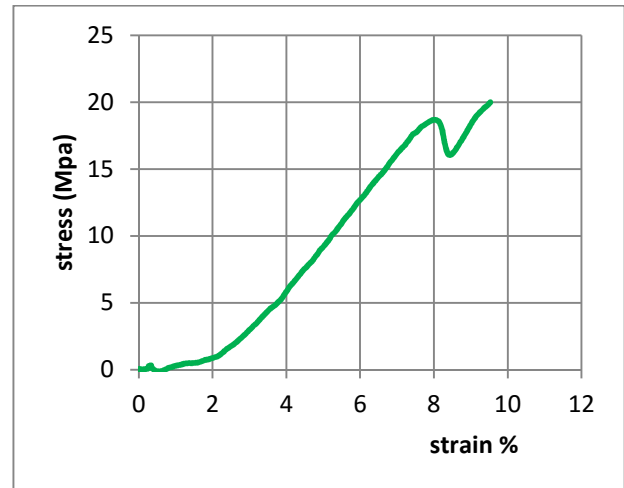


Figure. III. 11 stress-strain curve for the second experiment of GFT-CFT plate.

In the first experiment figure.III.11, the sandwich plate's behavior is divided into two phases, the first is linear until yield stress point which is equal to 3.9 MPa, and the second phase is linear disturbed until maximum stress 5,56 MPa is reached. The maximum deformation is about 4.4 %.

From figure.III.12, we notice the same disturbance at the beginning of the curve for the same reason as the previous specimen, also we notice a reduction in stress 18.3MPa and 17.09MPa then an augmentation in stress which is due to the different faces sheets materials properties, the maximum stress 20.71MPa, the maximum deformation 9.52%.

4.3 Plate with carbon fiber texture faces sheets (CFT)

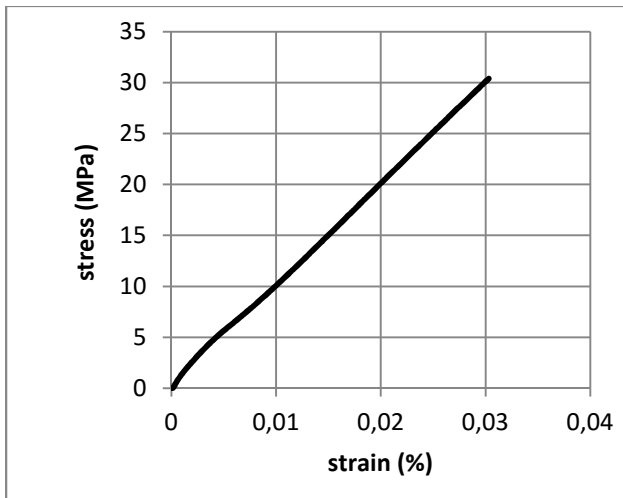


Figure. III. 14 stress-strain curve for the first experiment of CFT plate.

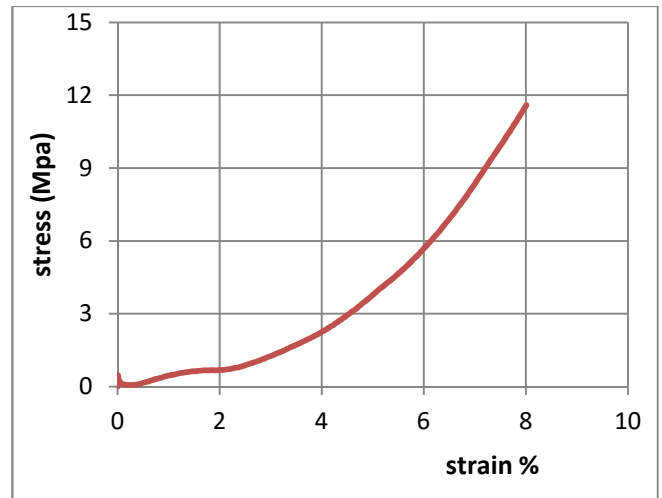


Figure. III. 13 Stress-strain curve for the second experiment of CFT Plate.

In figure III.13, the curve is linear until maximum stress (which is also yield stress) 30.39 MPa, also the maximum strain is 3 %.In figure.III.14 We notice the same disturbance in the beginning of the curve as the previous two cases, we observe that the maximum stress is equal to the yielding stress which is 11.59Mpa; also the maximum strain is 8%. The superior stress value in the first experiment was due to the sliding between grippes and test specimen, but, unlike the previous similar cases, this time the gripping force caused a deformation which results an important augmentation in traction force which in the end results an augmentation in stress value.

From figure III.13, the curves were about the first experiment, we must know from it that some point must be taken in consideration during the experience, here are the major ones:

- The dimension of the sample depends highly on some regulations as: JIS, ASTM, ISO...and also on the type of the machine test.

- When we put the machine gripes on the ends of the sample it may cause non desirable deformation on the honeycomb core as shown in figure III.15 which cause a disturbance in the results.

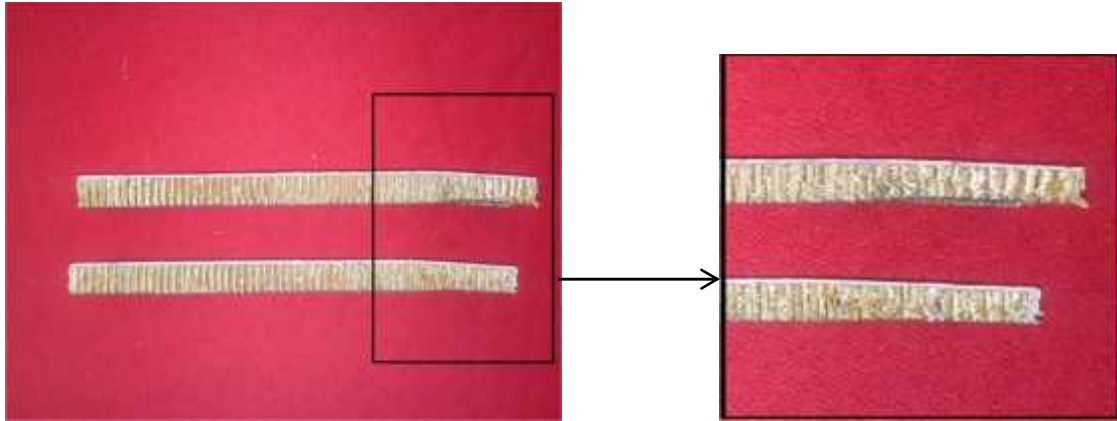


Figure. III. 15 deformation caused by the gripping force of jaws

4.4 Honeycomb core

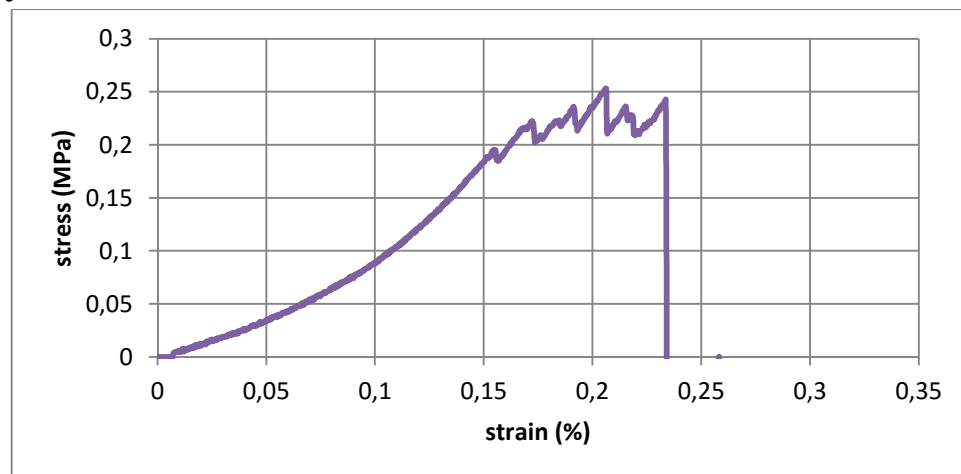


Figure. III. 16 Stress-strain curve for honeycomb core in tensile test

In this figure we have the force by elongation curve for the Nomex honeycomb core. It starts in linear form 0 N until it reaches the value 57 N, from which we notice a multiple disturbance in the force magnitude, then, a massive decrease at the value of stress = 71 N, then, small disturbances to the final rupture. The explanation for the disturbances is that when the cells are deboning in a non-uniform form. The calculation of in-plan characteristics shows that the elasticity modulus of the honeycomb core is very much weaker than the skins materials, which allows us to say that behavior showed by the plates is due to skins properties.

5 Flexural strength

It is also known as modulus of rupture, bend strength, or fracture strength. The flexural strength represents the highest stress experienced within the material at its moment of rupture. It is determined from three points or four points bending tests. When an object formed of a single material, like a wooden beam or steel rod, is bent, it experiences a range of stresses across its depth. At the edge of the object on the inside of the bend (concave face) the stress will be at its maximum compressive stress value. At the outside of the bend (convex face) the stress will be at its maximum tensile value. These inner and outer edges of the beam or rod are known as the “extrem fibers”. For a rectangular cross-section calculation of the flexural stress:

Calculation of the flexural stress:

$$\sigma_f = \frac{3F}{2b} \quad (III.1)$$

Calculation of the flexural strain:

$$\epsilon_f = \frac{6D}{L^2} \quad (III.2)$$

Calculation of flexural modulus

$$E_f = \frac{L^3 m}{4bd^3} \quad (III.3)$$

Where:

F: the applied force (N).

L: the sample length (mm).

b: the sample width (mm).

d: the sample depth (mm).

D: the deflection of the test sample (mm) $D = \frac{FL^3}{4E}$

I: second moment of area (mm⁴). It is defined by: $I = \frac{a^3 b}{12}$

E: Young`s modulus (MPa).

σ_f : Flexural strain (MPa).

ε : Deformation of the sample (%).

M: the gradient (slop) between the initial straight line portion of the load deflection (N/mm).

$$m = \frac{F}{D}$$

ε_f : Flexural deformation.

E_f : Flexural modulus (MPa).

5.1 Three points bending experiment process

The following experiment was performed at UR-PMC at University of Boumerdes.

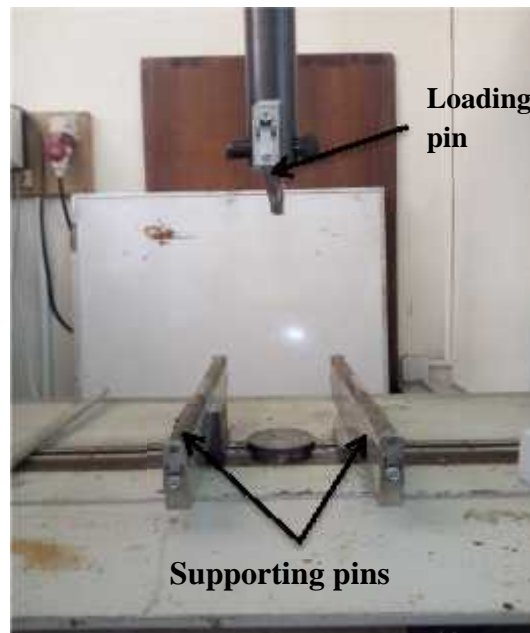


Figure. III. 17 Three points bending test machine

The load pin has a maximum load up to 100KN.

The test speed is 10N/s.

6 Experimental data

6.1 Plate with glass fiber texture faces sheets (GFT)

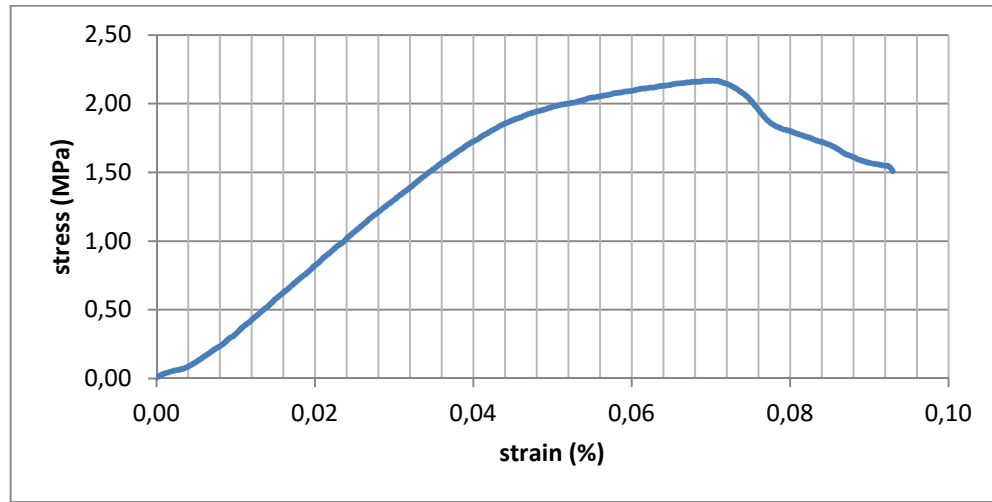


Figure. III. 18 Stress-strain curve for GFT honeycomb sandwich plate

In this figure, we can clearly see that the resistance of the sandwich plate starts to weaken before maximum force applied is reached, and then when fracture occurs, the stress of the plate does not decrease extensively, the maximum stress is about 2.7Mpa and the maximum strain is 7%.

6.2 Plate with glass fiber and carbon fiber textures faces sheets (GFT-CFT)

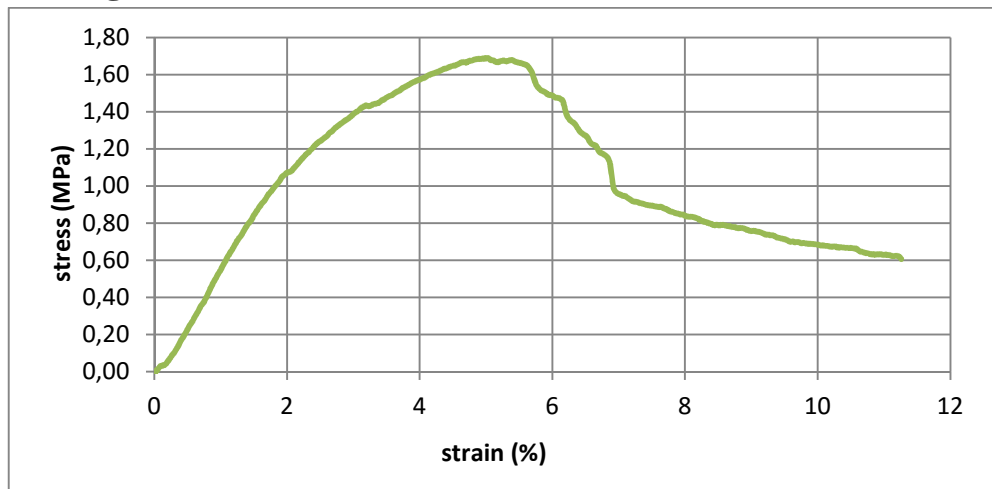


Figure. III. 19 Stress-strain curve for GFT-CFT honeycomb sandwich plate

In this figure III.19 we have the stress-strain curve for GFT-CFT honeycomb sandwich plate. We can notice that the maximum stress is about 1.69% and the maximum strain is 19%.

6.3 Plate with carbon fiber texture faces sheets (CFT)

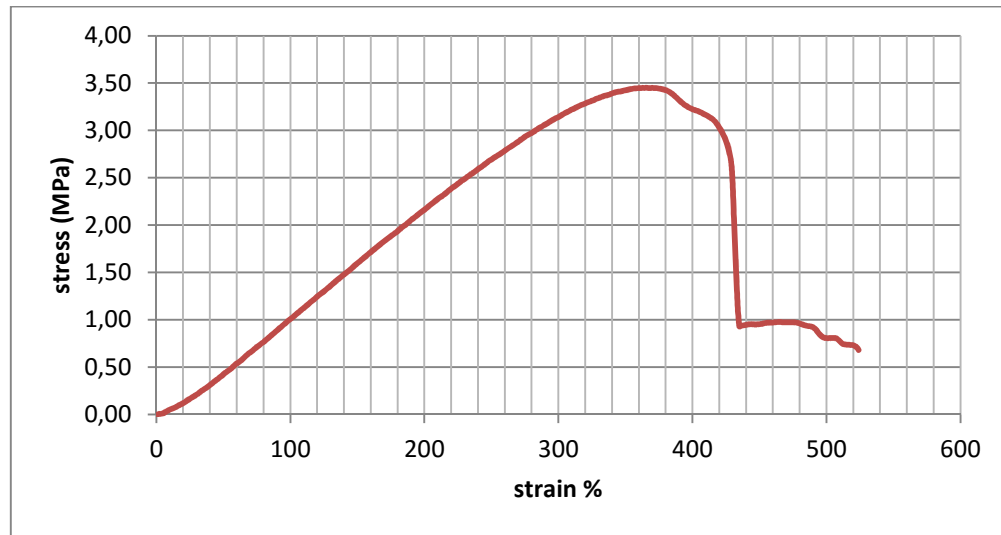


Figure. III. 20 stress strain curve for CFT honeycomb sandwich plate

Figure III.20 is about stress-strain curve for carbon fiber texture (CFT) faces sheets honeycomb sandwich plate. In this curve the maximum stress is 3.45Mpa and the maximum strain 9%.

7 Results and discussion

7.1 Tensile test

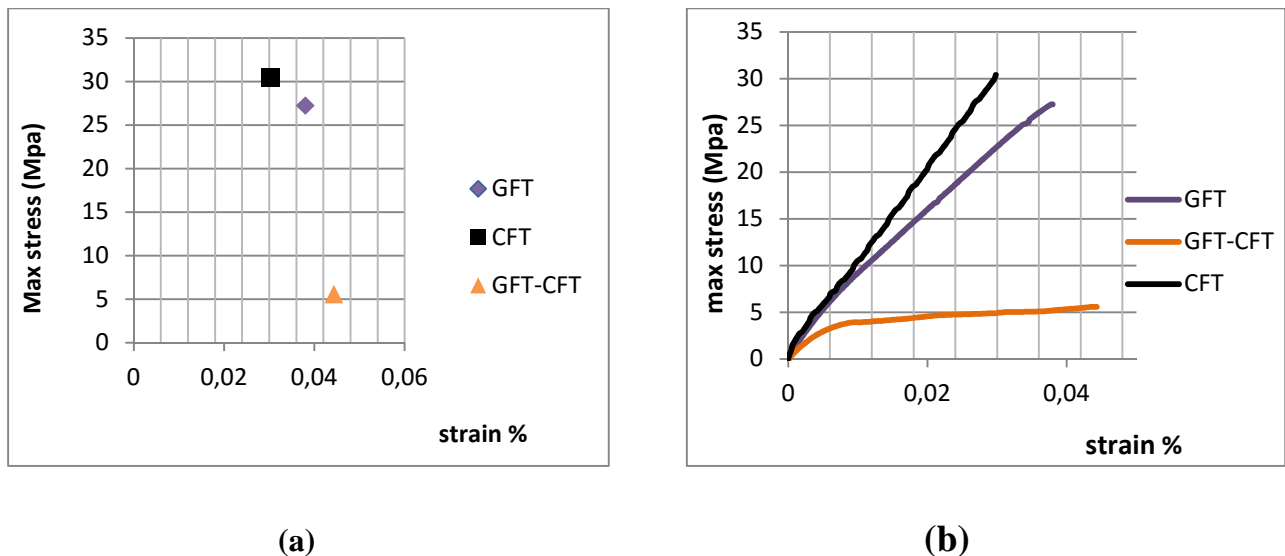
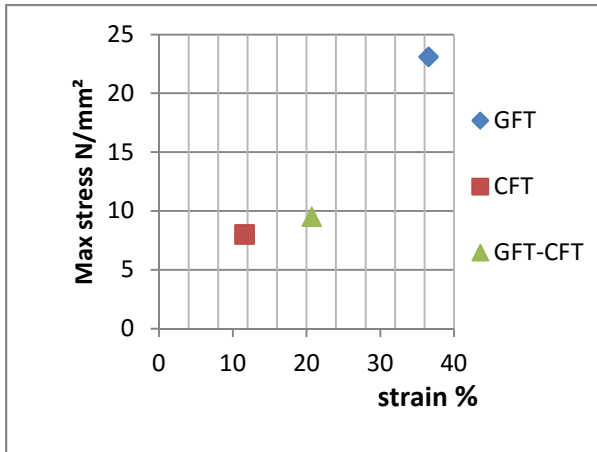
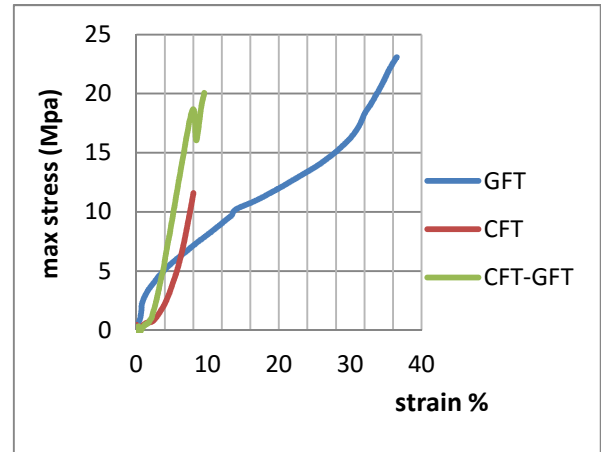


Figure. III. 21 (a),(b) stress by strain curve of the first tensile experiment for the test specimens



(c)



(d)

Figure. III. 22 (c),(d) stress by strain curve of the second tensile experiment for the test specimens

From figures (III.21. (a) and (b)), we can notice that in the first tensile test CFT honeycomb sandwich plate shows a superior resistance comparing with the two other plates but with the smallest value of allowable deformation and the weakest behavior in tension is shown by the plate of GFT-CFT and the biggest deformation comparing to the other plates .

From figures (III.22. (c) And (d)), we can see that in the second tensile test . GFT honeycomb sandwich plate shows a superior resistance (when compare to the other two plates) with the biggest value of allowable deformation which place it as the best plate in tension, and the weakest behavior is shown by the plate with carbon fiber texture face sheets which place it as the unlikely most favorite plate in the performed experiment. The results are numerically calculated following procedure in ISO 527.

Table. III. 2 Characteristics obtained from the first tensile experiment

Test case	$F_{\max}(\text{N})$	σ_m (MPa)	ϵ (%)	E_A (MPa)	G_A (MPa)	θ
GFT	8170	27.23	3.798	7.16	2.68	0.3
GFT-CFT	1673.30	5.57	4.43	1.257	0.471	0.3
CFT	9118	30.39	3.031	10.02	3.75	0.3

Table. III. 3 Characteristics obtained from the second tensile experiment

Test case	F_{\max} (N)	σ_m (MPa)	ε (%)	E_A (MPa)	G_A (MPa)	θ
GFT	12790	36.54	23.1	158.18	60.83	0.3
GFT-CFT	7250	20.71	9.5	218	83.84	0.3
CFT	4060	11.59	8	144.87	55.71	0.3

As we can see from the table, the plate with higher elastic characteristics in plan is from test case 2, which is the sandwich plate with different skins materials and characteristics, and the plate with the largest elongation is from test case one that is the one with both skins made of 3 ply of glass fiber texture. That's leaves us with the last test specimen the one with both skins made of carbon fiber texture, and we can say about it that it is the most stiff plate in our experiment comparing to the other two.

7.2 Three point Bending test

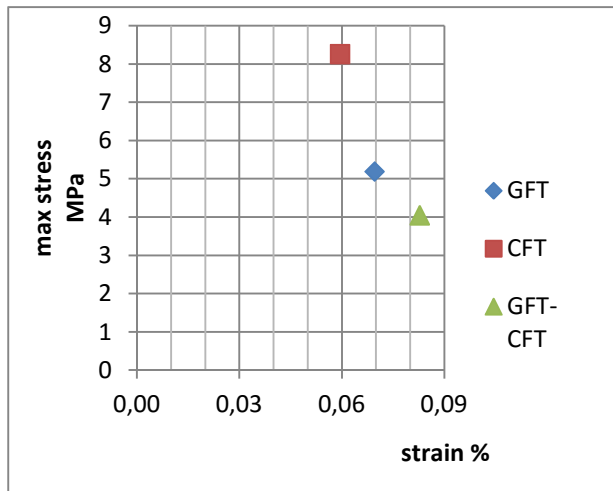


Figure. III. 24 Maximum stress by deformation for bending test specimens

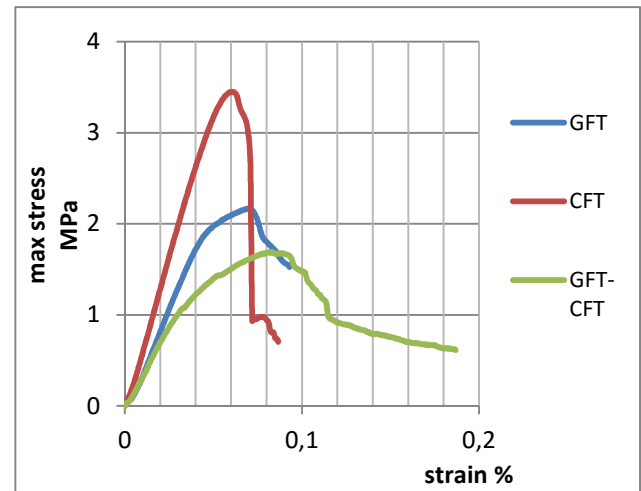


Figure. III. 23 Stress by strain for the bending test of the three specimens

From figures (III.23, 24), the sandwich plate with carbon fiber texture face sheets have the maximum stress and the lowest deformation, comparing to the second test specimen, we notice that it has the maximum deformation between the three plates and the smallest value of stress.

The plate with glass fiber texture face sheets has the middle position in bending test, unlike in the tensile experiment. Also, these figures allows us to notice that the bending behavior is similar and can be described in three phases: the first phase is initial linear elastic behavior followed by a non-linear one in which the maximum loading is achieved. In the last phase, a reduction in the load applied is observed till the total rupture of the samples occurs. The linear behavior corresponds to the work of the skins in traction and compression, whereas, the non-linear behavior mainly depends on the core properties under the effect of shear stress, which also explain the similarity of pattern in figures (*) knowing that our test samples have the similar core material.

Table. III. 4 Flexural characteristics obtained from bending test

Test case	D (mm)	σ_f (MPa)	ε_f (%)	E_f (MPa)
GFT	79.95	5.19	0.47	74.56
GFT-CFT	95.23	4.045	0.57	48.75
CFT	68.34	8.26	0.41	138.75

From the calculated data in table (III.7), we can notice a difference in the behavior of the three test specimens in bending stress, the honeycomb sandwich plate with different face sheets materials has the biggest deflection in the case of three point bending, however, it's flexural elasticity modulus and shear modulus is the weakest comparing to the other two specimens.

The sandwich plate with carbon fiber texture skins material shows the most favorite behavior in bending, even if it has the lowest deflection value between the three plates, the 3rd test specimen has the better flexural characteristic in three point bending test.

8 Simulation

Our analysis are about shear stress in both tensile and three points bending experiments on a honeycomb sandwich panel specimens with the same skins material properties as those used in previous section about the experimental study.

8.1 Tensile test

8.1.1 GFT (glass fiber texture)

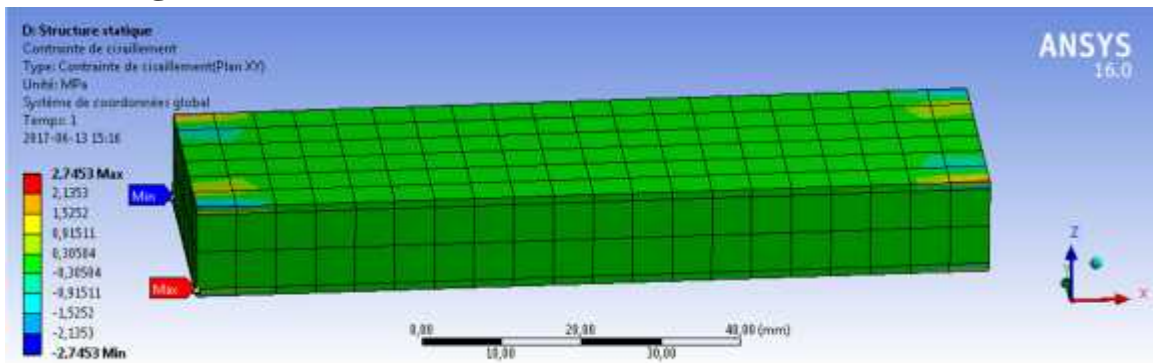


Figure. III. 25 Shear stress in tensile test for the GFT plate

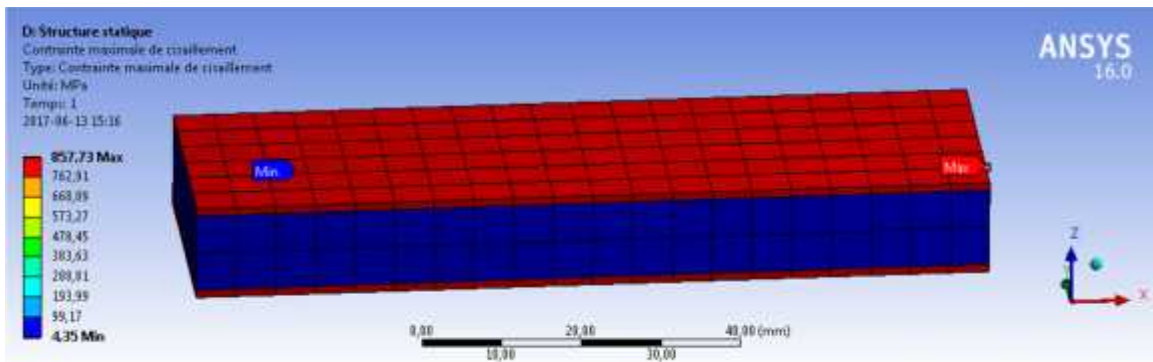


Figure. III. 26 Maximum shear stress in tensile test for the GFT plate

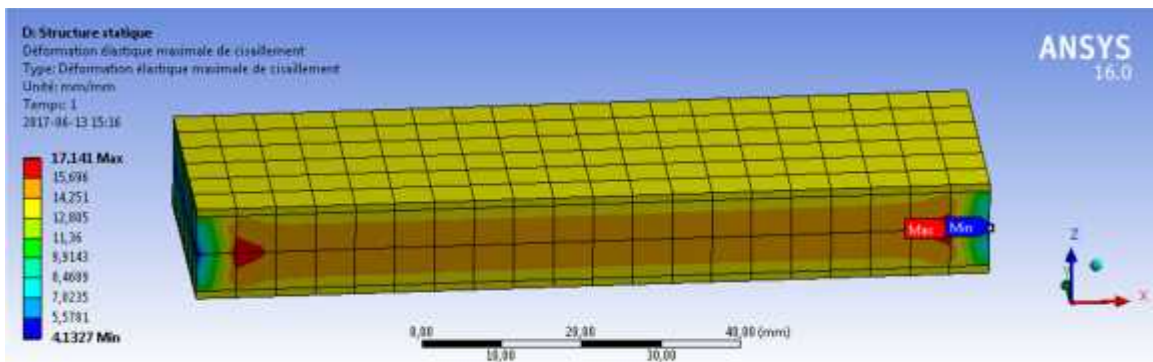


Figure. III. 27 Maximum shear deformation in tensile test for the GFT plate

8.1.2 GFT-CFT (glass fiber texture – carbon fiber texture)

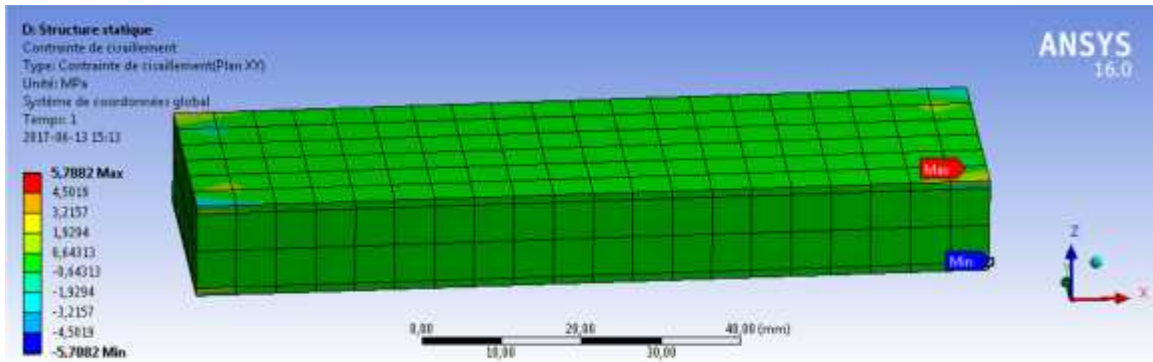


Figure. III. 28 shear stress in tensile tests for the GFT-CFT plate

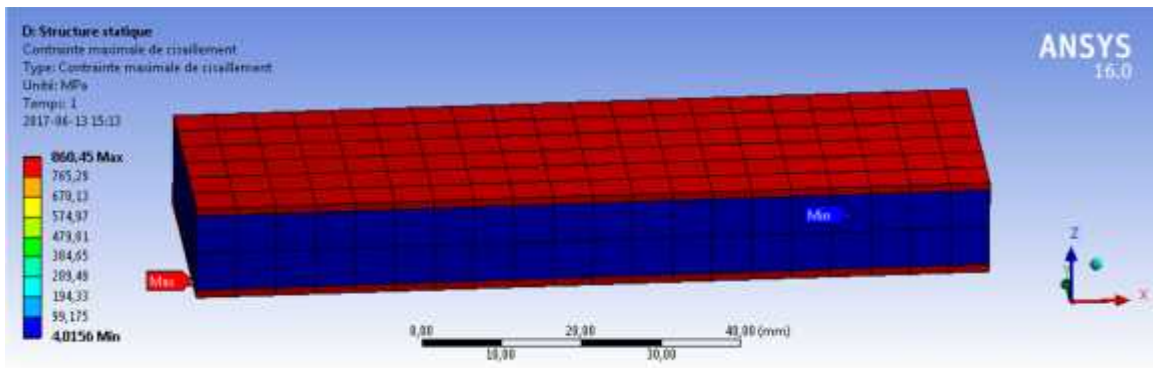


Figure. III. 29 Maximum shear stress in tensile test for the GFT-CFT plate

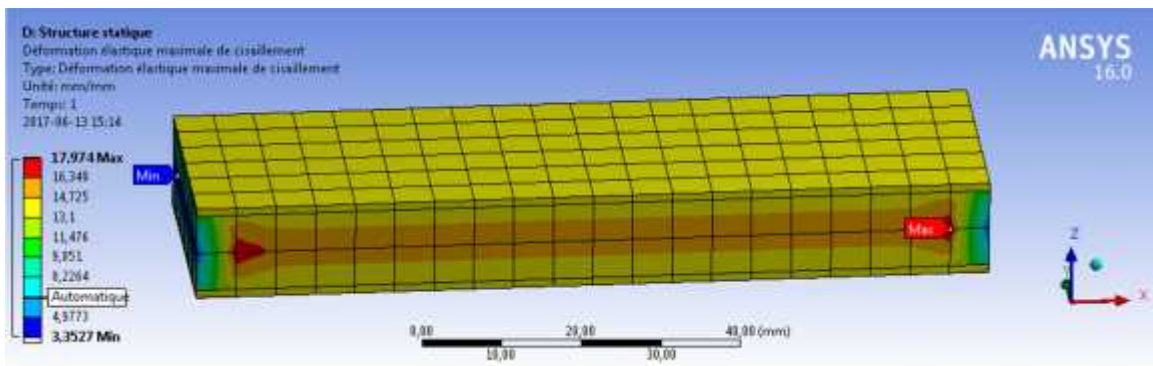


Figure. III. 30 Maximum shear deformation in tensile test for the GFT-CFT plate

8.1.3 CFT (carbon fiber texture)

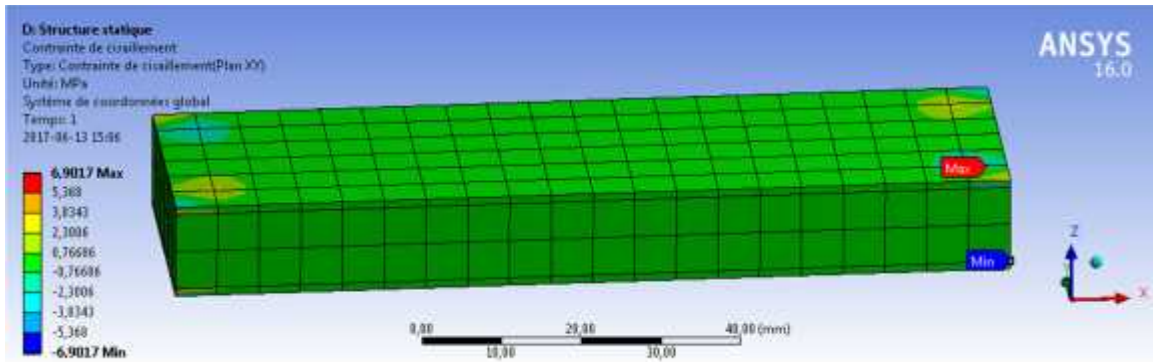


Figure. III. 31 shear stress in tensile tests for the CFT plate

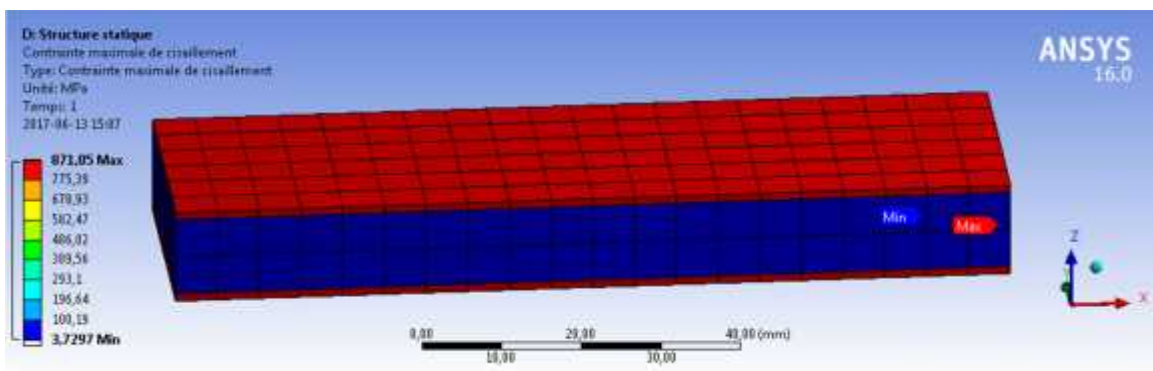


Figure. III. 32 Maximum shear stress in tensile test for the CFT plate

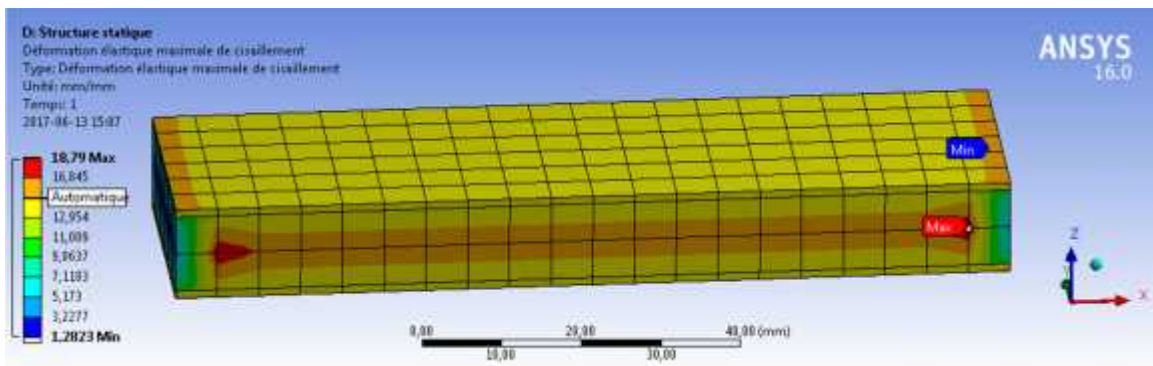


Figure. III. 33 Maximum shear deformation in tensile test for the CFT plate

8.2 Bending test

8.2.1 GFT (glass fiber texture)

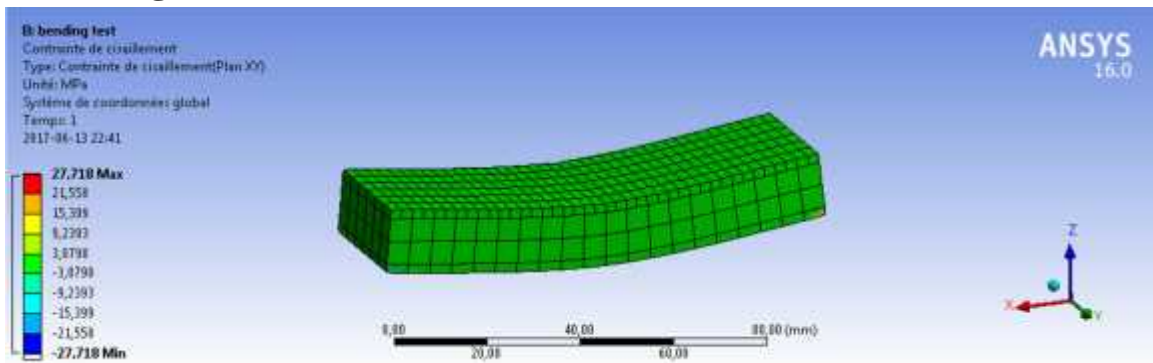


Figure. III. 34 shear stress in three point bending tests for the GFT plate

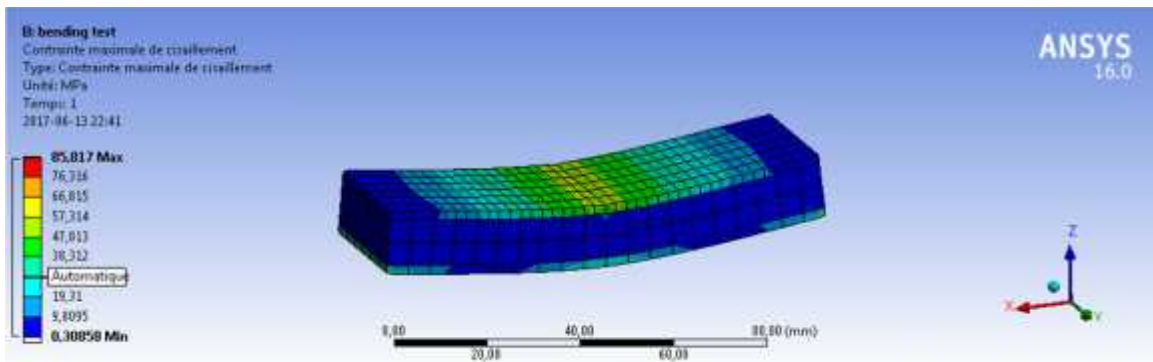


Figure. III. 35 Maximum shear stress in three point bending tests for the GFT plate

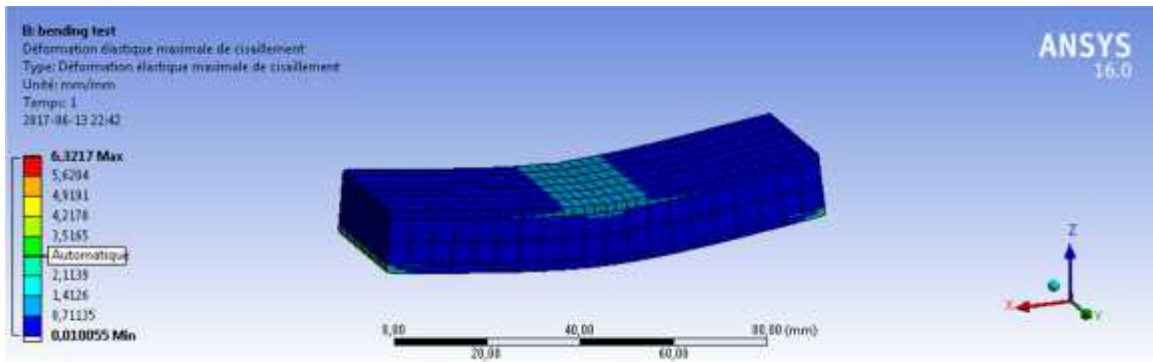


Figure. III. 36 Maximum shear deformation in three point bending tests for the GFT plate

8.2.2 GFT-CFT (carbon fiber texture- glass fiber texture)

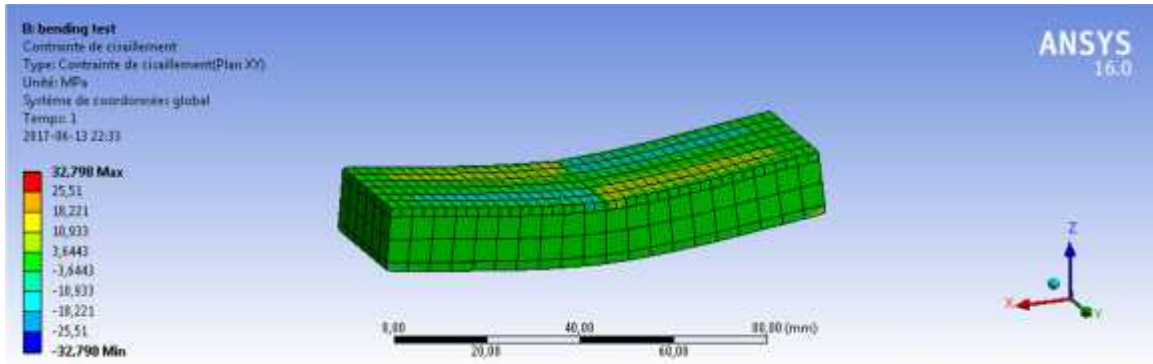


Figure. III. 37 shear stress in three point bending tests for the GFT plate

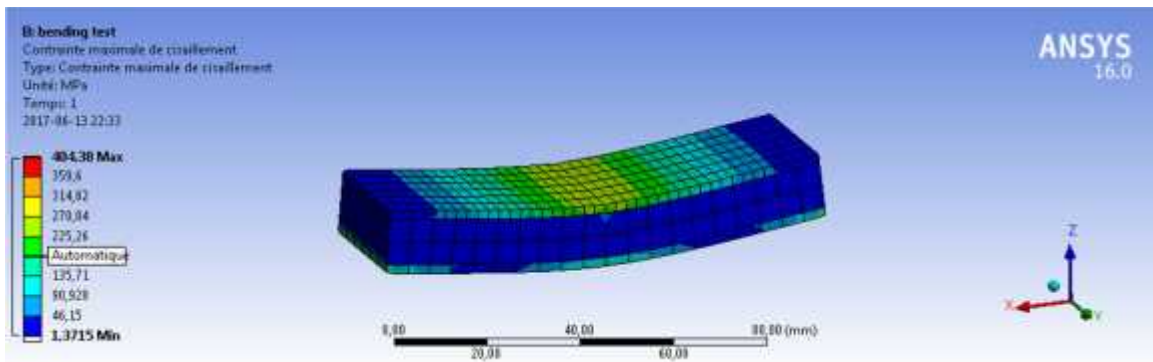


Figure. III. 38 Maximum shear stress in three point bending tests for the GFT-CFT plate

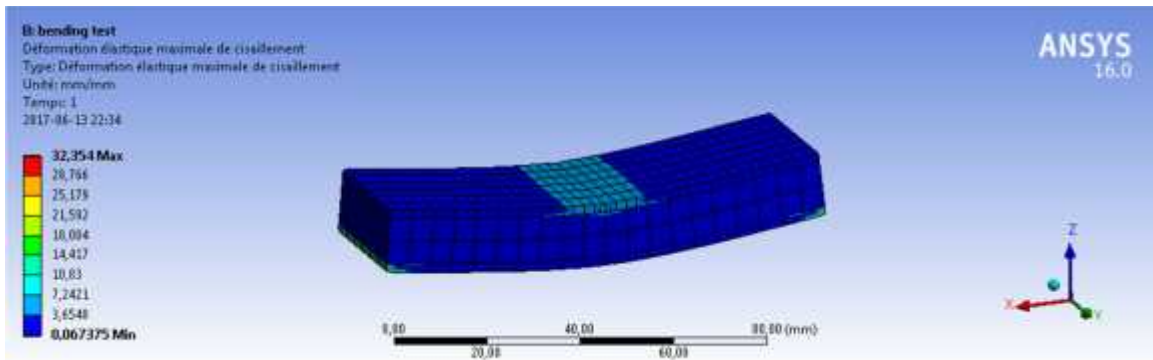


Figure. III. 39 Maximum shear deformation in three point bending tests for the GFT-CFT plate

8.2.3 CFT (carbon fiber texture)

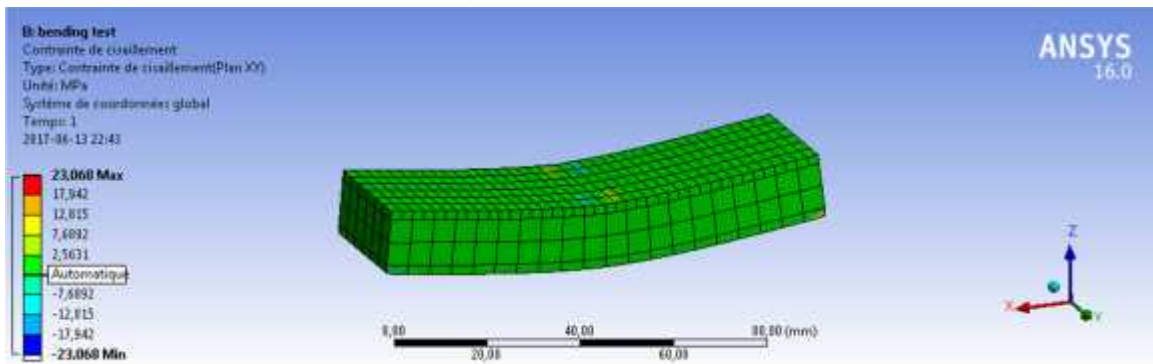


Figure. III. 40 shear stress in three point bending tests for the GFT plate

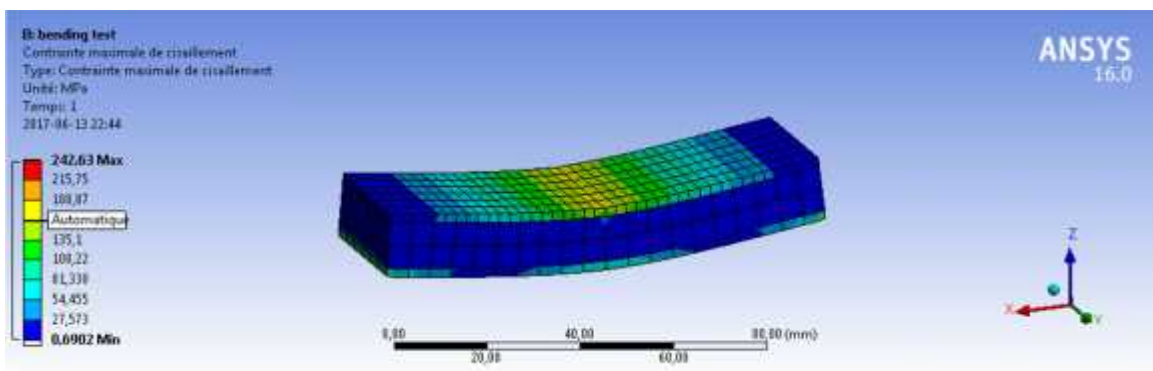


Figure. III. 41 Maximum shear stress in three point bending tests for the CFT plate

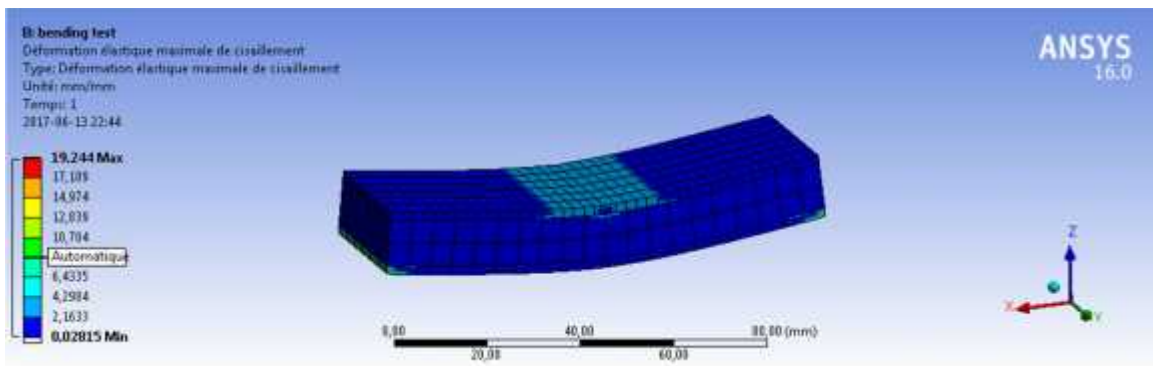
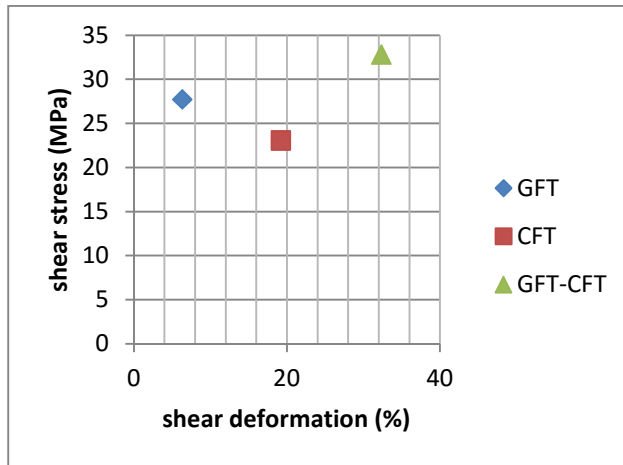
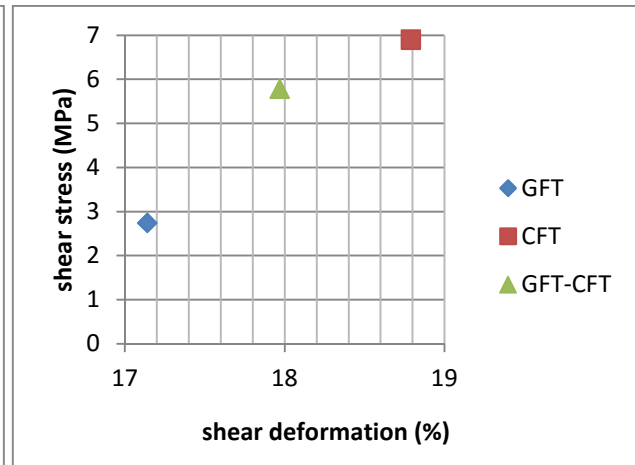


Figure. III. 42 Maximum shear deformation in three point bending tests for the CFT plate

Table. III. 5 data obtained from software analysis

Test plate	Tensile test			3 points bending test		
	Shear stress (MPa)	Max shear deformation	Yield stress (MPa)	Shear stress (MPa)	Max shear deformation	Yield stress (MPa)
GFT	2.74	17.14	19.42	27.71	6.32	2.38
GFT-CFT	5.78	17.97	15.14	32.79	32.35	1.58
CFT	6.9	18.79	11.59	23.06	19.24	3.79

**Figure. III. 44 shear stress by shear deformation for three points bending specimens****Figure. III. 43 shear stress by shear deformation for tensile specimens**

We notice from the simulation analysis that the shear stress in the bending test is greater than in tensile test. Also from the data table that in tensile experiment the maximum shear deformation in GFT sandwich plate is superior to the other two test specimens, however, in bending the GFT-CFT sandwich plate have the upper values of shear stresses. Also, as we can observe from table (III.5) that shear stress is much important in bending than yield stress, and it is the opposite in traction, which means that shear stress is the more influent in the deformation of the sandwich plates in bending.

9 Conclusion

In this chapter we manufactured three honeycomb plates with the same core material made of an aramid paper called Nomex and with different skins materials where we used carbon fiber tissue and glass fiber tissue, then, we exposed these specimens to tensile and bending forces by

performing tensile and three point bending tests respectively in order to study the behavior by analysing the stress concentration zones and influence. Finally, to complete our study we used ANSYS software to get an idea about the shear stress effect on the plates in both experiments.

The analysis of the results obtained from tensile and three point bending tests leads us to the following conclusions:

- The behavior of the honeycomb plates is anisotropic.
- The plate with both skins made of glass fiber tissue endures an important deformation in the first direction.
- The plate with both skins made of carbon fiber tissue withstands important loads in the transvers direction.
- Shear stress plays a big part in the deformation caused by bending forces.

This analysis and the quality of results allows us to say that due the anisotropic behavior of the honeycomb plates, this kind of materials is quite challenging to define. Also, some points can be developed in the future.

1 Introduction

We learned previously that the importance of composite materials and sandwich structures is in their high performance characteristics, and to determine these characteristics there is some procedures to follow and experiments to perform, in this chapter, we are going to see two of the basic experiments used to characterize a sandwich plate: tensile test, and three point flexural test, and a simulation using ANSYS software.

2 Manufacturing of sandwich plate

2.1 Manufacturing process

The manufactures of the plates were made at the level of plastic and composite workshop at Algerian airlines reparation base. We start with the preparation of place and material needed for this process. First we mixes the resin and the hardener at 15/100 ratio (figure.III.1)



Figure. III. 1 preparation of resin (adhesive)

After that, we cut the tissues of carbon (a) and glass fiber (c) and the honeycomb (b) with the desired measurements (100x200 mm), the tissue is deposited on the impregnation layer and then spread another resin layer on each layer (one layer for the carbon tissue (a) and 3 layers for fiber glass tissue (c)). The honeycomb core (b) is placed directly after the last impregnated ply by a layer of resin. Then we put another layer of the tissue (fiber glass (c) or carbon (a)) then spread another resin layer on this fold



a) Carbon fiber texture

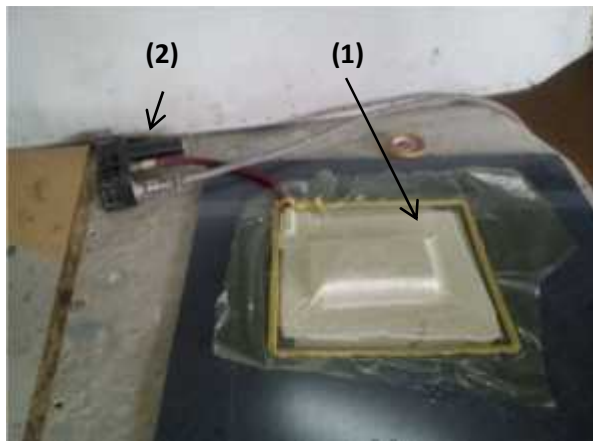
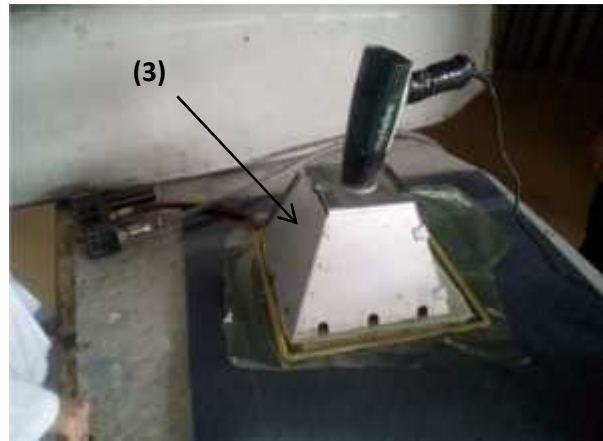
b) Aramide paper (Nomex)
honeycomb core

c) Glass fiber texture

Figure. III. 2 (a), (c), Skins and, (b) core materials

The next step is to cut the tear-off fabric widely enough to cover the sandwich plate and then placed on it and we cut also the absorption fabric in rectangular form which covers the entire previous surface without trespass the sealing tape.

Finally, the vacuum bag system is closed by using the plastic film; the purpose of its use is to seal the system assembly and to achieve the protection of the mold, and to have mostly perfect resin absorption (figure.III.3. (a)), then we put a heat chamber over this system (figure.III.3. (b)).

a) (1)Vacuum bag system
(2)Vacuum pump

b) (3) Heat chamber

Figure. III. 3 Final phase of manufacturing process (a), (b)

2.2 Tensile and bending tests specimens



Figure. III. 5 (a) GFT



Figure. III. 4 GFT- CFT



Figure. III. 6 CFT

- (a) GFT: Glass Fiber Texture faces sheets plate: each face contains 3 layers of GFT.
- (b) GFT-CFT: Glass Fiber Texture and Carbon Fiber Texture faces sheets plate: one face sheet made with 1 layer of CFT, the other one is made with 3 layers of GFT.
- (c) CFT: Carbon Fiber Texture faces sheets plate: each face contains 1 layer of CFT.

Table.III.1. Dimension of test specimens

Length L (mm)	Width b (mm)	Depth d (mm)
100	30	10

3 Tensile test

Tensile testing is a fundamental material science test in which a sample is subjected to a controlled tension until failure. Properties that are directly measured via a tensile test are ultimate tensile strength, maximum elongation and reduction in area. From these measurements the following properties can also be determined: Young's modulus, Poisson's ratio, yield strength, and strain-hardening characteristics. These characteristics can be determined from stress-strain curve (figure.III.5) obtained from the experimental data.

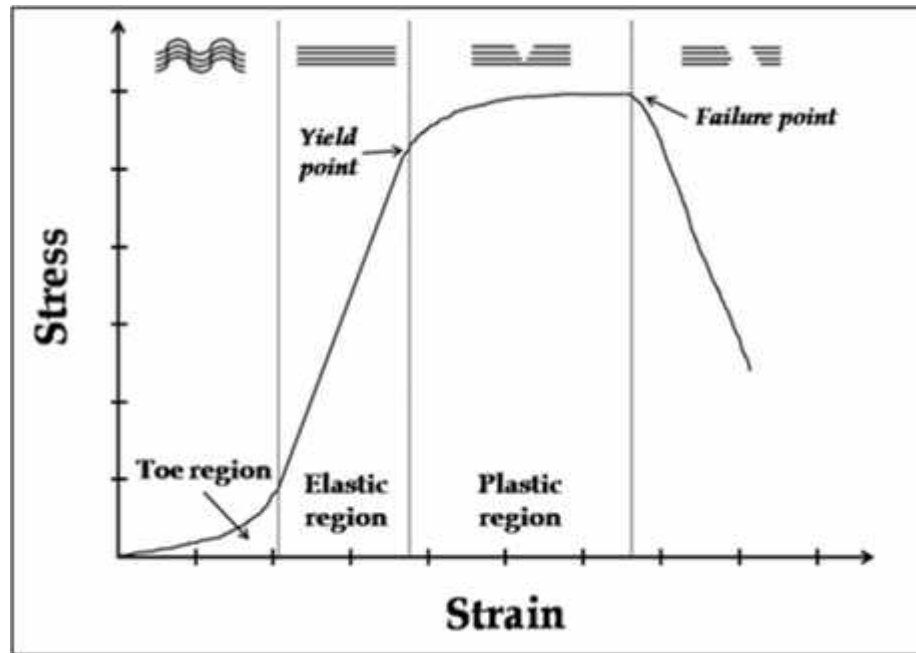


Figure. III. 7 Stress-strain curve

In the following paragraph, we are going to represent three test cases performed in two separate occasions; the first was at the laboratory of mechanics at the higher college of aerial defense of the territory at Reghaia (ESDAT). The second one was at materials science laboratory located at the department of mechanical engineering at HOUARI BOUMEDIENE Sciences and Technology University, but, in this case we putted hills in both ends of the test specimens glued with the adhesive used in patch repairs.

3.1 Tensile experiment process

The tensile test is generally carried out by introducing a test piece into a Universal traction machine (figure.III.6). This machine consists of a flat base and a piston Hydraulic system having a linear motion perpendicular to this same base. Jaws (hydraulic or manual) are located on the piston as well as on the piston based. The latter are installed in such a way that their axes are collinear with that of the piston. Then, once the test piece is inserted into the jaws, the piston is displaced vertically and the axial force required for this displacement is recorded. In addition, strain gauges are glued to the test piece to measure deformations involved in the calculation of the mechanical properties.



Figure. III. 8 HOYTOM universal traction machine

Our work is to recover and process and analyze these Tests using a spreadsheet (Excel) to determine the values of the characteristics Mechanical properties of the 3 test specimens. The maximum force of the test machine is 50 KN, and the test speed is 50 mm/min.

4 Experimental data

4.1 Plate with glass fiber texture faces sheets (GFT)

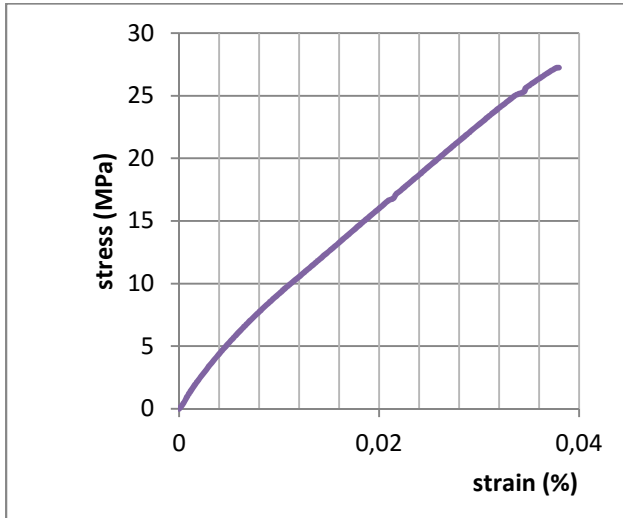


Figure. III. 10 stress-strain curve for first experiment of GFT plate

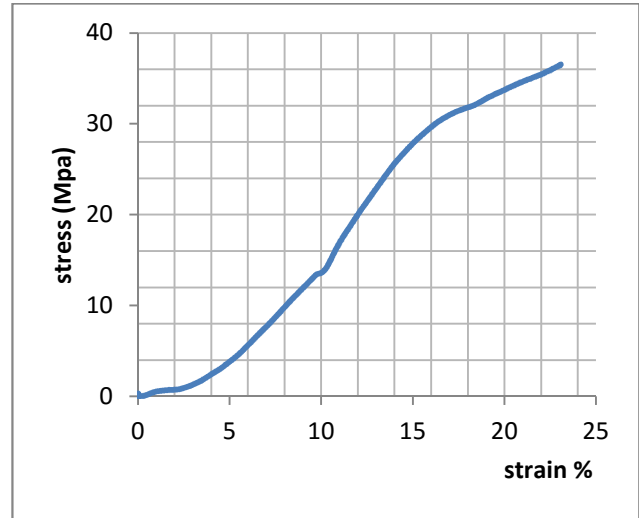


Figure. III. 9 stress-strain curve for the second experiment of GFT plate

From figure III.10 we see that curve is mostly linear, the maximum stress is 27.23 MPa, and the yield stress is 25.2 MPa. The maximum deformation is 3 %. From figure.III.9 we notice that the maximum stress is about 36.54 MPa, and the yield stress 19.42 MPa, and the maximum deformation after the yielding point 23.1%. We also observe a small disturbance at the beginning of the curve; it was due to a small sliding between the grips and the test specimen.

4.2 Plate with glass fiber and carbon fiber textures faces sheets (GFT-CFT)

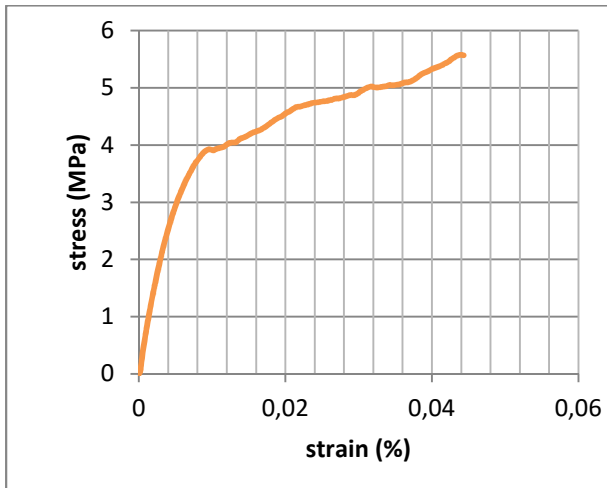


Figure. III. 12 stress-strain curve for the first experiment of GFT-CFT plate

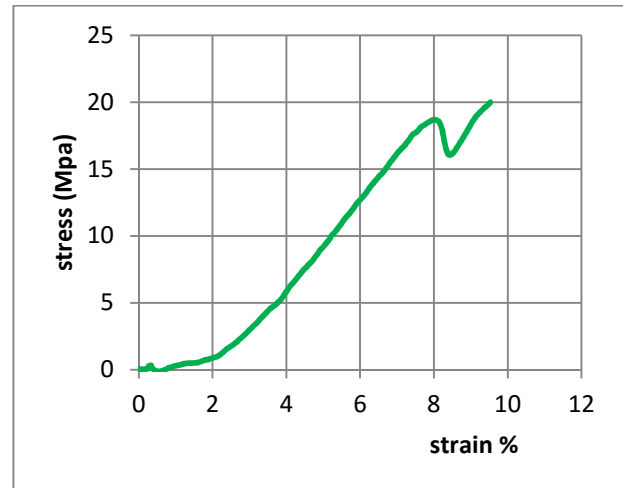


Figure. III. 11 stress-strain curve for the second experiment of GFT-CFT plate.

In the first experiment figure.III.11, the sandwich plate's behavior is divided into two phases, the first is linear until yield stress point which is equal to 3.9 MPa, and the second phase is linear disturbed until maximum stress 5,56 MPa is reached. The maximum deformation is about 4.4 %.

From figure.III.12, we notice the same disturbance at the beginning of the curve for the same reason as the previous specimen, also we notice a reduction in stress 18.3MPa and 17.09MPa then an augmentation in stress which is due to the different faces sheets materials properties, the maximum stress 20.71MPa, the maximum deformation 9.52%.

4.3 Plate with carbon fiber texture faces sheets (CFT)

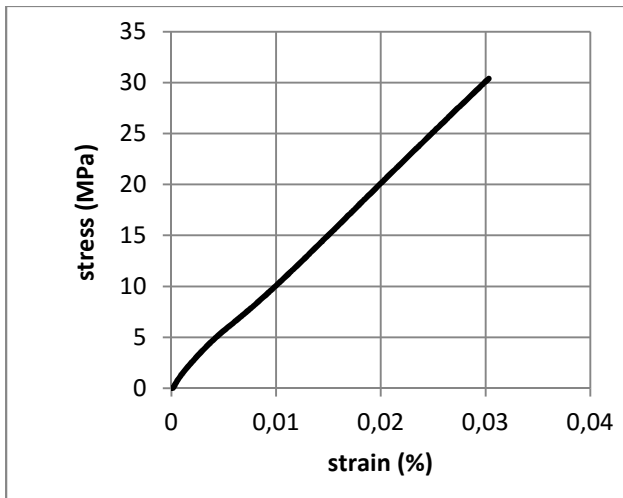


Figure. III. 14 stress-strain curve for the first experiment of CFT plate.

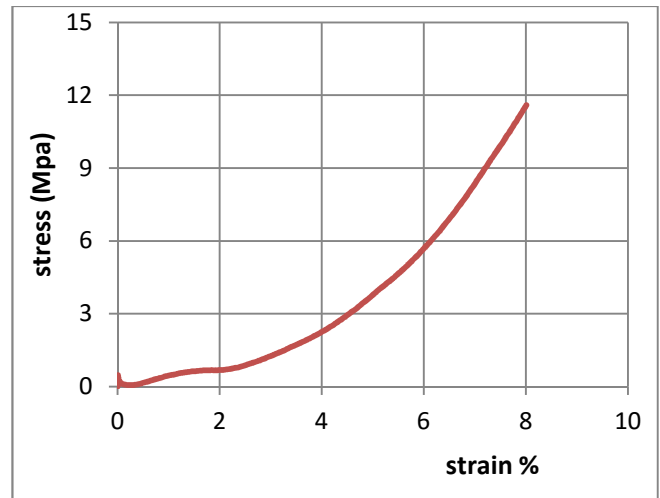


Figure. III. 13 Stress-strain curve for the second experiment of CFT Plate.

In figure III.13, the curve is linear until maximum stress (which is also yield stress) 30.39 MPa, also the maximum strain is 3 %.In figure.III.14 We notice the same disturbance in the beginning of the curve as the previous two cases, we observe that the maximum stress is equal to the yielding stress which is 11.59Mpa; also the maximum strain is 8%. The superior stress value in the first experiment was due to the sliding between grippes and test specimen, but, unlike the previous similar cases, this time the gripping force caused a deformation which results an important augmentation in traction force which in the end results an augmentation in stress value.

From figure III.13, the curves were about the first experiment, we must know from it that some point must be taken in consideration during the experience, here are the major ones:

- The dimension of the sample depends highly on some regulations as: JIS, ASTM, ISO...and also on the type of the machine test.

- When we put the machine grips on the ends of the sample it may cause non desirable deformation on the honeycomb core as shown in figure III.15 which cause a disturbance in the results.

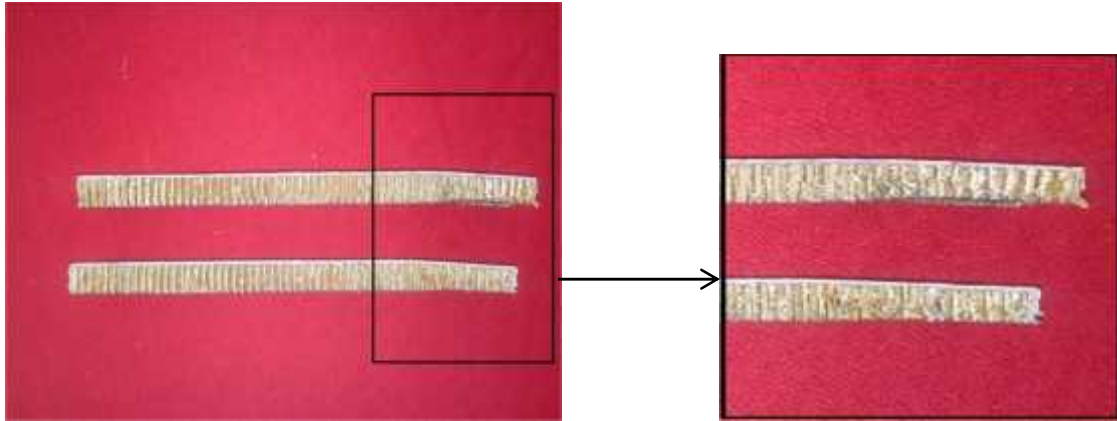


Figure. III. 15 deformation caused by the gripping force of jaws

4.4 Honeycomb core

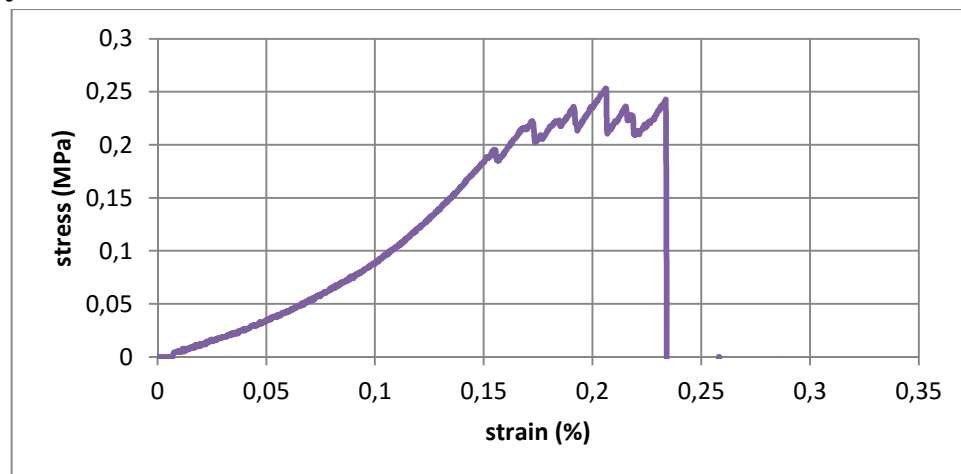


Figure. III. 16 Stress-strain curve for honeycomb core in tensile test

In this figure we have the force by elongation curve for the Nomex honeycomb core. It starts in linear form 0 N until it reaches the value 57 N, from which we notice a multiple disturbance in the force magnitude, then, a massive decrease at the value of stress = 71 N, then, small disturbances to the final rupture. The explanation for the disturbances is that when the cells are deboning in a non-uniform form. The calculation of in-plan characteristics shows that the elasticity modulus of the honeycomb core is very much weaker than the skins materials, which allows us to say that behavior showed by the plates is due to skins properties.

5 Flexural strength

It is also known as modulus of rupture, bend strength, or fracture strength. The flexural strength represents the highest stress experienced within the material at its moment of rupture. It is determined from three points or four points bending tests. When an object formed of a single material, like a wooden beam or steel rod, is bent, it experiences a range of stresses across its depth. At the edge of the object on the inside of the bend (concave face) the stress will be at its maximum compressive stress value. At the outside of the bend (convex face) the stress will be at its maximum tensile value. These inner and outer edges of the beam or rod are known as the “extrem fibers”. For a rectangular cross-section calculation of the flexural stress:

Calculation of the flexural stress:

$$\sigma_f = \frac{3F}{2b} \quad (III.1)$$

Calculation of the flexural strain:

$$\epsilon_f = \frac{6D}{L^2} \quad (III.2)$$

Calculation of flexural modulus

$$E_f = \frac{L^3 m}{4bd^3} \quad (III.3)$$

Where:

F: the applied force (N).

L: the sample length (mm).

b: the sample width (mm).

d: the sample depth (mm).

D: the deflection of the test sample (mm) $D = \frac{FL^3}{4E}$

I: second moment of area (mm⁴). It is defined by: $I = \frac{a^3 b}{12}$

E: Young`s modulus (MPa).

σ_f : Flexural strain (MPa).

ε : Deformation of the sample (%).

M: the gradient (slop) between the initial straight line portion of the load deflection (N/mm).

$$m = \frac{F}{D}$$

ε_f : Flexural deformation.

E_f : Flexural modulus (MPa).

5.1 Three points bending experiment process

The following experiment was performed at UR-PMC at University of Boumerdes.

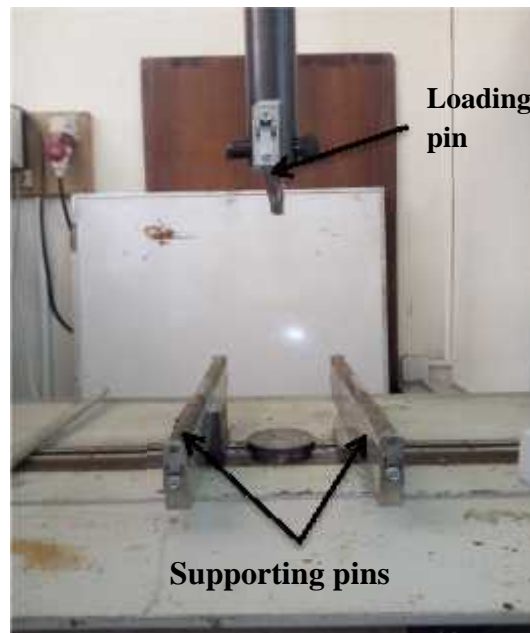


Figure. III. 17 Three points bending test machine

The load pin has a maximum load up to 100KN.

The test speed is 10N/s.

6 Experimental data

6.1 Plate with glass fiber texture faces sheets (GFT)

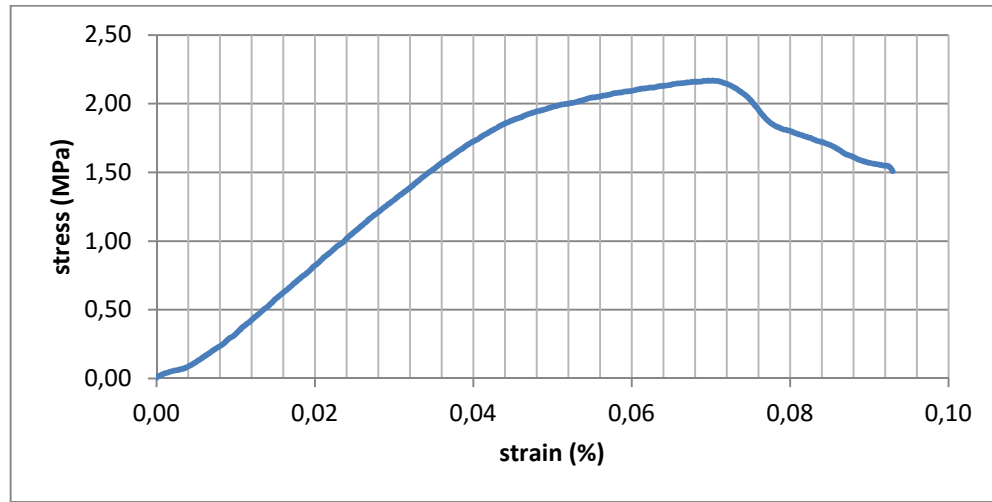


Figure. III. 18 Stress-strain curve for GFT honeycomb sandwich plate

In this figure, we can clearly see that the resistance of the sandwich plate starts to weaken before maximum force applied is reached, and then when fracture occurs, the stress of the plate does not decrease extensively, the maximum stress is about 2.7Mpa and the maximum strain is 7%.

6.2 Plate with glass fiber and carbon fiber textures faces sheets (GFT-CFT)

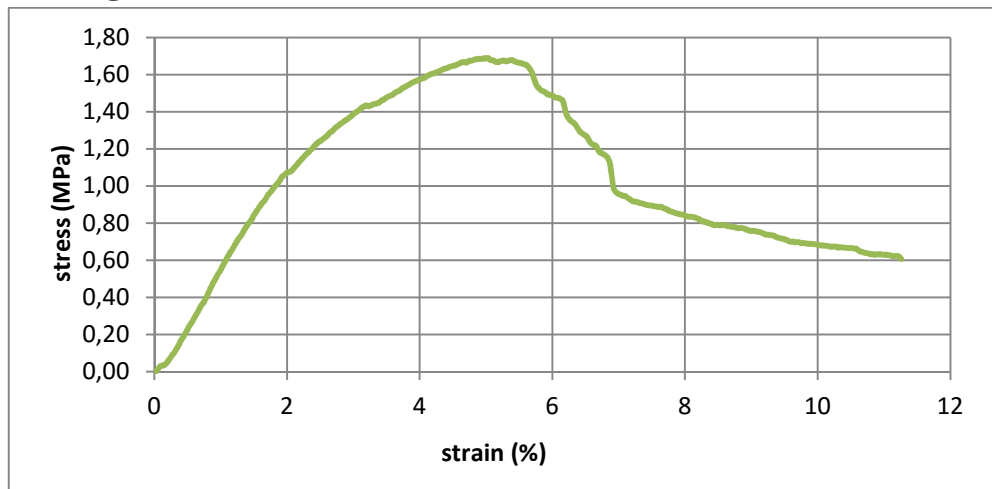


Figure. III. 19 Stress-strain curve for GFT-CFT honeycomb sandwich plate

In this figure III.19 we have the stress-strain curve for GFT-CFT honeycomb sandwich plate. We can notice that the maximum stress is about 1.69% and the maximum strain is 19%.

6.3 Plate with carbon fiber texture faces sheets (CFT)

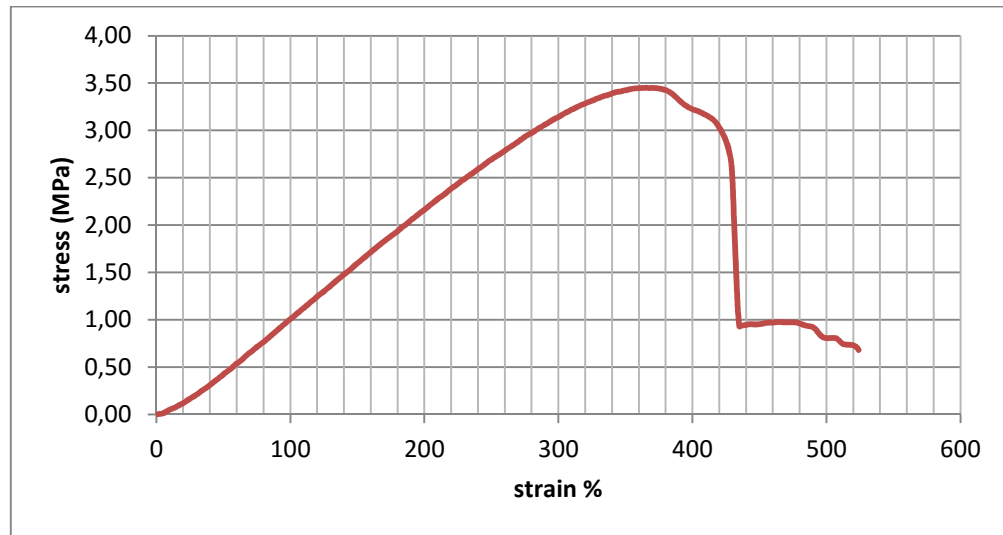


Figure. III. 20 stress strain curve for CFT honeycomb sandwich plate

Figure III.20 is about stress-strain curve for carbon fiber texture (CFT) faces sheets honeycomb sandwich plate. In this curve the maximum stress is 3.45Mpa and the maximum strain 9%.

7 Results and discussion

7.1 Tensile test

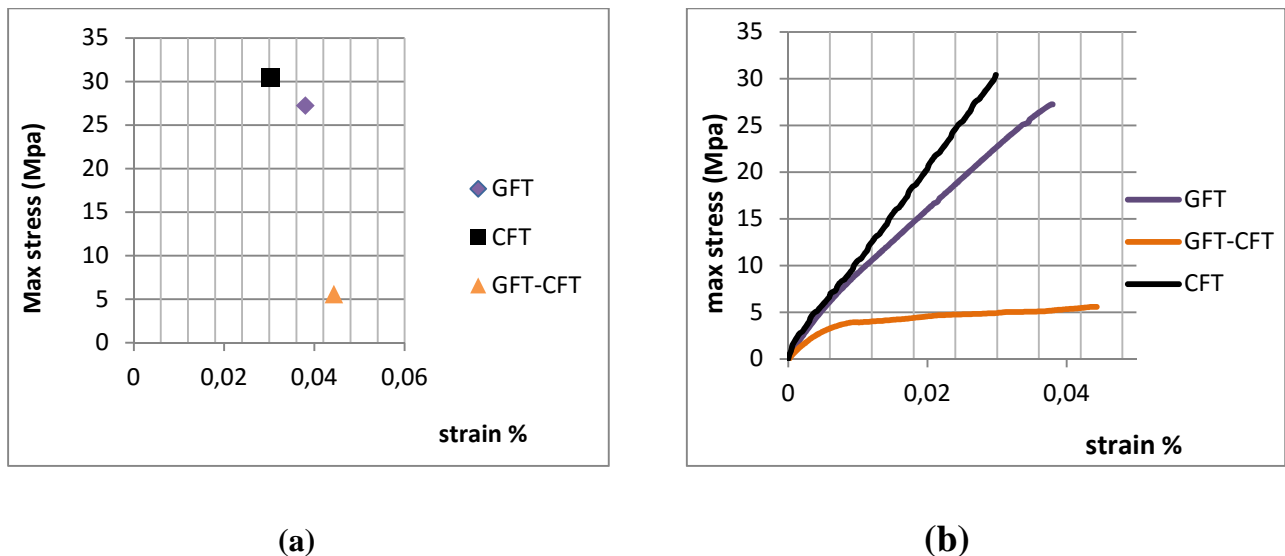
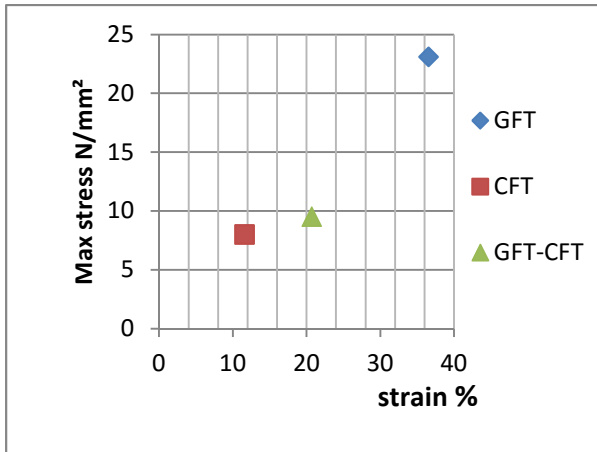
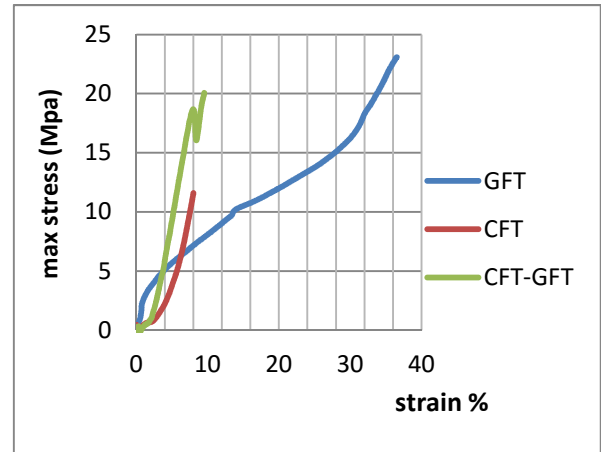


Figure. III. 21 (a),(b) stress by strain curve of the first tensile experiment for the test specimens



(c)



(d)

Figure. III. 22 (c),(d) stress by strain curve of the second tensile experiment for the test specimens

From figures (III.21. (a) and (b)), we can notice that in the first tensile test CFT honeycomb sandwich plate shows a superior resistance comparing with the two other plates but with the smallest value of allowable deformation and the weakest behavior in tension is shown by the plate of GFT-CFT and the biggest deformation comparing to the other plates .

From figures (III.22. (c) And (d)), we can see that in the second tensile test . GFT honeycomb sandwich plate shows a superior resistance (when compare to the other two plates) with the biggest value of allowable deformation which place it as the best plate in tension, and the weakest behavior is shown by the plate with carbon fiber texture face sheets which place it as the unlikely most favorite plate in the performed experiment. The results are numerically calculated following procedure in ISO 527.

Table. III.2. Characteristics obtained from the first tensile experiment

Test case	F_{\max} (N)	σ_m (MPa)	ϵ (%)	E_A (MPa)	G_A (MPa)	θ
GFT	8170	27.23	3.798	7.16	2.68	0.3
GFT-CFT	1673.30	5.57	4.43	1.257	0.471	0.3
CFT	9118	30.39	3.031	10.02	3.75	0.3

Table.III.3. Characteristics obtained from the second tensile experiment

Test case	F_{\max} (N)	σ_m (MPa)	ε (%)	E_A (MPa)	G_A (MPa)	θ
GFT	12790	36.54	23.1	158.18	60.83	0.3
GFT-CFT	7250	20.71	9.5	218	83.84	0.3
CFT	4060	11.59	8	144.87	55.71	0.3

As we can see from the table, the plate with higher elastic characteristics in plan is from test case 2, which is the sandwich plate with different skins materials and characteristics, and the plate with the largest elongation is from test case one that is the one with both skins made of 3 ply of glass fiber texture. That's leaves us with the last test specimen the one with both skins made of carbon fiber texture, and we can say about it that it is the most stiff plate in our experiment comparing to the other two.

7.2 Three point Bending test

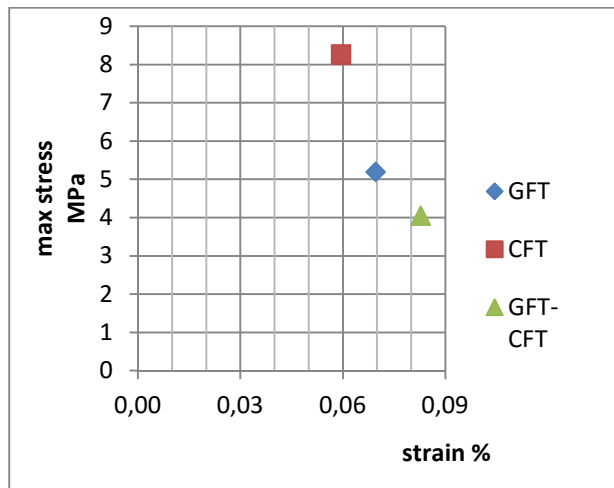


Figure. III. 24 Maximum stress by deformation for bending test specimens

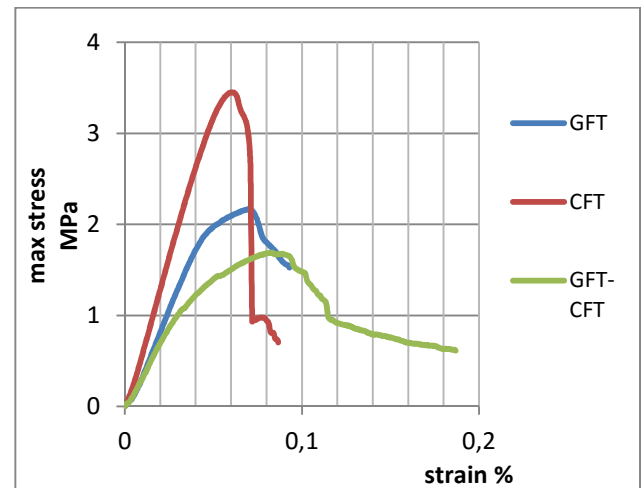


Figure. III. 23 Stress by strain for the bending test of the three specimens

From figures (III.23, 24), the sandwich plate with carbon fiber texture face sheets have the maximum stress and the lowest deformation, comparing to the second test specimen, we notice that it has the maximum deformation between the three plates and the smallest value of stress.

The plate with glass fiber texture face sheets has the middle position in bending test, unlike in the tensile experiment. Also, these figures allows us to notice that the bending behavior is similar and can be described in three phases: the first phase is initial linear elastic behavior followed by a non-linear one in which the maximum loading is achieved. In the last phase, a reduction in the load applied is observed till the total rupture of the samples occurs. The linear behavior corresponds to the work of the skins in traction and compression, whereas, the non-linear behavior mainly depends on the core properties under the effect of shear stress, which also explain the similarity of pattern in figures (*) knowing that our test samples have the similar core material.

Table.III.4. Flexural characteristics obtained from bending test

Test case	D (mm)	σ_f (MPa)	ε_f (%)	E_f (MPa)
GFT	79.95	5.19	0.47	74.56
GFT-CFT	95.23	4.045	0.57	48.75
CFT	68.34	8.26	0.41	138.75

From the calculated data in table (III.7), we can notice a difference in the behavior of the three test specimens in bending stress, the honeycomb sandwich plate with different face sheets materials has the biggest deflection in the case of three point bending, however, it's flexural elasticity modulus and shear modulus is the weakest comparing to the other two specimens.

The sandwich plate with carbon fiber texture skins material shows the most favorite behavior in bending, even if it has the lowest deflection value between the three plates, the 3rd test specimen has the better flexural characteristic in three point bending test.

8 Simulation

Our analysis are about shear stress in both tensile and three points bending experiments on a honeycomb sandwich panel specimens with the same skins material properties as those used in previous section about the experimental study.

8.1 Tensile test

8.1.1 GFT (glass fiber texture)

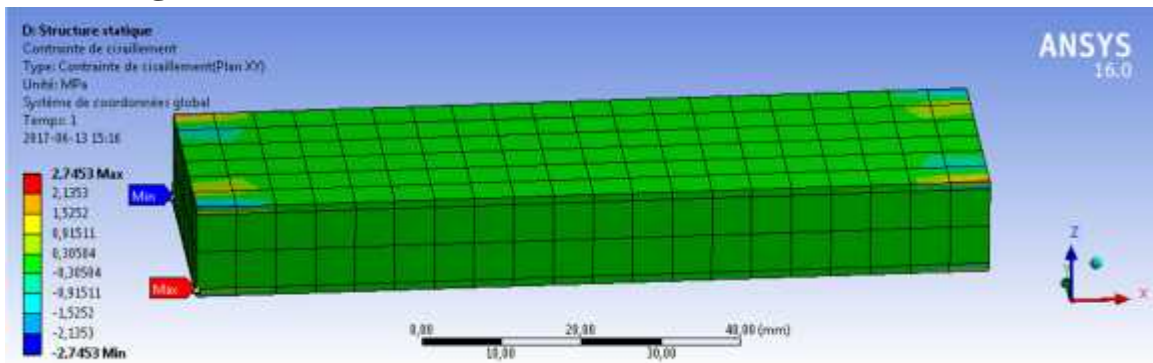


Figure. III. 25 Shear stress in tensile test for the GFT plate

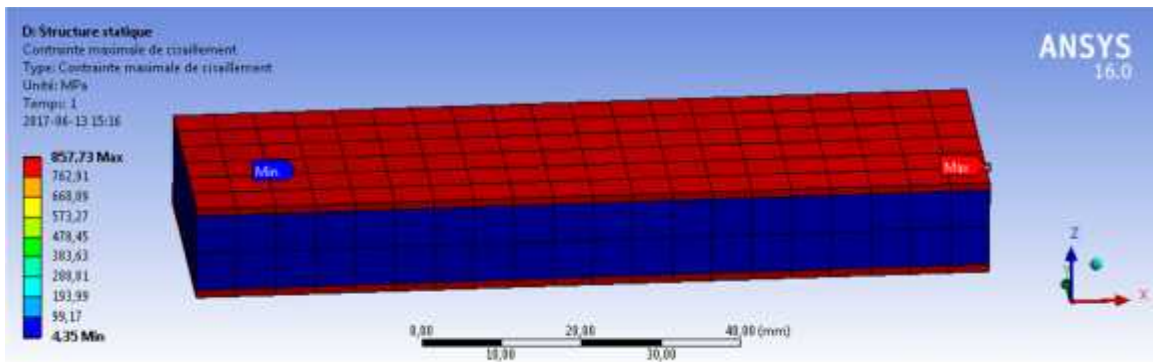


Figure. III. 26 Maximum shear stress in tensile test for the GFT plate

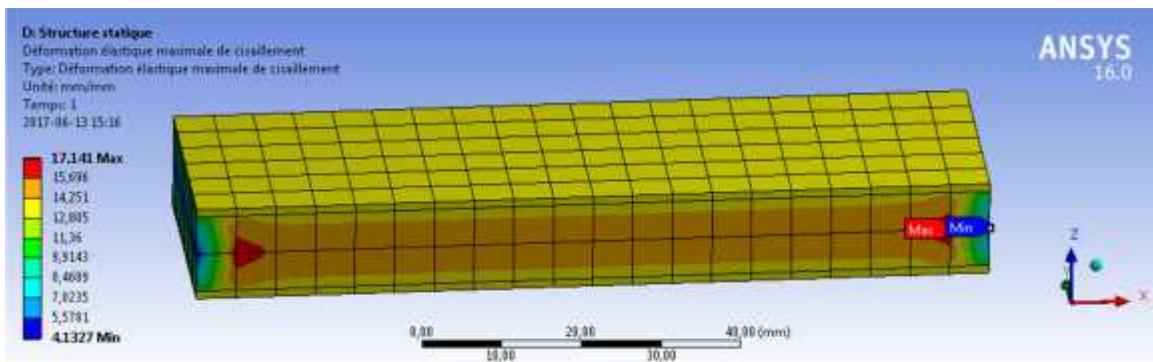


Figure. III. 27 Maximum shear deformation in tensile test for the GFT plate

8.1.2 GFT-CFT (glass fiber texture – carbon fiber texture)

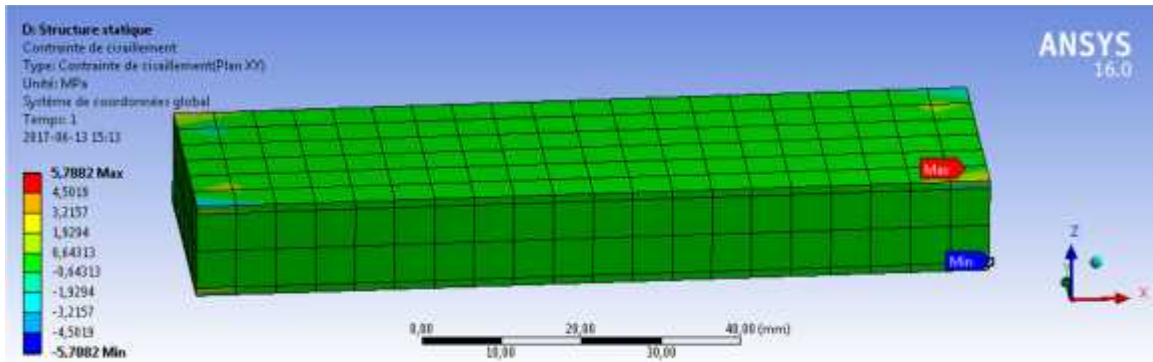


Figure. III. 28 shear stress in tensile tests for the GFT-CFT plate

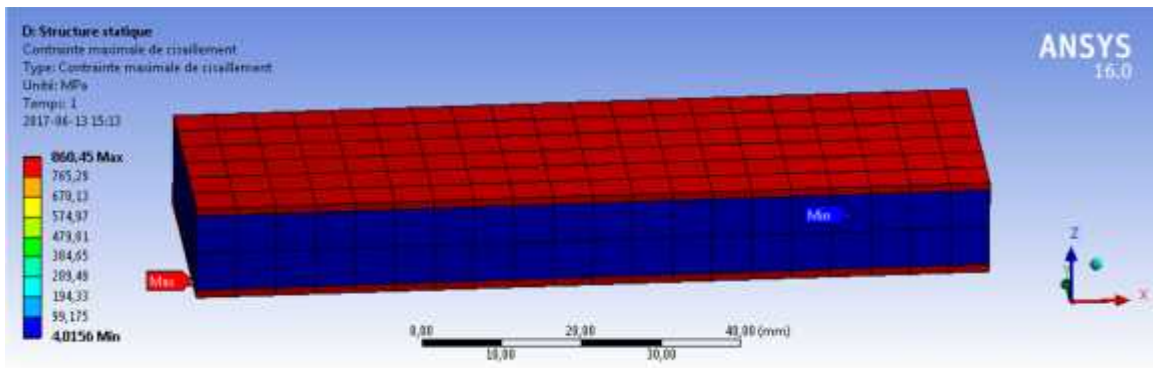


Figure. III. 29 Maximum shear stress in tensile test for the GFT-CFT plate

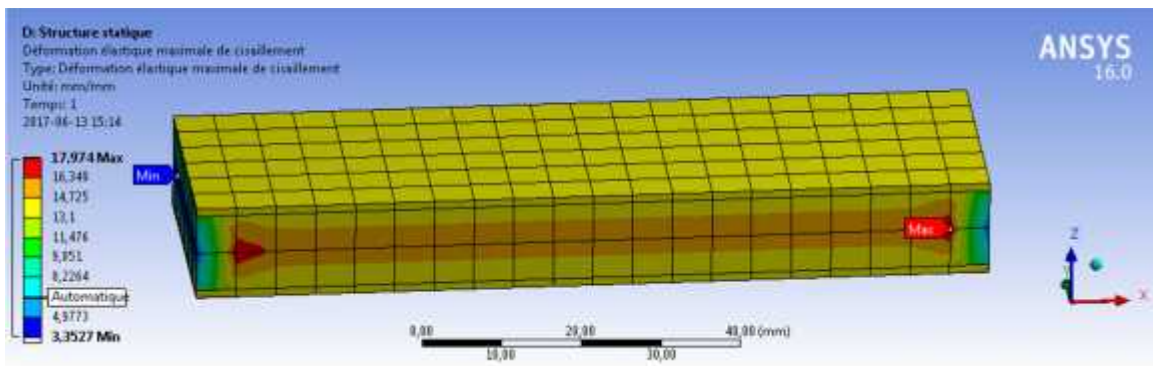


Figure. III. 30 Maximum shear deformation in tensile test for the GFT-CFT plate

8.1.3 CFT (carbon fiber texture)

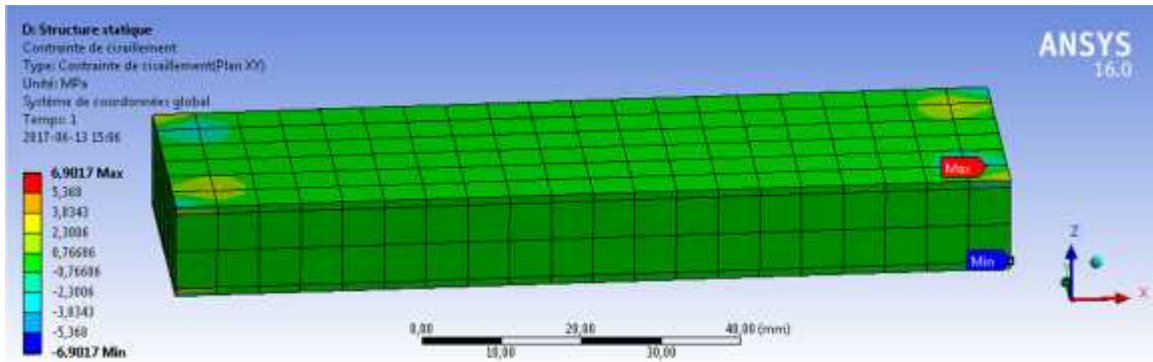


Figure. III. 31 shear stress in tensile tests for the CFT plate

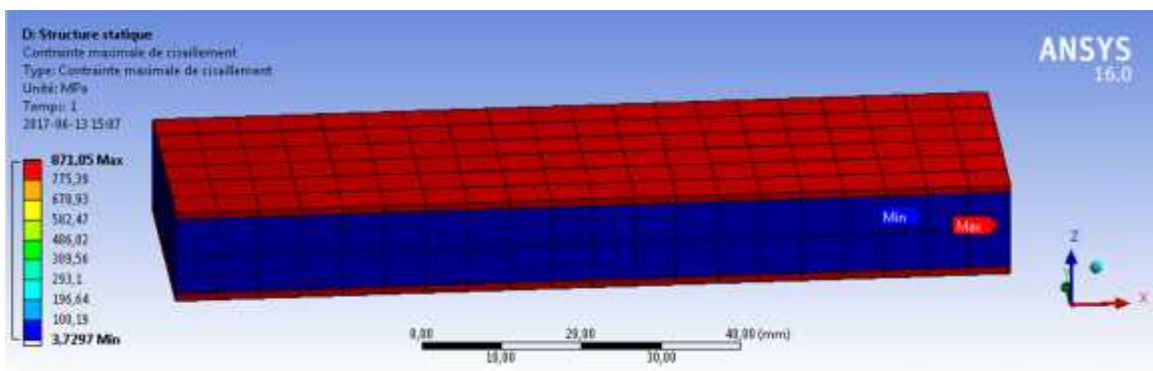


Figure. III. 32 Maximum shear stress in tensile test for the CFT plate

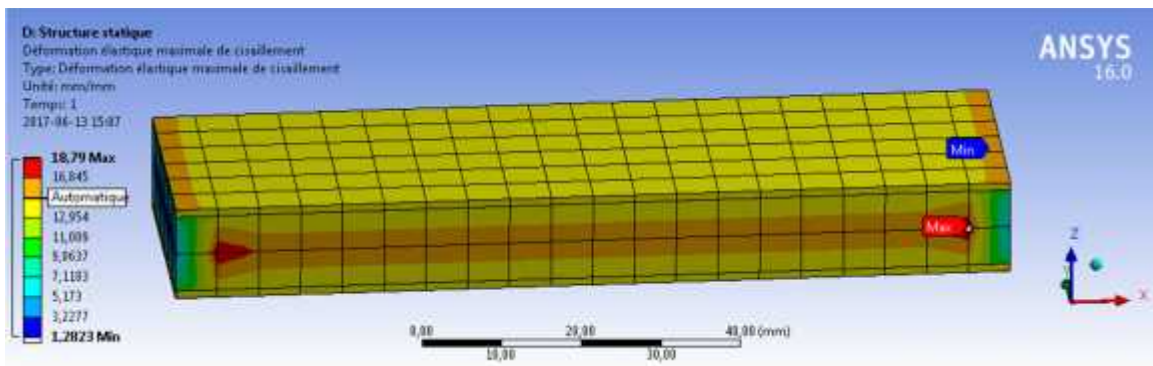


Figure. III. 33 Maximum shear deformation in tensile test for the CFT plate

8.2 Bending test

8.2.1 GFT (glass fiber texture)

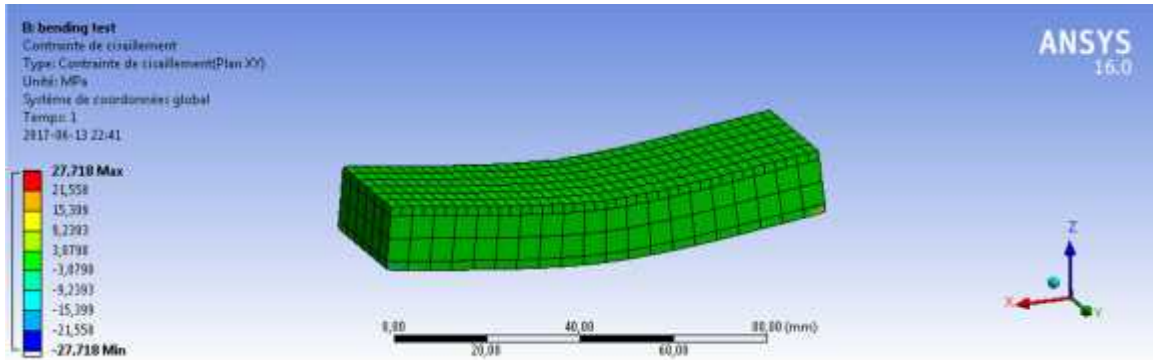


Figure. III. 34 shear stress in three point bending tests for the GFT plate

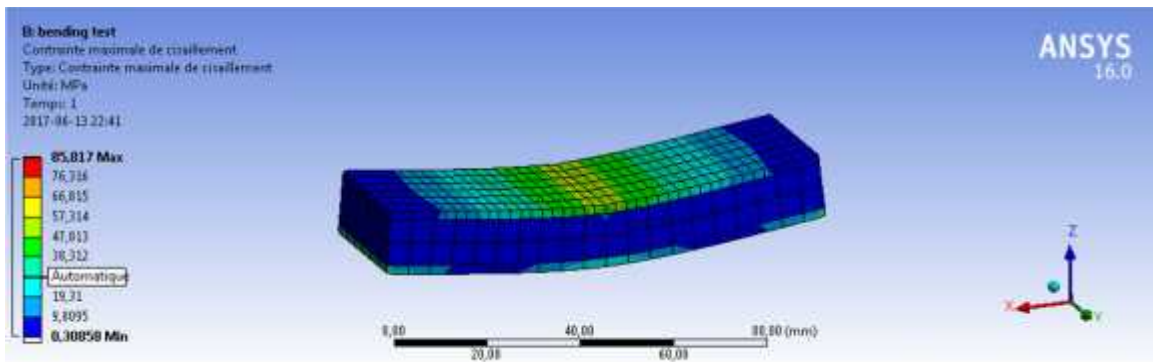


Figure. III. 35 Maximum shear stress in three point bending tests for the GFT plate

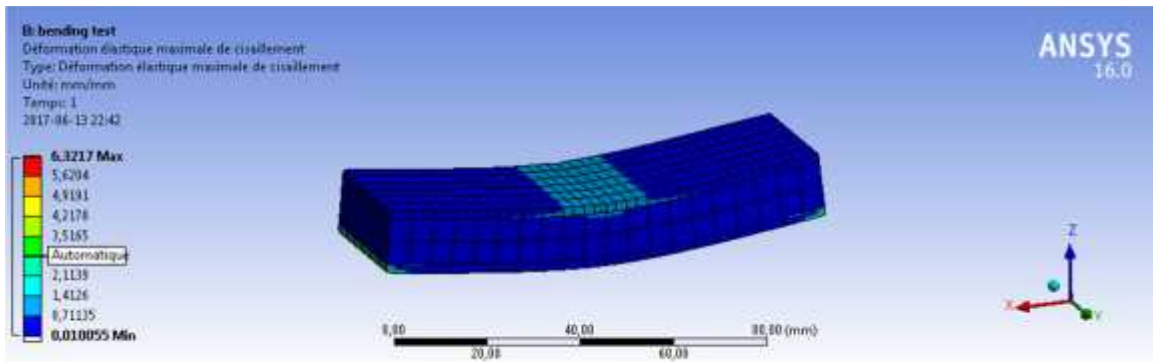


Figure. III. 36 Maximum shear deformation in three point bending tests for the GFT plate

8.2.2 GFT-CFT (carbon fiber texture- glass fiber texture)

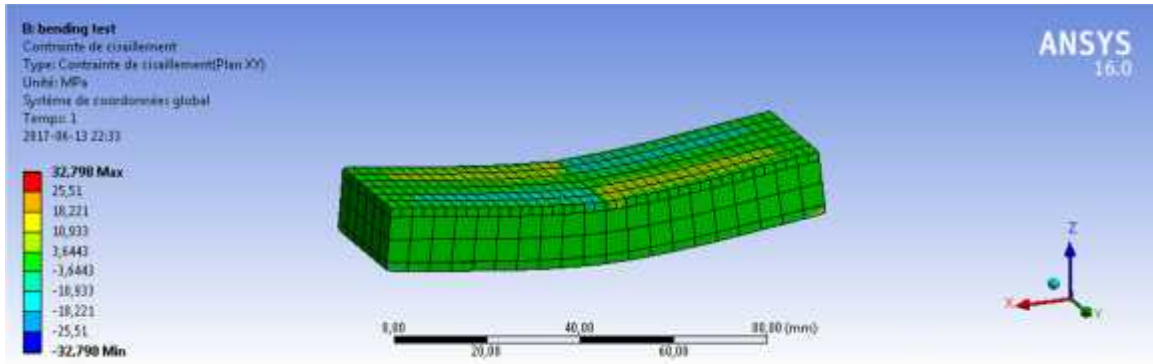


Figure. III. 37 shear stress in three point bending tests for the GFT plate

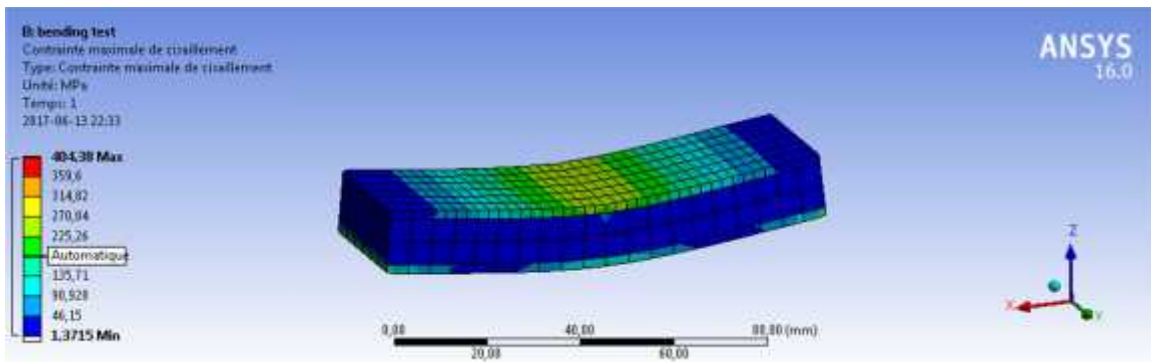


Figure. III. 38 Maximum shear stress in three point bending tests for the GFT-CFT plate

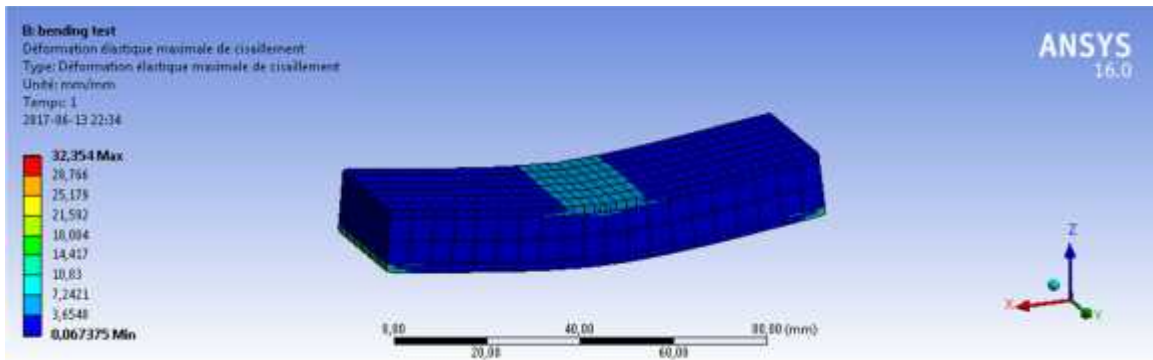


Figure. III. 39 Maximum shear deformation in three point bending tests for the GFT-CFT plate

8.2.3 CFT (carbon fiber texture)

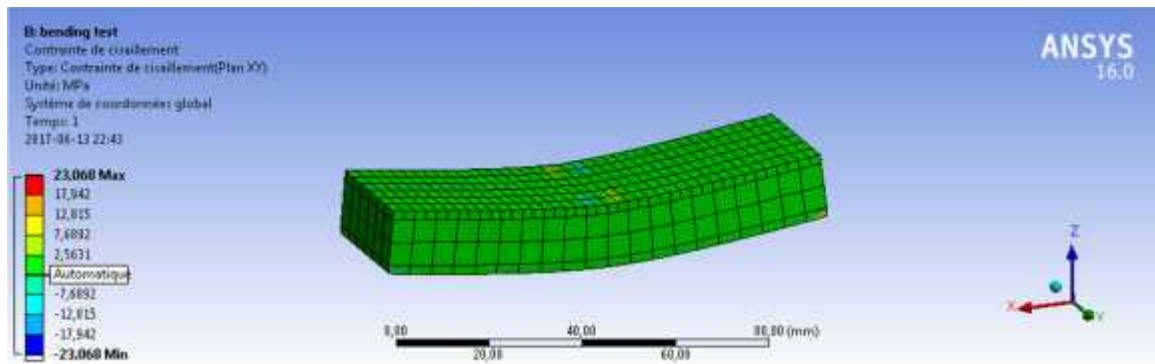


Figure. III. 40 shear stress in three point bending tests for the GFT plate

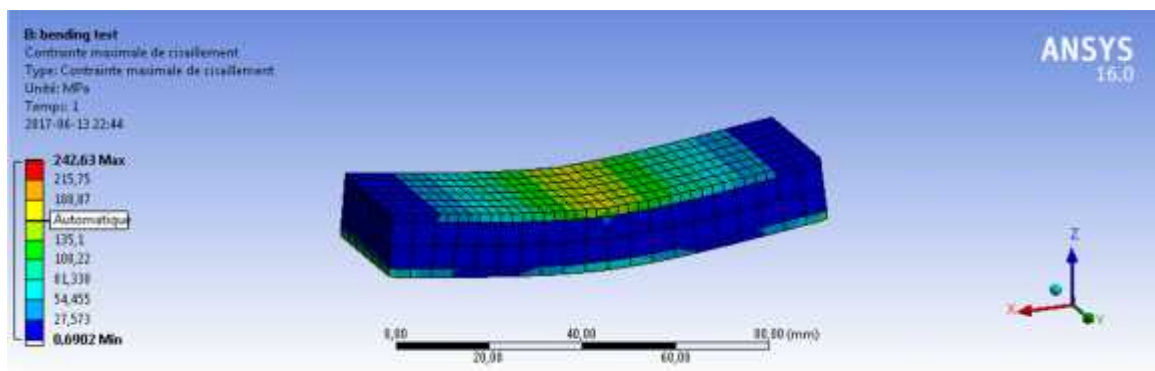


Figure. III. 41 Maximum shear stress in three point bending tests for the CFT plate

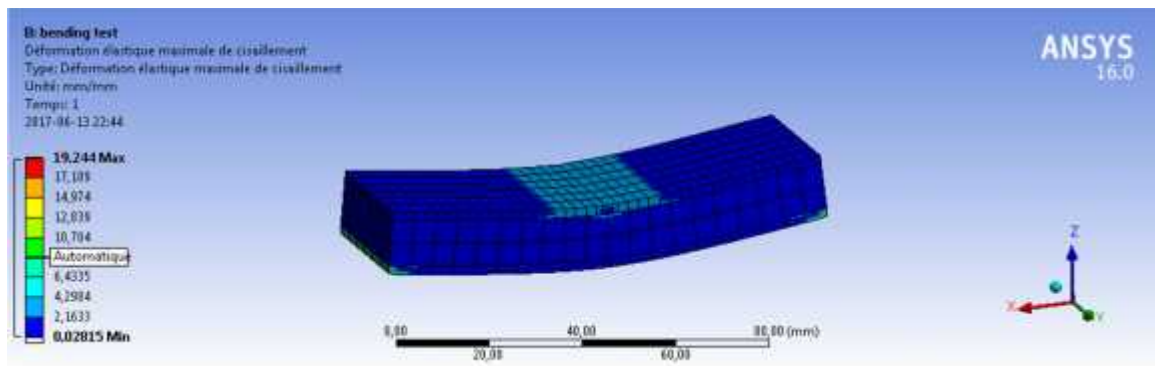
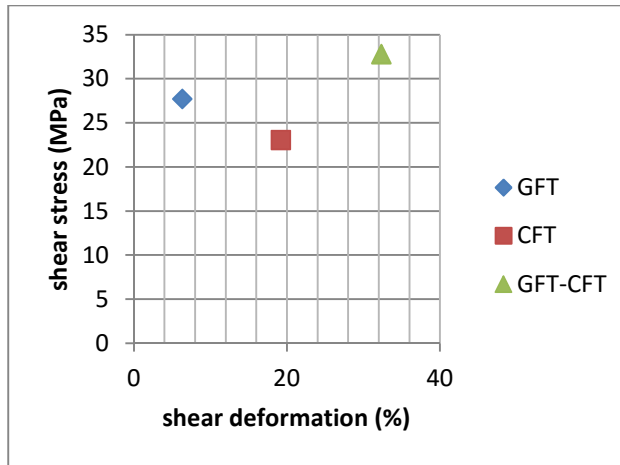
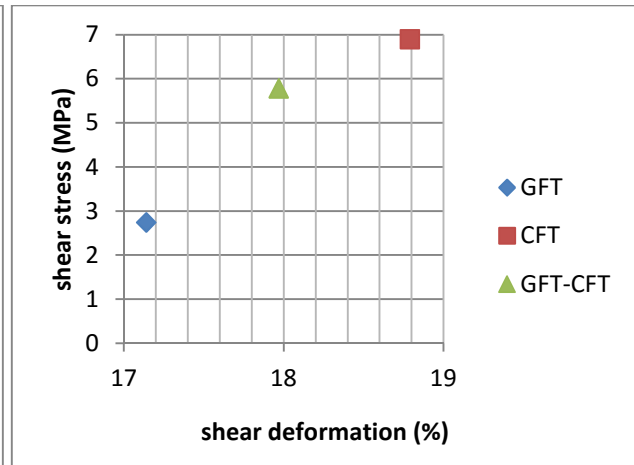


Figure. III. 42 Maximum shear deformation in three point bending tests for the CFT plate

Table.III.5. data obtained from software analysis

Test plate	Tensile test			3 points bending test		
	Shear stress (MPa)	Max shear deformation	Yield stress (MPa)	Shear stress (MPa)	Max shear deformation	Yield stress (MPa)
GFT	2.74	17.14	19.42	27.71	6.32	2.38
GFT-CFT	5.78	17.97	15.14	32.79	32.35	1.58
CFT	6.9	18.79	11.59	23.06	19.24	3.79

**Figure. III. 44 shear stress by shear deformation for three points bending specimens****Figure. III. 43 shear stress by shear deformation for tensile specimens**

We notice from the simulation analysis that the shear stress in the bending test is greater than in tensile test. Also from the data table that in tensile experiment the maximum shear deformation in GFT sandwich plate is superior to the other two test specimens, however, in bending the GFT-CFT sandwich plate have the upper values of shear stresses. Also, as we can observe from table (III.5) that shear stress is much important in bending than yield stress, and it is the opposite in traction, which means that shear stress is the more influent in the deformation of the sandwich plates in bending.

9 Conclusion

In this chapter we manufactured three honeycomb plates with the same core material made of an aramid paper called Nomex and with different skins materials where we used carbon fiber tissue and glass fiber tissue, then, we exposed these specimens to tensile and bending forces by

performing tensile and three point bending tests respectively in order to study the behavior by analysing the stress concentration zones and influence. Finally, to complete our study we used ANSYS software to get an idea about the shear stress effect on the plates in both experiments.

The analysis of the results obtained from tensile and three point bending tests leads us to the following conclusions:

- The behavior of the honeycomb plates is anisotropic.
- The plate with both skins made of glass fiber tissue endures an important deformation in the first direction.
- The plate with both skins made of carbon fiber tissue withstands important loads in the transvers direction.
- Shear stress plays a big part in the deformation caused by bending forces.

This analysis and the quality of results allows us to say that due the anisotropic behavior of the honeycomb plates, this kind of materials is quite challenging to define. Also, some points can be developed in the future.

General conclusion

General conclusion

As we write the final word, we are divided between joy to have finished with a long-winded quest and the bitterness of not having pushed the audacity further on, and as Louis Aragon said: "and if it were to be redone, I would do it again"

The composite materials are then unanimous. Because they can be shaped by adjusting their properties to the specific requirements of an application, they are solutions of choice in sectors as varied as transportation, building, mechanics, electronics, sports, And even paramedical equipment.

They bring many functional advantages: mechanical, chemical and physical

These main performances can be summarized by their lightness, their reduced maintenance, their long life and their freedom of shaping.

Unlike similar materials, the design of composite parts requires precise knowledge of future use.

Due to the anisotropy of the structure, the designer must ensure that the workpiece is resistant to all particular modes of loading.

Validation with the help of tests of each stage of design (choice of fibers, resin, and adhesion between the two) is then paramount when studying composite part.

The work presented in this thesis was aimed at studying the tolerance of Damage to composite sandwich structures subjected to impact stresses of the type Low speed. The sandwich structure in question consists of composite fiber skins of Glass, carbon, resin and an aramid paper made core (Nomex). The panels were made by infusion in the composites workshop at the reparation base of Algerian Airlines Company.

And the behavior under impact of the sandwich structures, two tests were carried out the first experiment is the tensile test that was done at the laboratory level of ESDAT laboratory at Reghaia and the laboratory of SDM in university level of USTHB and for the second test was the three-point bending test that was realized at the level of UR-MPC laboratory at the university of Boumerdes UMBB.

General conclusion

In the first part of this work, the emphasis was mainly on the response to the impact of sandwich panels on the various structural parameters and experiments. The impact tests were carried out on machines with a falling mass instrumented. Then, the results were presented in the form of the curves giving the evolution of the stress as a function of the deformation. This representation graphs allowed to characterize the materials and also to make the comparison between the behaviors of the three test specimens under the effect of the tests

The second part of this work was devoted to understanding the behavior of Sandwich structures under static impacts. The objective was to be able to better interpret the transition in drop mass impact tests. In this context, the effect of the rate of stress on the behavior of our samples has been studied.

Finally, trials static tests were carried out on a three-point traction and flexion machine. The analysis of the results allowed us to characterize the parameters of the materials well and the second part of this work was devoted to the understanding of the behavior of the tests on the test pieces.

The simulation performed by ANSYS software was to complete the experimental study.

In conclusion, the results of this study contribute to the understanding of Behavior of sandwich structures subjected to in-plan and flexural loads. Nevertheless, some points can be developed and studied in the future.

Bibleography

References

- [1] Lubin, ``Hand book of composites``, Van Nostrand, New York 1982.
- [2] Achilles Petras, `` Design of sandwich structures``, Cambridge University Engineering Department, December 1998.
- [3] M. F. Ashby, `` Materials Selection in Mechanical Design``, Pergamon Press, Oxford 1983.
- [4] R. W. Birmingham and J. A. D. Wileox, `` Charting the links between material selection and elemental form in structural design``, Journal of Engineering Design, 4(2), 1993, pp. 127-140.
- [5] Nikhil. V. Nayak, `` Composite materials in aerospace applications``, International Journal of Scientific and Research Publications, Vol 4, Issue 9, September 2014, ISSN 2250-3153.
- [6] J.Odorico. G. Leiba, ``Evolution of materials on civil aircrafts structure and helicopters". Material and Techniques, N° 1-2 / January - February 1988.
- [7] M.-L. Sanmartin, "New sandwich material", C.I.A.T / ATS materials center of research. Materials and Techniques, N° 6 / June 1988.
- [8] K.B. Spaulding JR. "Fiberglass boats in naval service", Naval Engineers Journal. Volume 78. Issue 2, pages 333-340. April 1966. Article first published online: 18 MAR 2009. DOI: 10.1111/j.1559- 3584.1966.tb05634.x.
- [9] C. Bathias, "Damage in composite materials: mechanisms et mise en evidence". Materials and Techniques, N° 4-5 / April - Mai 1988.
- [10] J.Z. Zhu AND O.C. Zienkiewicz, "Adaptive Techniques In The Finite Element Method". Department of Civil Engineering. University of Swaua, SA2, BPP. U. K. communications in applied numerical methods, 0748-8025/88/020197, Vol. 4, 197-204 (1988).
- [11] J Babushka and W. C. Rheinboldt, "Error estimates for adaptive finite element computations``, SIAM J. Num". Anal., 15(1978), pp. 736-754
- [12] P. Ladeveze and D. Leguillon. "Error Estimate Procedure in the Finite Element Method and Applications SIAM Journal on Numerical Analysis. Vol. 20, No. 3 : pp. 485-509. (doi: 10.1137/0720033) , 1983. Ladeveze P. Oden J.T. "

BIBLIOGRAPHY

- Advances in Adaptative Computational Methods in Mechanics". Studies in Applied Mechanics, Elsevier, doi: 10.1016/S0922-5382(98)80001-9. Volume 47 (1998).
- [13] P. Ladeveze, Jean-Pierre Pelle. "Maitrise du calcul en mecanique lineaire et non lineaire", Paris, France.ISBEN 0-387-21294-9 Printed on acid-free paper. Hennes-Lavoisier Science Publishers, (2001).
- [14] D. Lang. "Initiation et propagation des endommagements dans les composites verre-epoxy", Materials and Techniques, N° 4-5 / Avril - Mai 1988.
- [15] J. E. Mottershead. M.I Friswell, "Model Updating in Structural, Dynamics: A Survey", Journal of Sound and Vibration, 0022-460X/93/230347, 167(2), 347-375 (1993).
- [16] Pascual R. Golinval J .C, Razeto M, " Comparison of model updating methods adapted to local error detection ", Inti. C'onf. on Noise & Vib. Eng, 21th ISM A. Leuven, Belgium. (1996).
- [17] P. Moine. L. Billet et D. Aubry. "Two updating methods for dissipative models with non-symmetnc matrices". Proceedings of the 15st International Modal Analysis Conference (IMAC-XV). pages 1931- 1936. Orlando. Floride. fevrier 1997.
- [18] R. Pascual Gimenez, J.-C. Golinval et M. Razeto. "On the reliability of error localization indicators" . Proceedings of the 23rd International Conference on Noise and Vibration Engineering (ISMA 23). Leuven. Belgique, September 1998.
- [19] Humbert. F. Thouverez et L. Jezequel, "Finite element dynamic model updating using modal thermoelastic fields". Journal of Sound and Vibration. 228(2) : 397-420, 1999.
- [20] E. Balmes. "Review and evaluation of shape expansion methods". Proceedings of the 18th International Modal Analysis Conference (IMAC-XVM). San Antonio, Texas, fevrier 2000.
- [21] P. Ladeveze, "Erreur en relation de comportement en dynamique : theorie et application au recalage de modeles de structures". Rapport interne 150, LMT-Cachan. 1993.

BIBLIOGRAPHY

- [22] P. Ladeveze, A. Chouaki. "Application of a posteriori error estimation for structural model updating". Inverse Problems. 15 : 49-58. 1999.
- [23] Decouvreur, P. Bouillard, A. Deraemaeker et P. Ladeveze. " Updating 2D acoustic models with the constitutive equation error method". Journal of Sound and Vibration, 278(4-5) : 773-787, 2004.
- [24] T. Y. YANG, "Finite element structural analysis", PRENTICE HALL. INC—Englewood Cliffs— N.J.07632 (1986).
- [25] Young W. kwon et hyochoong bang. "The finite element method using MATHLAB ". Library of Congress Cataloging-in-publication Data. 1997 by CRC Press LLC.
- [26] M. Grediac, "A finite element study of the transverse shear in honeycomb cores", Int. j. solids Struct, 30 (13): 1777- 88 (1993).
- [27] K .Renji, P. S. Nair, and S. Narayanan, "Modal density of composite honeycomb sandwich Panels", J. Sound and Vibration, 195 (5): 687-99 (1996).
- [28] W. Becker. "The in-plane stiffness's of a honeycomb core including the thickness effectv. Archive of Applied Mech, 68: 334-41 (1998).
- [29] K. Renji and S. Shankar Narayan. "Loss Factors Of Composite Honeycomb Sandwich Panels", journal of sound and vibration (2002) 250(4), 745-761.
- [30] Vinson, J, `` The Behavior of Sandwich Structures of Isotropic and Composite Materials ``. Pennsylvania, Technomic Publishing Company, Inc, 1999.
- [31] C.C. Foo, L.K. Seah, G.B. Chai,`` Low-Velocity Impact Failure of Aluminum Honeycomb Sandwich Panels``, Composite Structures 85(2008) 20-28.
- [32] V. Curpi, G. Epasto, E. Guglielmino, `` Collapse Mode in Aluminum Honeycomb Sandwich Panels under bending and Impact Loading `` , International Journal of Impact Engineering 43(2012) 6-15.
- [33] H.R. Ali, B. Manafi, V. Shaterna shhadi and A. Salimi,`` Analysis and investigation of a Honeycomb Sandwich Panel Parameters Under Static Three-

BIBLIOGRAPHY

- point Bending`, Mechanical Engineering, 17009-17012, ISSN: 2229-712x, Elixir Mech. Engg. 61(2013).
- [34] Sakhi Jan, Rafi Ullah Khan, Sajjad Ahmad, Muhammad Amjad, Saeed Badshah, Mutahir Ahmad,` Flexural strength of Honeycomb Sandwich Structures`, Int. Journal of Applied Sciences, ISSN 2277-8442. 1, Vol. 4, No. 2015.
- [35] Mamalis, A. G., Manolakos, D. E., Ioannidis, M. B., and D. P. Papapostolou
- [36] Khurram, Shehzad; Xu, Yang; Chao, Gao; Xianfeng, Duan (2016). ``Three-dimentional macro-structures of two-dimensional nanomaterials``. Chemical Society Reviews. (doi: 10.1039/C6CS0218H)
- [37] J. M. Berthelot, ``MATERIAUX COMPOSITES: comportement mécanique et analyse des structures``, 4th Edition, mai 2005.
- [38] Sushrut Vaidya, Linhui Zhang, Dharma Maddala., Rainer Hebert, Jefferson, T. Wright, Arun Shukla, Jeong-Ho Kim,`` Quasi-static response of Sandwich Steel Beams with Corrugated Cores``, Journal homepage Engineering Structures 97(2015) 80-89.
- [39] Y.M. Li, M.P. Hoang, B. Abbes, F. Abbes, Y.Q. Guo,`` Analytical homogenization for stretch and bending of honeycomb sandwich plates with skin and height effects``, Composite Structures 120(2015) 406-416.
- [40] Adams, Donald F. Sandwich panels test methods. High performance composites, No. 5 4-6. 2006
- [41] Wadley H., Fleck N., and Evans A. ``Fabrication and Structural Performance of Periodic Cellular Metal Sandwich Structures``. Composite Science and Technology, 36, 2003: 2331-2343.
- [42] Evans A., Hutchinson J., Fleck N., Ashby M., and Wadley H. `` the Topological Design of Multifunctional Cellular Metals``. Progress in Materials science, 46, 2001: 309-327.
- [43] D. Radford, V. Deshpande and N. Fleck, `` The response of Clamped Sandwich Beams Subjected to Shock Loading``. International Journal of Impact Engineering, 2006, 32, pp. 968-987.

BIBLIOGRAPHY

- [44] S. Gu, T. Lu and A. Evans, ``On the Design of 2D Cellular Metals For Combined Heat Dissipation and Structural Load Capacity``. International Journal of Heat and Mass Transfer, 2001, 44, pp. 2163-2175.
- [45] DIAB core guide rev 1-december 2012 <http://www.diabgroup.com/en-GB/Knowledge/Sandwich-technology>, Last accessed date March 2017.
- [46] ``Honeycomb``
- [47] M. Yamashita and M. Gotoh , Int. J. Impact Eng. 32(1), 618.
- [48] L. J. Gibson and M. F. Ashby , Cellular Solids: Structure and Properties (Cambridge University Press, Cambridge, 1999).
- [49] Composite materials and sandwich structures - A primer Mohan M. Ratwani, Ph. R-Tec 28441 Highridge Road, Suite 530 Rolling Hills Estates, CA 90274-4886 USA.
- [50] Robert M. J, `` Mechanics of composite materials``, Hemisphere Publishing Corp, 1975.
- [51] Ochoa O. O. Reddy J. N. `` finite element analysis of composite laminates``, Kluwer Academic Publishers, 1992.
- [52] Masters I. G, Evans K. E. `` Models for the elastic deformation of honeycombs``, Composite Structures, Vol. 35, 1996, pp 403-422.
- [53] Liu Q, Zhao Y, `` effect of soft honeycomb core on flexural vibration of sandwich panel using low order and high order shear deformation models``, Journal of sandwich structures and materials, Vol. 9, 2007, pp 95-108.
- [54] Abb-el-Sayed F, Burgess I. W, Jones R, `` A theoretical approach to the deformation of honeycomb-based composite materials``, Composites, 1979, pp 209-214.
- [55] Grediac M, `` A finite element study of the transverse shear in honeycomb cores``, Int. J. Solids structures, Vol. 30, 1993, pp 1777-1788.
- [56] Shi G, Tong P, `` Equivalent transverse shear in honeycomb cores``, Solids Structures, Vol. 32, 1995, pp 1383-1393.
- [57] Kelsey S, Gellatly R. A, Clarck B. W, `` The shear modulus of foil honeycomb cores``, Aircraft Engng, Vol. 30, 1958, pp 294-302.

BIBLIOGRAPHY

- [58] Becker W, `` Closed form analysis of the thickness effect of regular honeycomb core Materials``, Composite Structures, Vol. 48, 2000, pp 67-70.
- [59] Zhang J, Ashby M. F, `` The out-of-plane prop ties of honeycombs``, Int. J. Mech. Sci, Vol. 34, No. 6, 1992, pp 475-489.
- [60] Nast E, `` On honeycomb-Type core moduli``, AIAA/ASME/AHS adaptive structures forum, kissimmee, FL, Apr. 7-10, 1997, collection of technical papers, Pt,2 (A97-24112 05-39).
- [61] A. T. Settet, A. Nour, H. Zahloul, H. Naceur,`` Evaluation of damage and fracture mechanisms of different characteristic honeycomb structures under thermo mechanical loading``, Mechanics of composite materials, Vol. 50, No. 5, November 2014, DOI 10.1007/s11029-014-9452-9.
- [62] www.structures.ethz.ch- 13:20 ; 12/03/2017
- [63] www.Technically.speaking.brachiolopemedia.co- 16:48 ; 12/03/2017

Annex

Annex 1

Tensile test

This procedure was carried out following ISO 527 system

$$E = \frac{\sigma}{\varepsilon}$$

$$\sigma = \frac{F_m}{A}$$

$$\varepsilon = \frac{\Delta L}{L_0}$$

$$G = \frac{3}{8} E$$

CFT plate

$$\sigma = 11,59 \text{ N/m}^2$$

$$\varepsilon = 8\%$$

$$E = 144,87 \text{ N/m}^2$$

$$G = 54,32 \text{ N/m}^2$$

GFT-CFT plate

$$\sigma = 20,71 \text{ N/m}^2$$

$$\varepsilon = 9,5\%$$

$$E = 218 \text{ N/m}^2$$

$$G = 81,75 \text{ N/m}^2$$

GFT plate

$$\sigma = 36,54 \text{ N/m}^2$$

$$\varepsilon = 23,1\%$$

$$E = 158,18 \text{ N/m}^2$$

$$G = 59,32 \text{ N/m}^2$$

We mention that in the three test cases Poisson's ratio was supposed to be equal to 0,3.

3 point bending test

$$I = \frac{d^3 b}{12}$$

$$E = \frac{\sigma}{\varepsilon}$$

$$\sigma_f = \frac{3P}{2b^2}$$

$$\varepsilon = \frac{\Delta L}{L_0}$$

$$E = \frac{FL^3}{48I}$$

$$m = \frac{F}{D}$$

$$\varepsilon_f = \frac{6D}{L^2}$$

$$E_f = \frac{L^3 m}{4d^3}$$

CFT plate

$$I = 2500 \text{ m}^4$$

$$\sigma_f = 8.26 \text{ M}$$

$$\varepsilon = 5.95 \cdot 10^{-2}$$

$$E = 138.82 \text{ M}$$

$$D = 68.34 \text{ m}$$

$$m = 16.65 \text{ N/m}$$

$$\varepsilon_f = 0.41$$

$$E_f = 138.75 \text{ M}$$

GFT-CFT plate

$$I = 2500 \text{ m}^4$$

$$\sigma_f = 4.045 \text{ M}$$

$$\varepsilon = 8.29 \cdot 10^{-2}$$

$$E = 48.79 \text{ M}$$

$$D = 95.23 \text{ m}$$

$$m = 5.85 \text{ N/m}$$

$$\varepsilon_f = 0.57$$

$$E_f = 48.75 \text{ M}$$

GFT plate

$$I = 2500 \text{ m}^4$$

$$\sigma_f = 5.19 \text{ M}$$

$$\varepsilon = 6.96 \cdot 10^{-2}$$

$$E = 74.56 \text{ M}$$

$$D = 79.95 \text{ m}$$

$$m = 8.94 \text{ N/m}$$

$$\varepsilon_f = 0.47$$

$$E_f = 74.56 \text{ M}$$

We mention that the dimensions are all the same for the three test cases specimens.

Annex 2

Interpolation equations for data of the experiments

Tensile test

6-fold trend curve of the traction test in the 1st experiment for the GFT

$$y = -1E+10x^6 + 2E+09x^5 - 1E+08x^4 + 4E+06x^3 - 68157x^2 + 1327,5x - 0,0391$$

6-fold trend curve of the traction test in the 2nd experiment for the GFT honeycomb sandwich

$$y = 3E-06x^6 - 0,0001x^5 + 0,0023x^4 - 0,0149x^3 + 0,1834x^2 + 0,0035x + 0,1045$$

6-fold trend curve of the traction test in the 1st experiment for the GFT-CFT honeycomb sandwich

$$y = -2E+10x^6 + 3E+09x^5 - 2E+08x^4 + 6E+06x^3 - 106378x^2 + 1020,3x - 0,1364$$

6-fold trend curve of the traction test in the 2nd experiment for the GFT-CFT honeycomb sandwich

$$y = 0,0012x^6 - 0,0302x^5 + 0,2855x^4 - 1,2627x^3 + 3,0932x^2 - 2,6526x + 0,5553$$

6-fold trend curve of the traction test in the 1st experiment for the CFT honeycomb sandwich

$$y = -2E+11x^6 + 2E+10x^5 - 8E+08x^4 + 2E+07x^3 - 161391x^2 + 1631,6x - 0,1$$

6-fold trend curve of the traction test in the 2nd experiment for the CFT honeycomb sandwich

$$y = -6E-05x^6 + 0,0018x^5 - 0,0209x^4 + 0,1389x^3 - 0,3134x^2 + 0,5302x + 0,0663$$

Three point bending test

6-fold trend curve of the bending test for the GFT honeycomb sandwich

$$y = 1E+08x^6 - 3E+07x^5 + 3E+06x^4 - 163996x^3 + 4352x^2 - 1,5074x + 0,035$$

6-fold trend curve of the bending test for the GFT-CFT honeycomb sandwich

$$y = -6E-17x^6 + 2E-13x^5 - 2E-10x^4 + 9E-08x^3 - 2E-05x^2 + 0,0083x - 0,1008$$

6-fold trend curve of the bending test for the CFT honeycomb sandwich

$$y = 3E-14x^6 - 4E-11x^5 + 2E-08x^4 - 5E-06x^3 + 0,0005x^2 - 0,0128x + 0,1668$$